Government of **Western Australia**
Department of **Mines and Petroleum**

RECORD 2017/2

GSWA 2017 EXTENDED ABSTRACTS
Promoting the prospectivity of Western Australia

Geological Survey of Western Australia

Government of **Western Australia**
Department of **Mines and Petroleum**

Record 2017/2

GSWA 2017 EXTENDED ABSTRACTS
Promoting the prospectivity of Western Australia

February 2017

Perth 2017

Geological Survey of Western Australia

MINISTER FOR MINES AND PETROLEUM
Hon. Sean K L'Estrange MLA

ACTING DIRECTOR GENERAL, DEPARTMENT OF MINES AND PETROLEUM
Tim Griffin

EXECUTIVE DIRECTOR, GEOLOGICAL SURVEY OF WESTERN AUSTRALIA
Rick Rogerson

REFERENCE
The recommended reference for this publication is:

(a) For reference to an individual contribution:
Duuring, P, Teitler, Y and Hagemann, S 2017, Tools for discovering BIF-hosted iron ore deposits in the Pilbara Craton, *in* GSWA 2017 extended abstracts: Geological Survey of Western Australia, Record 2017/2, p. 1–3.

(b) For reference to the publication:
Geological Survey of Western Australia 2017, GSWA 2017 extended abstracts: promoting the prospectivity of Western Australia: Geological Survey of Western Australia, Record 2017/2, 47p.

National Library of Australia Card Number and ISBN PDF 978-1-74168-731-6; print 978-1-74168-740-8

Published 2017 by Geological Survey of Western Australia
This Record is published in digital format (PDF) and is available online at <www.dmp.wa.gov.au/GSWApublications>.

Further details of geological products and maps produced by the Geological Survey of Western Australia are available from:
Information Centre
Department of Mines and Petroleum
100 Plain Street
EAST PERTH WESTERN AUSTRALIA 6004
Telephone: +61 8 9222 3459 Facsimile: +61 8 9222 3444
www.dmp.wa.gov.au/GSWApublications

Cover image: Elongate salt lake on the Yilgarn Craton — part of the Moore–Monger paleovalley — here viewed from the top of Wownaminya Hill, 20 km southeast of Yalgoo, Murchison Goldfields. Photograph by I Zibra for the Geological Survey of Western Australia.

Contents

GSWA 2017 — Geological Survey Open Day — 24 February 2017

8.15 – 8.45	**REGISTRATION**		
SESSION 1			
8.45 – 9.00	Welcome and opening remarks		
9.00 – 9.25	Tools for discovering BIF-hosted iron ore deposits in the Pilbara Craton	EXPLORATION INCENTIVE SCHEME	Paul Duuring
9.25 – 9.50	Mafic dyke swarms and large igneous provinces in Western Australia get a digital makeover		Michael Wingate
	Morning tea 9.50 – 10.45 in the display area		
SESSION 2			
10.45 – 11.10	From subduction magmatism to cratonization: an isotopic perspective from the Capricorn Orogen	EXPLORATION INCENTIVE SCHEME	Simon Johnson
11.10 – 11.35	In situ phosphate dating of orogenic gold mineralization at Paulsens mine, southern Pilbara	EXPLORATION INCENTIVE SCHEME	Imogen Fielding, Curtin University
11.35 – 12.00	Making sense of the Eastern Goldfields stratigraphic story		Matt De Paoli
	Lunch 12.00 – 1.30		
	Ongoing demonstrations of online systems		
SESSION 3			
1.30 – 1.55	A hydrogeochemistry atlas for Western Australia	EXPLORATION INCENTIVE SCHEME	Dave Gray, CSIRO
1.55 – 2.20	Regolith and spinifex chemistry from the Ngururrpa area, northeastern Western Australia	EXPLORATION INCENTIVE SCHEME	Paul Morris
2.20 – 2.45	Digging up the dirt on Western Australian coal exploration, northern Perth Basin	EXPLORATION INCENTIVE SCHEME	Alan Millar
	Afternoon tea 2.45 – 3.15 in the display area		
SESSION 4			
3.15 – 3.40	Revised tectono-stratigraphy of the Kimberley Basin, northern Western Australia		Christopher Phillips
3.40 – 4.05	Structural evolution of the S-bend region, east Albany–Fraser Orogen	EXPLORATION INCENTIVE SCHEME	Mark Munro
4.05 – 4.30	Post-Giles Event evolution of the Musgrave Province constrained by (multi-method) thermochronology	EXPLORATION INCENTIVE SCHEME	Raphael Quentin de Gromard

Tools for discovering BIF-hosted iron ore deposits in the Pilbara Craton

by

P Duuring, Y Teitler[1,2], and S Hagemann[2]

A consequence of the mostly upward trajectory of iron ore prices from 2007 to 2011 was a broadening of the exploration and research scope in Western Australia, from a historical focus on the mining centres of the Hamersley Basin, to the inclusion of smaller but high-grade (>55 wt% Fe) iron ore deposits in the Yilgarn and Pilbara Cratons. Genetic models for banded iron-formation (BIF)-hosted iron ore deposits were initially influenced by the synthesis of detailed studies completed in the Hamersley Basin (e.g. Morris, 1980; Barley et al., 1999; Taylor et al., 2001), but later evolved to incorporate results from district-scale studies in the Yilgarn Craton (e.g. Angerer et al., 2015). Only recently have iron ore deposits of the Pilbara Craton been examined in order to develop a statewide understanding of iron ore styles and genesis for these deposits. This contribution summarizes the main outcomes of a collaborative project coordinated by the Minerals Research Institute of Western Australia (MRIWA), involving Atlas Iron Ltd Pty, the Centre for Exploration Targeting (CET) at The University of Western Australia, RWTH Aachen University, and the Geological Survey of Western Australia (GSWA) (recently published as GSWA Report 163; Duuring et al., 2016).

Characteristics of iron ore deposits in the Pilbara Craton

The Pilbara Craton contains Archean granite–greenstone terranes unconformably overlain by the Fortescue and Hamersley Basins (Fig. 1). The Hamersley Basin hosts >76% of Western Australia's reported iron resources (44 962 Mt from a total 58 845 Mt of combined resource and reserve estimates; Department of Mines and Petroleum's (DMP) MINEDEX database, November 2016), whereas the Yilgarn and Pilbara Cratons contain about 12 and 11%, respectively. Greenschist-facies metamorphosed greenstone sequences in the Pilbara Craton comprise mainly volcanic and clastic sedimentary rocks, with minor intervals of Mesoarchean BIF that are thickest and most laterally extensive in the East Pilbara Terrane.

Iron ore deposits in the craton are classified by Cooper (2015) on the basis of their genetic and host-rock associations into primary magnetite-rich BIF (21–37 wt% Fe), high-grade supergene-enriched BIF (>55 wt% Fe), pisolitic/channel-iron deposits (CID) ores formed in paleochannels (52–57 wt% Fe), detrital ores (<58 wt% Fe), and orthomagmatic Fe–V–Ti ore hosted by layered mafic igneous rocks (~44 wt% Fe) (Fig. 1). Primary and supergene-enriched iron deposits are the main source of iron ore, representing >96 % of all iron resources in terms of their contained Fe (i.e. 6173 Mt from a total 6401 Mt Fe of combined resources plus reserves; DMP MINEDEX database, November 2016). However, the higher costs of refining primary magnetite-rich BIF ores have so far prevented their development into producing mines (e.g. the Maitland River, Mt Marie, and Mt Oscar deposits; Fig. 1). Instead, high-grade supergene-enriched BIF occurrences remain the primary target and have been mined from various camps throughout the Pilbara Craton, including McPhee Creek (136 Mt Fe; combined resource and reserve estimates), Goldsworthy (122 Mt Fe; comprising the satellite deposits of Mt Goldsworthy, Nimingarra, Shay Gap, Sunrise Hill and Yarrie), Mt Webber (39 Mt Fe), Corunna Downs (37 Mt Fe), Wodgina (18 Mt Fe), Abydos (11 Mt Fe), and Pardoo (6 Mt Fe). Pisolitic, detrital, and orthomagmatic Fe–V–Ti iron ore prospects in the Pilbara Craton are generally too small for mining.

BIF of the 3022–3016 Ma Cleaverville Formation are the main host to high-grade iron ore deposits, with only minor iron ore hosted by older BIF units of the Kangaroo Caves and Paddy Market Formations. BIF within the Cleaverville Formation are thicker (up to 1 km) and generally more iron rich (31–39 wt% Fe). Iron orebodies are mostly centred on kilometre-scale fold hinges that are intersected by shear zones or fault zones (e.g. Corunna Downs, Wodgina, and Pardoo camps), demonstrating the importance of secondary thickening of BIF units and their coincidence with broad damage zones. The enhanced permeability of these zones promotes hydrothermal fluid flow and chemical exchange with BIF, resulting in intense alteration and upgrade to high-grade orebodies (e.g. the ALX pit at Pardoo, Fig. 2a).

1 Centre for Exploration Targeting, The University of Western Australia, Crawley WA 6009

2 Université de Lorraine, GeoRessources, UMR 7359, BP 70239, Vandoeuvre-lés-Nancy, France F-54506

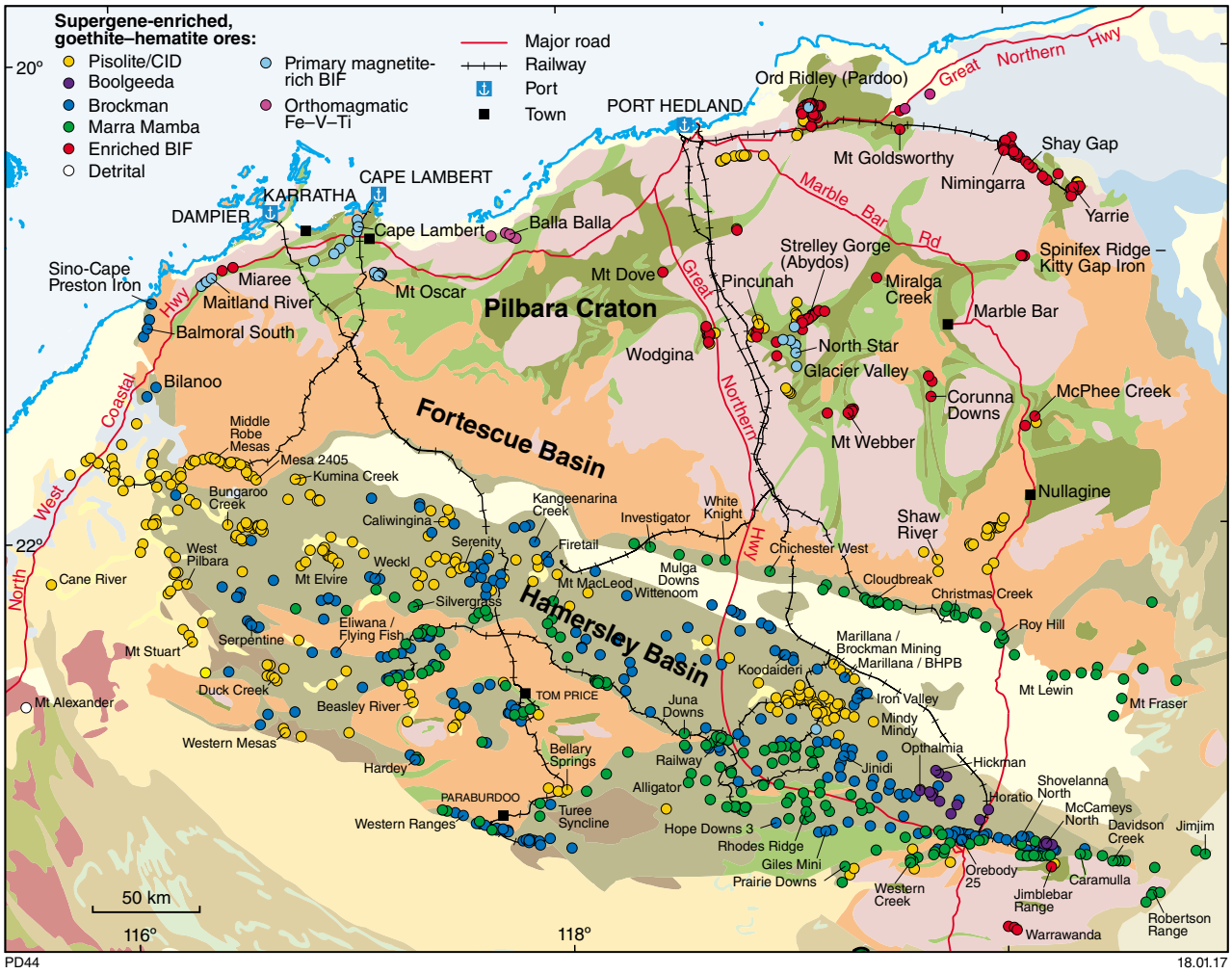

Figure 1. Comparison of iron ore occurrences in the northern half of the Pilbara Craton (the focus of this study) with those in the Hamersley Basin. In the Pilbara Craton, green polygons represent greenstone belts and pink polygons indicate granites. Other colours represent Proterozoic and Phanerozoic rocks that surround the Pilbara Craton. Iron ore occurrences are sourced from DMP's MINEDEX database, June 2016; the geology is sourced from the Geological map of Western Australia, 1:2 500 000, 2015.

Common to all studied deposits is their complex deformation and fluid alteration histories, which include early folding and multistage hypogene fluid alteration events, followed by supergene alteration by meteoric fluids along fault zones (e.g. the Wodgina camp; Teitler et al., 2016). Hypogene magnetite ± hematite ± quartz ore zones are steeply dipping and extend to depths of >200 m, but are narrow (<10 m wide) and low to moderate grade (37–55 wt% Fe). Overprinting supergene goethite ± martite ores are broader and high grade, and they extend from surface to depths of about 100 m (Figs 2b,c).

Hypogene-altered BIF is depleted in Si and enriched in Fe compared with unweathered least-altered BIF. At the Pardoo camp, hypogene-altered BIF are commonly enriched in W. Supergene goethite ± martite ores are depleted in Si and enriched in Fe, P, and volatile (loss on ignition) components, and commonly enriched in Mn, Ni, Co, As, Zn, and Cu, and more locally in U, Ca, Mg, Pb, and Ba compared with unweathered least-altered BIF. The variable enrichment patterns in supergene-altered BIF between iron ore camps are likely the product of chemical exchange between BIF and country rocks with diverse compositions.

Exploration for BIF-hosted iron ore in the Pilbara

Craton-wide predictive exploration strategies are ideally based on a synthesis of detailed deposit- and camp-scale studies obtained from diverse geographical and geological settings. A mineral systems analysis (sensu Wyborn et al., 1994) of enriched BIF-hosted iron ore deposits in the Pilbara Craton identifies the following critical elements for their genesis: (i) the presence of thick BIF; (ii) broad, interconnected damage zones that act as fluid pathways; (iii) a large volume of silica-undersaturated fluid; (iv) exhumation and surficial modification of BIF; and (v) the preservation of orebodies. The occurrence of all critical elements in a locality is required for it to be prospective.

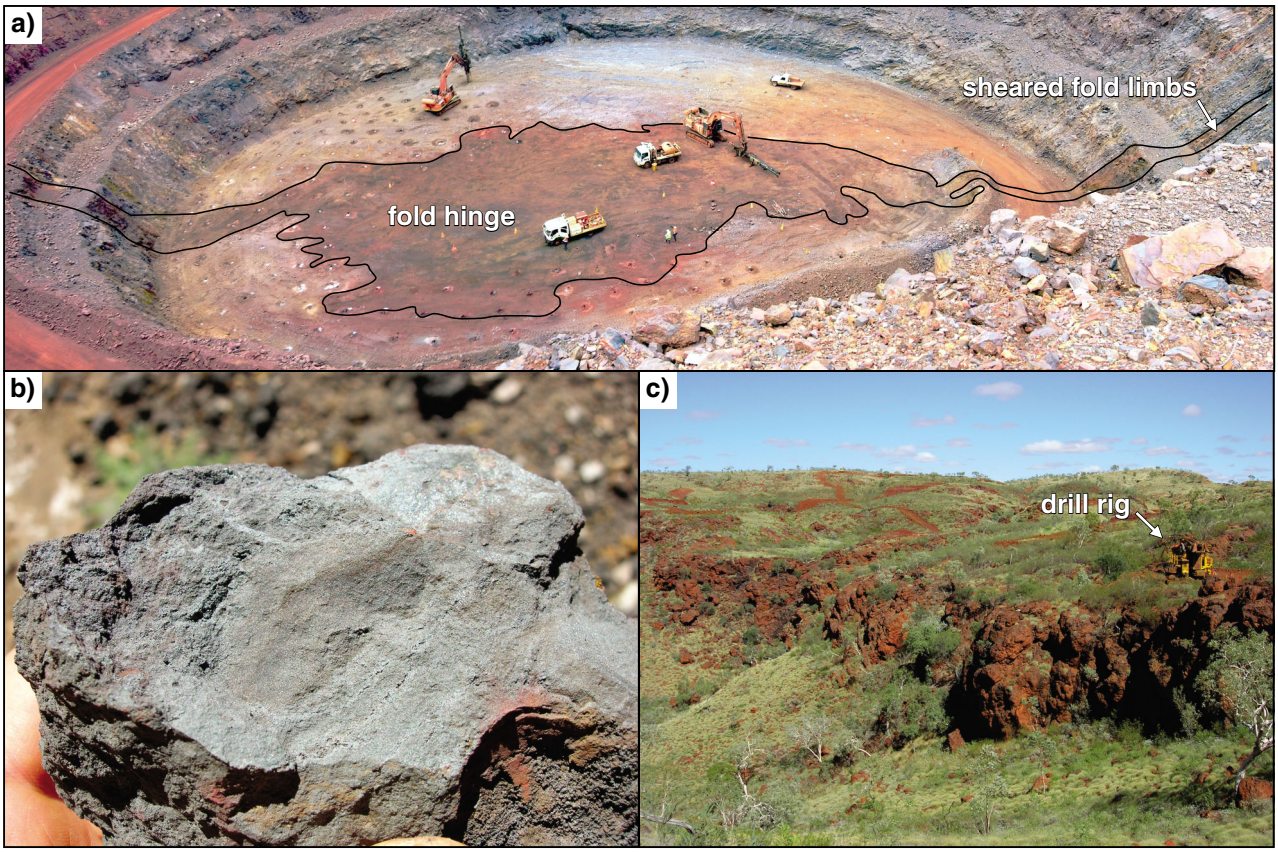

Figure 2. Examples of supergene-modified hypogene ore and supergene ore in the Pilbara Craton: a) Alice Extension pit in the Pardoo camp showing a folded hypogene magnetite-rich orebody that is overprinted by supergene goethite–martite alteration; b) hand specimen of supergene goethite ± martite ore from the Anson pit in the Wodgina camp; c) near-surface, >20 m-thick, subhorizontal layer of high-grade supergene goethite ± martite ore at the Corunna Downs prospect

Concept-driven orebody targeting is best conducted initially at a greenstone belt scale, but requires subsequent testing of specific detection criteria. For example, there is significant geochemical variability in pathfinder element suites for high-grade iron orebodies between camps, illustrating the need to establish baseline petrochemical trends within a camp rather than applying a craton-wide exploration formula. Pathfinder anomalies must be explained in terms of ore-forming processes, and their limitations understood. The greatest potential for the discovery of new iron ore deposits in the Pilbara Craton arguably lies in detecting supergene or hypogene orebodies concealed beneath transported sediment and surface veneers of weathered BIF.

References

Angerer, T, Duuring, P, Hagemann, SG, Thorne, W and McCuaig, TC 2015, A mineral system approach to iron ore in Archaean and Palaeoproterozoic BIF of Western Australia, *in* Ore Deposits in an Evolving Earth *edited by* GRT Jenkin, PAJ Lusty, I McDonald, MP Smith, AJ Boyce and JJ Wilkinson: Geological Society of London, Special Publication 393, p. 81–115.

Barley, ME, Pickard, AL, Hagemann, SG and Folkert, SL 1999, Hydrothermal origin for the 2 billion year old Mount Tom Price giant iron ore deposit, Hamersley Province, Western Australia: Mineralium Deposita, v. 34, no. 6, p. 784–789.

Cooper, RW 2015, Iron ore deposits of the Pilbara region — 2015 (1:750 000 scale): Geological Survey of Western Australia.

Duuring, P, Teitler, Y, Hagemann, S and Angerer, T 2016, MRIWA Report Project M426: exploration targeting for BIF-hosted iron deposits in the Pilbara Craton, Western Australia: Geological Survey of Western Australia, Report 163, 263p.

Morris, RC 1980, A textural and mineralogical study of the relationship of iron ore to banded iron-formation in the Hamersley Iron Province of Western Australia: Economic Geology, v. 75, no. 2, p. 184–209, doi:10.2113/gsecongeo.75.2.184.

Taylor, D, Dalstra, HJ, Harding, AE, Broadbent, GC and Barley, ME 2001, Genesis of high-grade hematite orebodies of the Hamersley Province, Western Australia: Economic Geology, v. 96, no. 4, p. 837–873, doi:10.2113/gsecongeo.96.4.837.

Teitler, Y, Duuring, P and Hagemann, SG 2016, Genesis history of iron ore from Mesoarchean BIF at the Wodgina mine, Western Australia: Australian Journal of Earth Sciences, in press, doi:10.1080/08120099.2017.1266387.

Wyborn, LAI, Heinrich, CA and Jaques, AL 1994, Australian Proterozoic mineral systems: essential ingredients and mappable criteria, *in* Australian mining looks north — the challenges and choices *edited by* PC Hallenstein: Australian Institute of Mining and Metallurgy; 1994 AusIMM Annual Conference, Darwin, Northern Territory, 5 August 1994, p. 109–115.

Mafic dyke swarms and large igneous provinces in Western Australia get a digital makeover

by

MTD Wingate

Digital dyke and LIP layers in the geological map of Western Australia

Since 1894, the Geological Survey of Western Australia (GSWA) has released 14 versions of the 'Geological Map of Western Australia'. The latest in this series, published in December 2015, is the first bedrock geology map compilation in digital form that covers the entire State, and can be viewed online and downloaded at no cost in a variety of formats. The new digital State map includes an updated mafic dyke layer compiled from published geological maps and interpreted from aeromagnetic data. Mafic dyke and sill suites are shown in significantly more detail than on previous State maps, reflecting improvement in the resolution of aeromagnetic datasets, advances in isotopic dating of mafic igneous rocks, and a greater appreciation of the importance of mafic igneous events in interpreting geological history. Most dykes and sills have been assigned to named suites (Figs 1, 2) based on age, orientation, magnetization, composition, and crosscutting relationships. Many dyke swarms are also components of at least seven large igneous provinces (LIP), which range in age from late Archean to early Cambrian (Figs 1, 2).

New developments and new questions

Western Australia is endowed with an impressive number of mafic dykes and sills. In the last few years, there have been several advances in our knowledge of these mafic suites and the large igneous provinces in Western Australia, and some of these are described below.

The 2775–2715 Ma Fortescue large igneous province

The oldest coherent mafic dyke swarm in Australia is the c. 2772 Ma Black Range Dolerite Suite, which fed the Mount Roe Basalt at the base of the Fortescue Group in the northern Pilbara Craton. A new baddeleyite age of 2770 ± 4 Ma for a large north-trending dyke in the Rocklea Inlier (GSWA 205904, Wingate et al., 2017) extends the Black Range swarm more than 200 km into the southwest Pilbara Craton, beneath the Fortescue and Hamersley Groups.

The 2408–2401 Ma Widgiemooltha large igneous province

Much of the Yilgarn Craton is transected by the Widgiemooltha dyke swarm, which includes dykes of two magnetic polarities: those that strike about 075° have upward magnetic inclinations and produce positive aeromagnetic anomalies, and those that strike about 085° have downward inclinations and negative anomalies. Until recently, geochronology and paleomagnetic studies have mainly targeted the first group, yielding U–Pb ages that average 2408 ± 3 Ma (Wingate, 2007, references within, and unpublished data), and paleomagnetic data (Smirnov et al., 2013) that confirm the affinity of dykes well into the northern Yilgarn Craton. Pisarevsky et al. (2015) reported data for 'negative' dykes, including a TIMS U–Pb age of 2401 ± 1 Ma and a mean inclination higher than that of the positive dykes, implying about 10° of poleward motion of the Yilgarn Craton between c. 2408 and 2401 Ma. If additional geochronology corroborates this age difference, it may be necessary to consider the Widgiemooltha dykes as two separate swarms, although perhaps emplaced during a single protracted event.

The c. 1210 Ma Marnda Moorn large igneous province

The c. 1210 Ma Marnda Moorn LIP consists of mafic dyke swarms subparallel to the western, southern, and southeastern margins of the Yilgarn Craton, and in parts of the western Yilgarn interior. However, recent geological mapping, geochemistry, geochronology, and metamorphic studies indicate that this circum-Yilgarn LIP is only one manifestation of a much more widespread event (Fig. 3). The Marnda Moorn LIP coincided with the early stages of the 1220–1100 Ma Maralinga Event (Spaggiari et al., 2016), which included high-strain deformation, extensive ultra-high-temperature reworking, and rapakivi-style granite magmatism in central Australia (Musgrave Orogeny, Howard et al., 2015), and high-temperature magmatism and metamorphism in the Madura and Coompana Provinces and Albany–Fraser Orogen (Spaggiari et al., 2016). There was also magmatism and metamorphism at this time in the Capricorn and Pinjarra Orogens (Fig. 3).

The areal extent of these events suggests the existence of a widespread mafic underplate. The restriction of mafic dykes to the Yilgarn Craton margins at c. 1210 Ma may indicate that the mafic magmas were able to penetrate the cold, dense craton, but remained at depth elsewhere due to their relatively low buoyancy in the presence of extensive partially molten lower crust. The short duration of the LIP may reflect a change in the regional stress regime; plate reorganization at c. 1210 Ma is indicated by a major bend in the apparent polar wander curve for Australia.

The c. 1075 Ma Warakurna large igneous province

The Warakurna LIP includes layered mafic–ultramafic intrusions and mafic to felsic volcanic rocks and dykes in central Australia, and a 1000 km-long mafic sill province and several mafic dyke swarms in Western Australia. New and recent geochronology and paleomagnetic studies have resolved a c. 1075 Ma age for the Round Hummock dyke swarm (D. Evans et al., written comm., 2016) and mafic sills in the Pilbara Craton, as well as mafic sills in the interior of the Yilgarn Craton, extending the LIP to the north and south and increasing its minimum area to about 2×10^6 km^2. Based on its short duration (1078–1070 Ma, Wingate et al., 2004) and wide extent, the LIP was initially considered to have formed above a mantle plume. However, recent work by GSWA has shown that mantle-derived magmatism in the Musgrave Province continued for >50 Ma and may instead reflect inheritance of the older (1220–1120 Ma), extreme thermal anomaly in central Australia (Fig. 3). Destabilization to produce the widespread 1078–1070 Ma mafic magmatic pulse of the Warakurna LIP may have been triggered by movement on crustal- and continent-scale shear zones (Smithies et al., 2015).

Mafic igneous events at 755–735 Ma

The c. 755 Ma Mundine Well Dolerite Suite is an extensive dyke swarm that intrudes the western Capricorn Orogen and Pilbara Craton, and may be comagmatic with the Northampton dykes of the Pinjarra Orogen (Wingate and Giddings, 2000). A new U–Pb baddeleyite age of c. 735 Ma has been determined for an east-southeastly trending dyke of the Nindibillup swarm that crosscuts Mesoproterozoic rocks of the eastern Albany–Fraser Orogen, and paleomagnetic directions in another east-southeastly trending dyke (Pisarevsky et al., 2014) are similar to those for the Mundine Well dykes. These new results suggest that east-southeastly trending dykes along the southern margin of the Yilgarn Craton and the Mundine Well dykes may have been emplaced during the same event.

The work continues…

There are still many dykes in Western Australia about which very little is known, although most can be grouped into swarms of dykes of similar orientation. Unfortunately, many are not exposed, and can only be identified on aeromagnetic images. However, samples for geochronology and geochemistry continue to be collected when dykes are encountered during regional mapping. Geochemical and isotope data currently being collated are expected to help elucidate the origins and tectonic settings of several dyke suites. The digital dyke layer is regularly updated with new information, and future improvements will include assigning each dyke suite to a unique GIS layer and integration with explanatory notes.

References

Howard, HM, Smithies, RH, Kirkland, CL, Kelsey, DE, Aitken, A, Wingate, MTD, Quentin De Gromard, R, Spaggiari, CV and Maier, WD 2015, The burning heart — the Proterozoic geology and geological evolution of the west Musgrave Region, central Australia: Gondwana Research, v. 27, p. 64–94.

Pisarevsky, SA, De Waele, B, Jones, S, Soderlund, U and Ernst, RE 2015, Paleomagnetism and U–Pb age of the 2.4 Ga Erayinia mafic dykes in the south-western Yilgarn, Western Australia: Paleogeographic and geodynamic implications: Precambrian Research, v. 259, p. 222–231.

Pisarevsky, SA, Wingate, MTD, Li, Z-X, Wang, X-C, Tohver, E and Kirkland, CL 2014, Age and paleomagnetism of the 1210 Ma Gnowangerup–Fraser dyke swarm, Western Australia, and implications for late Mesoproterozoic paleogeography: Precambrian Research, v. 246: p. 1–15.

Smirnov, AV, Evans, DAD, Ernst, RE, Soderlund, U and Li, Z-X 2013, Trading partners: Tectonic ancestry of southern Africa and western Australia, in Archean supercratons Vaalbara and Zimgarn: Precambrian Research, v. 224, p. 11–22.

Smithies, RH, Kirkland, CL, Korhonen, FJ, Aitken, ARA, Howard, HM, Maier, WD, Wingate, MTD, Quentin de Gromard, R and Gessner, K 2015 The Mesoproterozoic thermal evolution of the Musgrave Province in central Australia — plume vs. the geological record, Gondwana Research, 27: 1419–1429.

Spaggiari, CV, Smithies, RH, Wingate, MTD, Kirkland, CL and England, RN 2016, Exposing the Eucla basement: what separates the Albany–Fraser Orogen and the Gawler Craton?, *in* GSWA 2016 extended abstracts: promoting the prospectivity of Western Australia: Geological Survey of Western Australia, Record 2016/2, p. 36–41.

Wingate, MTD 2007, Proterozoic mafic dykes in the Yilgarn Craton: Proceedings of Geoconferences (WA) Inc., Kalgoorlie '07 conference: Geoscience Australia, Record 2007/14, p. 80–84.

Wingate, MTD and Giddings, JW 2000, Age and paleomagnetism of the Mundine Well dyke swarm, Western Australia: implications for an Australia–Laurentia connection at 755 Ma: Precambrian Research, v. 100, p. 335–357.

Wingate, MTD, Pirajno, F and Morris, PA 2004, The Warakurna large igneous province: a new Mesoproterozoic large igneous province in west-central Australia: Geology, v. 32, p. 105–108.

Wingate, MTD, Lu, Y and Johnson, SP 2017, 205904: metagabbro dyke, Black Hill Bore; Geochronology Record 1365: Geological Survey of Western Australia, 5p.

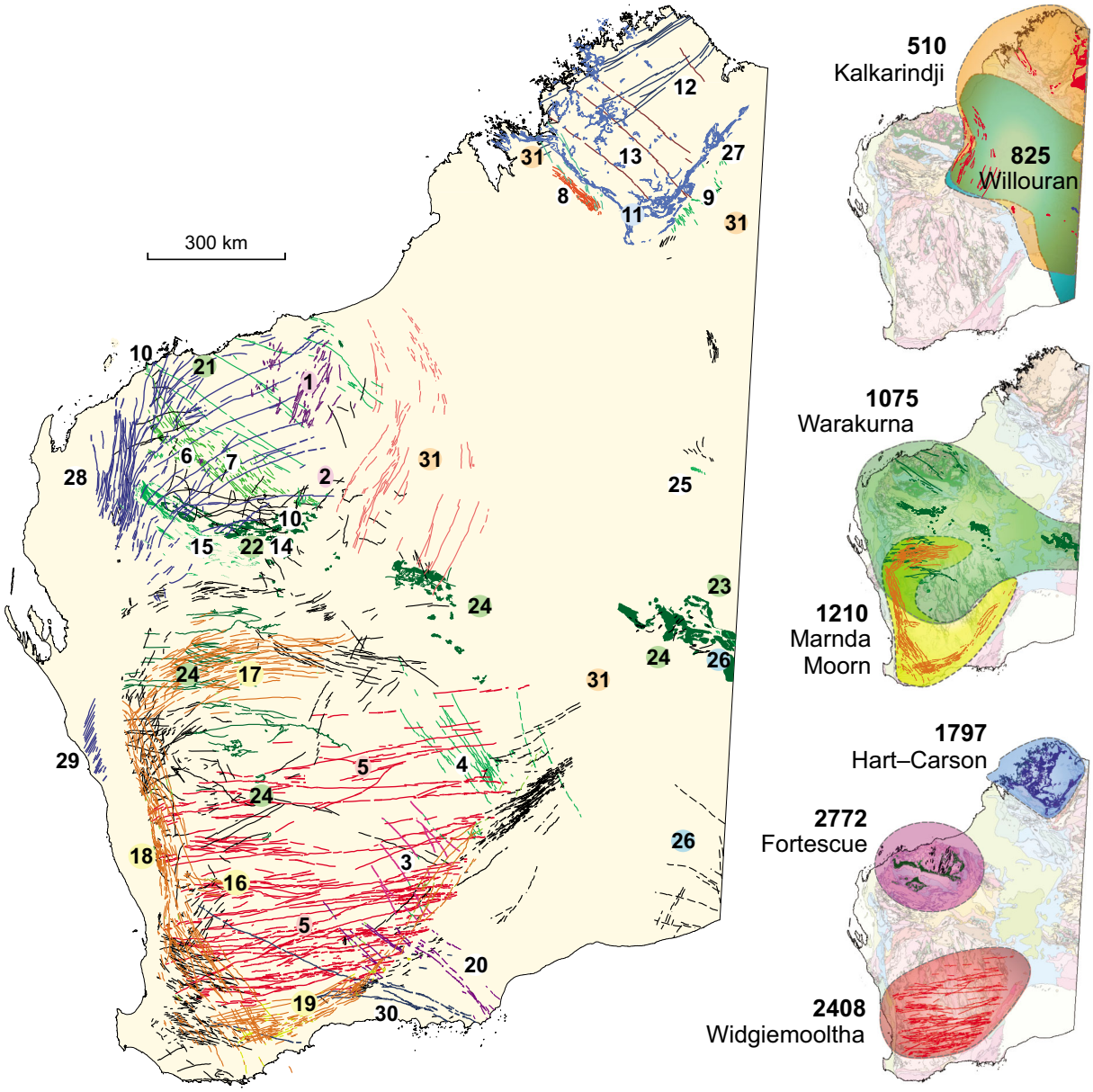

Figure 1. Dyke and sill suites in the digital map layer (left) and large igneous provinces in Western Australia (right). Ages are in Ma. Numbers identify dyke and sill suites listed in Figure 2.

	Dyke or sill suite	Age (Ma)	LIP	Location
31	Kalkarindji Supersuite	510	**Kalkarindji**	NW Officer Basin, Kimberley
30	Nindibillup Dyke Suite	735		S Yilgarn, Albany–Fraser Orogen
29	Northampton Dolerite Suite	748		Northampton Inlier
28	Mundine Well Dolerite Suite	755		Gascoyne Province, Pilbara Craton
27	Bow Hill Lamprophyre Suite	815		E Kimberley
26	Gairdner Dolerite	825	**Willouran**	Musgrave and Rudall Provinces
25	Central Desert Dolerite Suite	975		W Arunta region
24	Warakurna Supersuite	1075	**Warakurna**	Musgrave Province, Yilgarn Craton
23	Alcurra Dolerite	1075		Musgrave Province
22	Kulkatharra Dolerite (sills)	1075		Capricorn Orogen
21	Round Hummock Dolerite Suite	1075		Pilbara Craton
20	Beenong Dyke Suite	1210–541		SE Yilgarn, Albany–Fraser Orogen
19	Gnowangerup – Fraser Dyke S.	1210	**Marnda Moorn**	S Yilgarn Craton margin
18	Boyagin Dolerite Suite	1210		W Yilgarn Craton margin
17	Muggamurra Dolerite Suite	1210		N Yilgarn Craton margin
16	Wheatbelt Dyke Suite	1210		W & S Yilgarn Craton
15	Narimbunna Dolerite (sills)	1465		Capricorn Orogen
14	Waldburg Dolerite (sills)	1500		Capricorn Orogen
13	Prince Regent Dyke Suite	1797–510		Kimberley
12	Kalumburu Dyke Suite	1797–510		Kimberley
11	Hart Dolerite (mainly sills)	1797	**Hart–Carson**	Kimberley
10	Preston Dolerite Suite	1816		W Pilbara Craton
9	Warmun Dolerite Suite	1860–560		E Kimberley
8	Leopold Downs Dyke Suite	1860–560		W Kimberley
7	Panhandle Dyke Suite	2008		Hamersley region
6	Moodogara Dyke Suite	2208		Hamersley region
5	Widgiemooltha Supersuite	2408	**Widgiemooltha**	Yilgarn Craton
4	Cosmo Newbery Dyke Suite	2500–510		E Yilgarn Craton
3	Lakewood Dolerite Suite	2500–541		E Yilgarn Craton
2	Prairie Downs Dyke Suite	2745	**Fortescue**	S Pilbara Craton
1	Black Range Dolerite Suite	2772		E Pilbara Craton

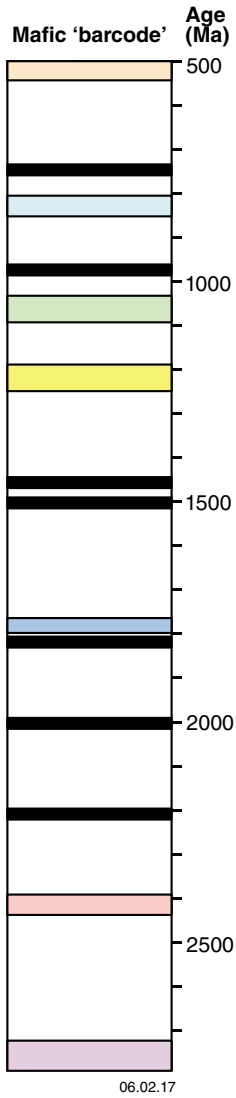

Figure 2. Named mafic dyke and sill suites in Western Australia, and their mafic 'barcode'. Numbers refer to Figure 1.

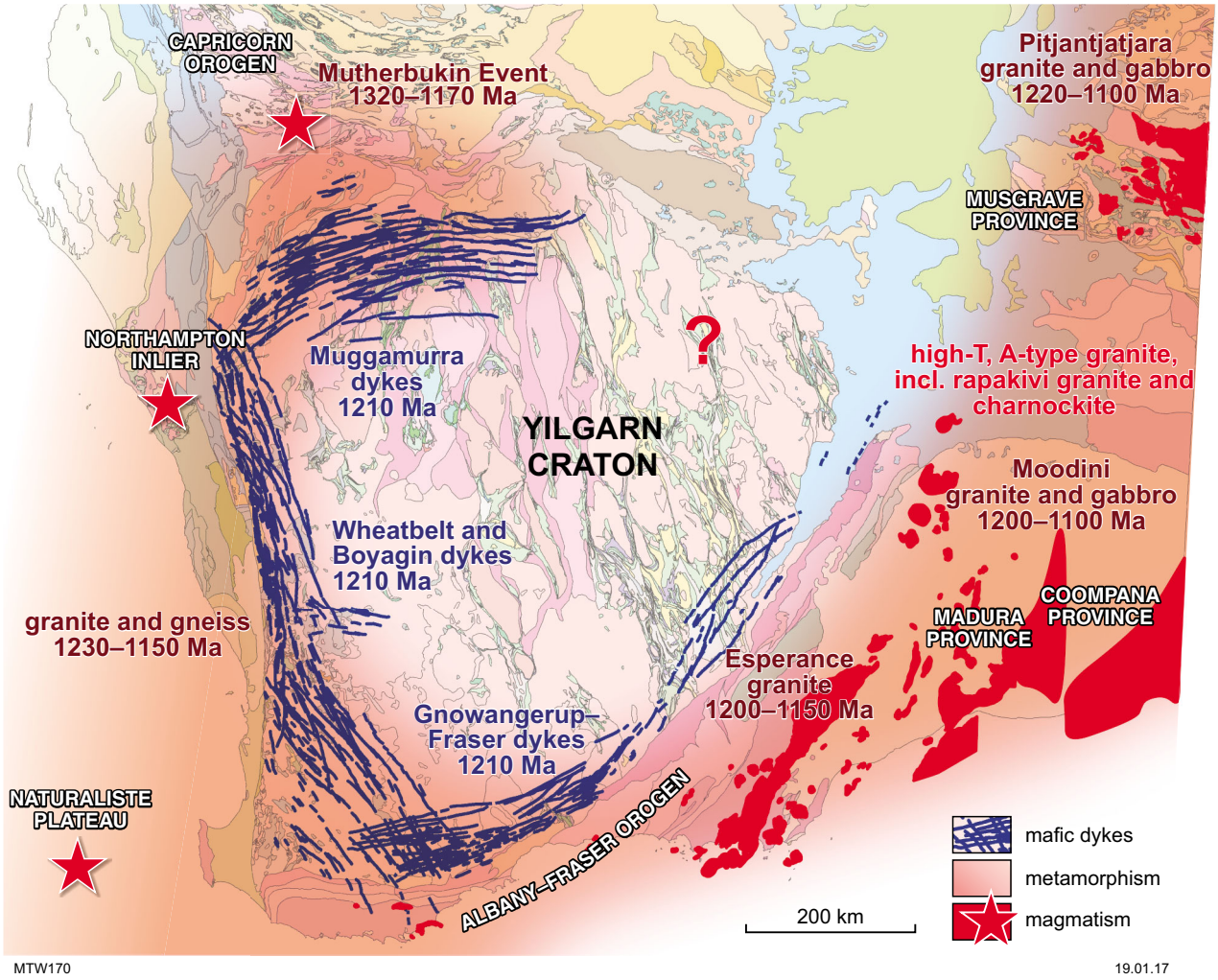

Figure 3. Mafic dyke swarms of the c. 1210 Ma Marnda Moorn large igneous province, and broadly coeval magmatic events in Western Australia

From subduction magmatism to cratonization: an isotopic perspective from the Capricorn Orogen

by

SP Johnson, FJ Korhonen, CL Kirkland[1], JB Cliff[2], EA Belousova[3], and S Sheppard[1]

The differentiation of continental crust is a fundamental process in the evolution of our planet. Partial melting of the deep crust and transport of those melts to shallower levels results in a chemically stratified crust, with a refractory, dehydrated lower portion overlain by a complementary enriched upper portion (e.g. Rudnick, 1995). This chemical differentiation process also fractionates the heat-producing elements (HPE; U–Th–K), which are generally enriched in crustal melts, preferentially moving them to shallower depths. The progressive chemical stratification of the crust greatly alters its thermal structure and rheology through time, ultimately promoting the long-term stability of the continents (McKenzie and Priestley, 2008; Afonso and Ranalli, 2004; Sandiford and McLaren, 2002).

Long-lived orogenic systems that preserve evidence for multiple tectono-magmatic episodes can provide a window into crustal differentiation and stabilization. However, since the deep crust is not accessible, these processes have to be investigated through indirect methods. Various isotopic systems, such as the Sm–Nd and Lu–Hf isotopic composition of whole rocks and zircons, respectively, can provide critical information on the timing of melt generation and melt sources in the deep crust as well as processes that might modify the melt during transportation and emplacement.

The Capricorn Orogen

The Proterozoic Capricorn Orogen of Western Australia is ideally suited for an isotopic study of crustal differentiation and stabilization processes because it has a long-lived tectonic history. The orogen exposes four cycles of magmatism that record a progressive evolution from subduction and continental convergence to intracontinental reworking and eventual cratonization (Johnson et al., 2016; Korhonen and Johnson, 2015; Sheppard et al., 2010a). The oldest component of the orogen is the Glenburgh Terrane, which is interpreted to be an exotic microcontinent within the Capricorn Orogen (Johnson et al., 2011a; Occhipinti et al., 2004). Neoarchean to Paleoproterozoic gneisses that make up this terrane represent the Cycle 1 magmatic rocks (Fig. 1).

The Glenburgh Terrane is interpreted to have collided with the Pilbara Craton during the 2215–2145 Ma Ophthalmia Orogeny (Johnson et al., 2011b; Occhipinti et al., 2004), although an associated magmatic arc on either the Pilbara Craton or Glenburgh Terrane margin has yet to be identified. Collision of the Pilbara Craton – Glenburgh Terrane with the Yilgarn Craton to form the West Australian Craton, took place during the latter part (1965–1950 Ma) of the Glenburgh Orogeny (Johnson et al., 2011b; Occhipinti et al., 2004) producing Cycle 2 rocks in a magmatic arc (Fig. 1). Following the final assembly of the West Australian Craton, the orogen was structurally and thermally reworked during at least five punctuated, intraplate orogenic events (Fig. 1). Many of the events, particularly the older ones, were accompanied by the intrusion of voluminous syntectonic felsic magmatic rocks, including Cycle 3 and 4 rocks (Fig. 1). These magmatic rocks all show similar 'calk-alkaline' major, trace and rare earth element whole-rock chemistries indicating that they were generated and emplaced entirely within an intraplate tectonic setting (Sheppard et al., 2010b). Following Cycle 4 magmatism, the orogenic crust displays a broad secular change to more rigid behaviour akin to that of the bounding Archean Yilgarn and Pilbara Cratons (Fig. 1), allowing the emplacement of abundant mafic dykes and sills into the shallow crust (Morris and Pirajno, 2005; Wingate, 2003), and the formation of thick intracontinental sedimentary basins (Cutten et al., 2016).

Isotopic data

Samarium–neodymium whole-rock data, and Lu–Hf and $\delta^{18}O$ isotopic data from previously well-dated magmatic and inherited zircon from the four main felsic magmatic cycles are used here to highlight the differentiation and thermal history of this tract of orogenic crust.

1 Department of Applied Geology, Western Australian School of Mines, Curtin University, Bentley WA 6102

2 Environmental Molecular Sciences Laboratory, Pacific Northwest National Laboratory, 3335 Innovation Boulevard, Richland, WA 99354, US

3 GEMOC, Department of Earth and Planetary Sciences, Macquarie University, Sydney, NSW 2109

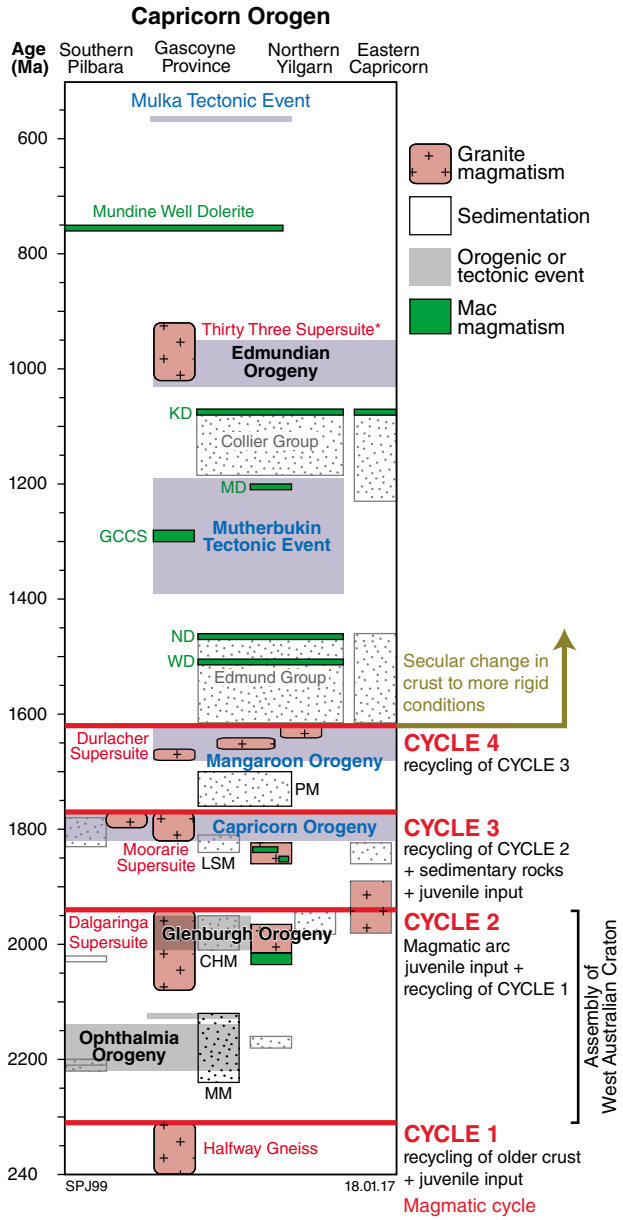

Figure 1. Time–space event summary of the Capricorn Orogen (after Korhonen and Johnson, 2015). Magmatic cycles shown in red; * denotes minor, localized intrusions. Magmatic evolution models from Johnson et al. (2011a,b, 2016). Orogenic events associated with the assembly of the West Australian Craton are shown in grey; reworking events are shown in blue. Abbreviations: CHM, Camel Hills Metamorphics; GCCS, Gifford Creek Carbonatite Suite; KD, Kulkatharra Dolerite; LSM, Leake Spring Metamorphics; MD, Muggamurra Dolerite; MM, Moogie Metamorphics; ND, Narimbunna Dolerite; PM, Pooranoo Metamorphics; WD, Waldburg Dolerite

Granitic and mafic rocks from each of the four magmatic cycles have a wide range of initial whole-rock Nd and zircon Hf isotopic compositions, forming vertical arrays that are generally more evolved than the Chondritic Uniform Reservoir (CHUR; Fig. 2). These arrays are commonly interpreted to indicate a simple two-component mixing between radiogenic (juvenile) crust and highly evolved crust, either in a deep crustal setting during magma generation, or by assimilation of evolved shallow crustal material during magma emplacement, or both. However, complimentary $\delta^{18}O$ isotopic data from the same zircon (Fig. 3) provide more detail on the source and transport history of the melt (Johnson et al., 2016).

Cycle 3 rocks were generated in a complex tectono-magmatic setting, from three main source components including minor amounts of mantle-derived material, shallow crustal rocks and a significant contribution from a previously unknown 2280–2115 Ma-aged deep- to mid-crustal component (D–MC, Fig. 3). Cycle 4 granitic rocks show no isotopic evidence for the involvement of mantle-derived source components, and appear to have been generated by the direct melting and recycling of rocks similar in isotopic composition to Cycle 3 rocks as well as interaction with the D–MC (Fig. 3).

Crustal differentiation and cratonization

The progression, from an active magmatic arc (Cycle 2) to reworking with minor amounts of new crustal growth (Cycle 3) to exclusive reworking (Cycle 4), was accompanied by a progressive decrease in the contribution from mantle-derived sources (Fig. 3), and a complimentary increase in radiogenic heat production (Fig. 4; Johnson et al., 2016; Korhonen and Johnson, 2015). This progression is also reflected by an increase in the Th/U content of magmatic zircon with time (Fig. 4; Korhonen and Johnson, 2015). The greatest step in heat production and zircon Th/U contents is recorded by Cycle 4 rocks (Fig. 4), following which the orogen did not experience any additional major felsic magmatic events (Fig. 1). In the Capricorn Orogen, the principal driver of differentiation of the crust was a decreasing accessibility to fertile mantle sources following collision. The generation of voluminous felsic magmatic rocks during Cycles 3 and 4 would have led to a complementary and rapid depletion in the lower crust, eventually leading to completely refractory lower crust during the generation of Cycle 4 rocks.

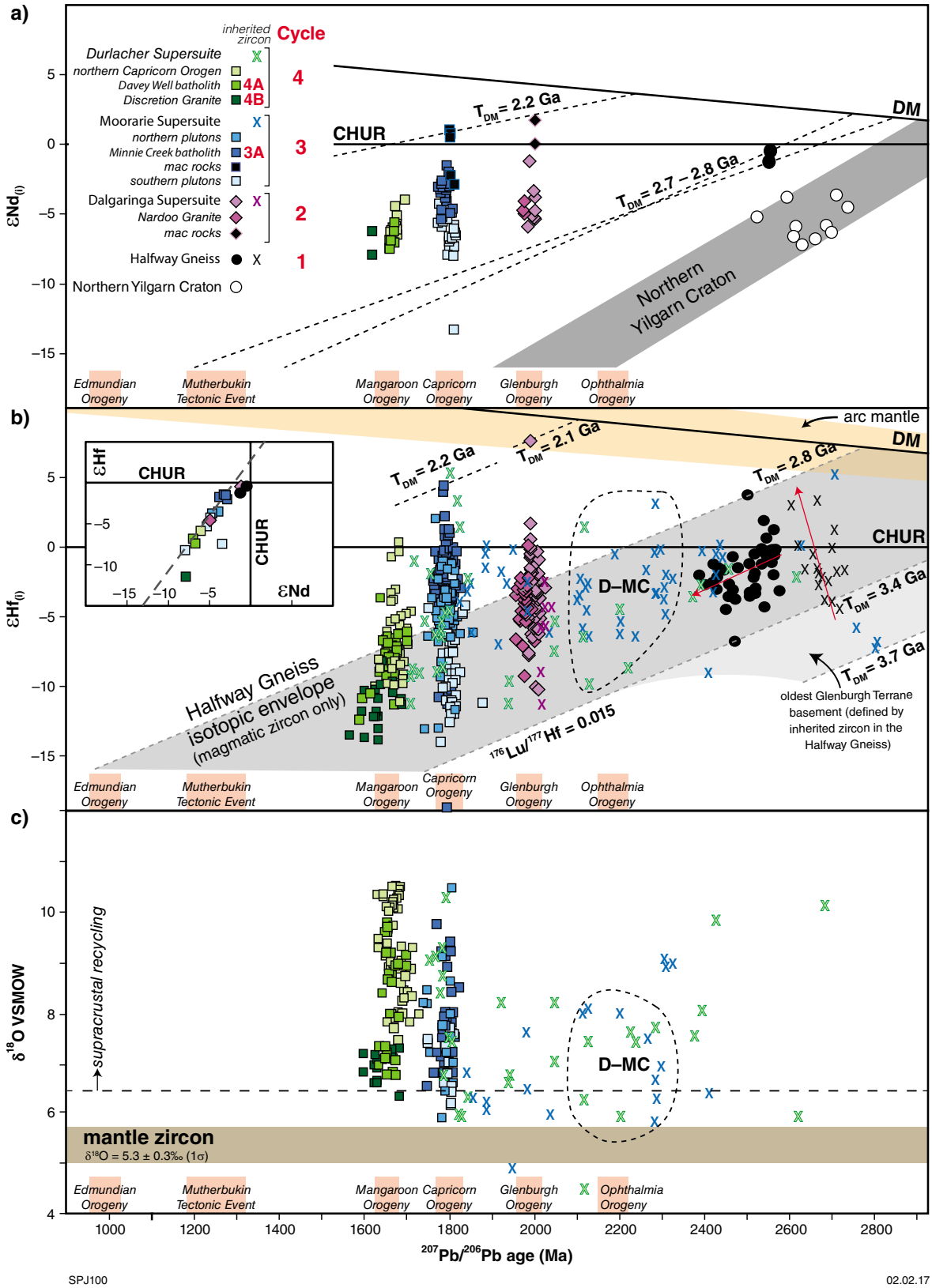

Figure 2. a) Whole-rock $\varepsilon Nd_{(i)}$ evolution diagram for both felsic and mafic magmatic rocks of the Capricorn Orogen and the northern Yilgarn Craton; b) $\varepsilon Hf_{(i)}$ evolution diagram for magmatic and inherited zircons from felsic magmatic rocks comprising the four main magmatic cycles. The field for arc mantle is based on the data of Dhumie et al. (2012); c) $\delta^{18}O$ VSMOW evolution diagram for magmatic and inherited zircons from Cycle 2 and Cycle 3 magmatic rocks. The compositional field for zircon in equilibrium with mantle-derived melts has a $\delta^{18}O$ VSMOW value of 5.3 ± 0.3‰ (1σ; Valley, 2003). The area labelled 'D–MC' (deep- to mid-crust) in b) and c), represents a previously unknown crustal source component that has contributed significantly to the isotopic composition of Cycle 3 and 4 magmatic rocks.

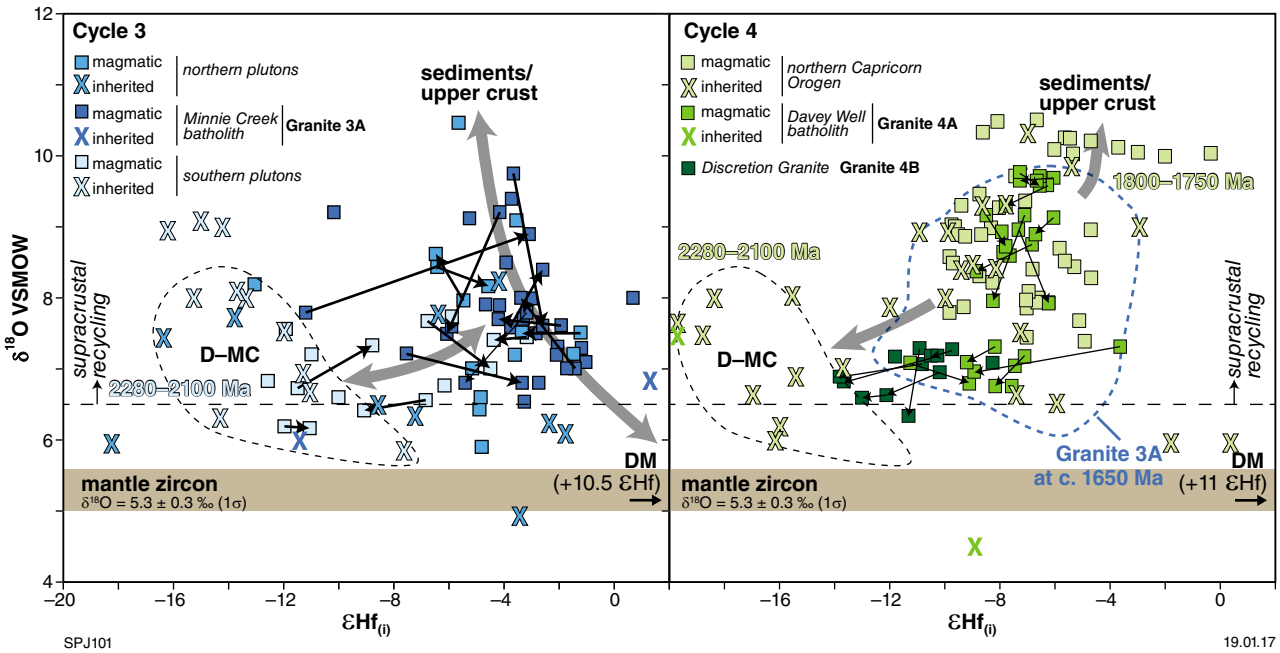

Figure 3. $\delta^{18}O$ vs $\varepsilon Hf_{(i)}$ plot for magmatic zircons in: a) Cycle 3 and; b) Cycle 4 granitic rocks formed during intracontinental reworking. Analyses were made in central and edge regions of magmatic grains where possible to track the isotopic evolution of individual magma pulses and batches — arrows show centre–edge pairs. The compositional field for zircon in equilibrium with mantle-derived melts has a $\delta^{18}O$ VSMOW value of 5.3 ± 0.3‰ (1σ; Valley, 2003). Abbreviations: D–MC — deep- to mid-crustal component

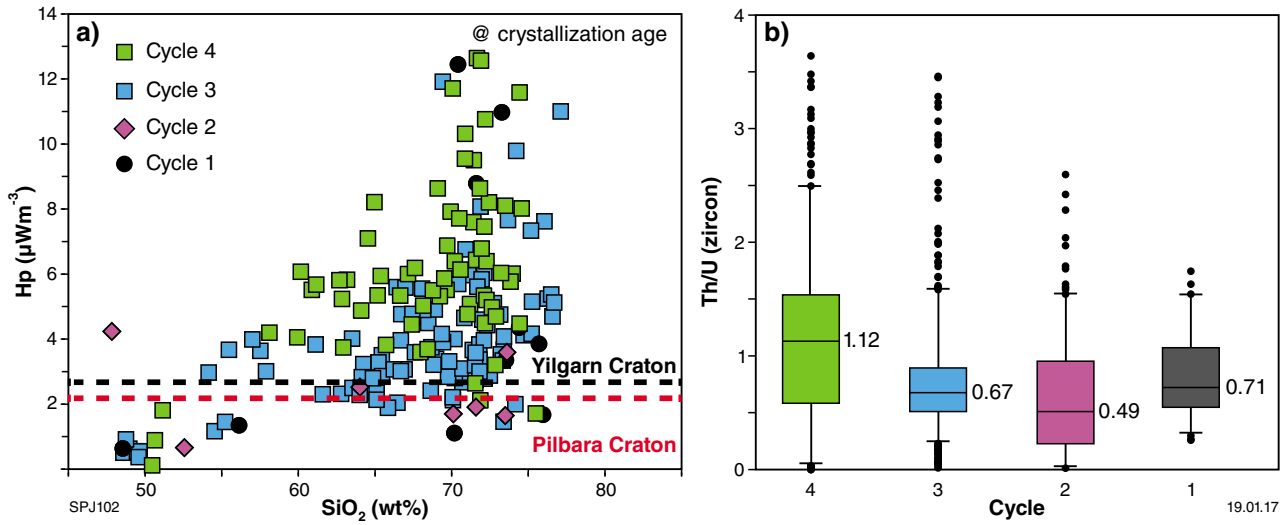

Figure 4. a) Calculated present-day heat production (Hp in μWm^{-3}) vs whole-rock SiO_2 content for the four main magmatic cycles. Dashed lines show average granite heat production for the Yilgarn and Pilbara Cratons; b) box-and-whisker plots (after Korhonen and Johnson, 2015) showing the median Th/U ratio of magmatic zircon from the four main magmatic cycles. Whiskers extend to 95th and 5th percentiles; outliers shown as closed dots

References

Afonso, JC and Ranalli, G 2004, Crustal and mantle strengths in continental lithosphere: is the jelly sandwich model absolute?: Tectonophysics, v. 394, p. 221–232.

Cutten, HN, Johnson, SP, Thorne, AM, Wingate, MTD, Kirkland, CL, Belousova, EA, Blay, OA and Zwingmann, H 2016, Deposition, provenance, inversion history and mineralization of the Proterozoic Edmund and Collier Basins, Capricorn Orogen: Geological Survey of Western Australia, Report 127, 74p.

Dhumie, B, Hawksworth, C and Cawood, P 2012, When continents formed: Science, v. 331, p. 154–155.

Johnson, SP, Korhonen, FJ, Kirkland, CL, Cliff, JB, Belousova EA and Sheppard S 2016, An isotopic perspective on growth and differentiation of Proterozoic orogenic crust: From subduction magmatism to cratonization: Lithos, v. 268–271, p. 76–86.

Johnson, SP, Sheppard, S, Rasmussen, B, Wingate, MTD, Kirkland, CL, Muhling, JR, Fletcher, IR and Belousova, EA 2011b, Two collisions, two sutures: punctuated pre-1950 Ma assembly of the West Australian Craton during the Ophthalmian and Glenburgh Orogenies: Precambrian Research, v. 189, p. 239–262.

Johnson, SP, Sheppard, S, Wingate, MTD, Kirkland, CL and Belousova, EA 2011a, Temporal and hafnium isotopic evolution of the Glenburgh Terrane Basement: an exotic crustal fragment in the Capricorn Orogen: Geological Survey of Western Australia, Report 110, 27p.

Korhonen, FJ and Johnson, SP 2015, The role of radiogenic heat in prolonged intraplate reworking: the Capricorn Orogen explained?: Earth and Planetary Science Letters, v. 428, p. 22–32.

McKenzie, DP and Priestley, KF 2008, The influence of lithospheric thickness variations on continental evolution: Lithos, v. 102, p. 1–11.

Morris, PA and Pirajno, F 2005, Mesoproterozoic sill complexes in the Bangemall Supergroup, Western Australia: geology, geochemistry, and mineralization potential: Geological Survey of Western Australia, Report 99, 75p.

Occhipinti, SA, Sheppard, S, Passchier, C, Tyler, IM and Nelson, DR 2004, Palaeoproterozoic crustal accretion and collision in the southern Capricorn Orogen: the Glenburgh Orogeny: Precambrian Research, v. 128, p. 237–255.

Rudnick, RL 1995, Making continental crust: Nature, v. 378, p. 571–578.

Sandiford, M and McLaren, S 2002, Tectonic feedback and the ordering of heat producing elements within the continental lithosphere: Earth and Planetary Science Letters, v. 204, p. 133–150.

Sheppard, S, Bodorkos, S, Johnson, SP, Wingate, MTD and Kirkland, CL 2010b, The Paleoproterozoic Capricorn Orogeny: intracontinental reworking not continent–continent collision: Geological Survey of Western Australia, Report 108, 33p.

Sheppard, S, Johnson, SP, Wingate, MTD, Kirkland, CL and Pirajno, F 2010a, Explanatory Notes for the Gascoyne Province: Geological Survey of Western Australia, Perth, Western Australia, 336p.

Valley, JW 2003, Oxygen isotopes in zircon: Reviews in Mineralogy and Geochemistry, v. 53, p. 343–385.

Wingate, MTD 2003, Age and palaeomagnetism of dolerite intrusions of the Southeastern Collier Basin and the Earaheedy and Yerrida Basins, Western Australia: Geological Survey of Western Australia, Record 2003/3, 35p.

In situ phosphate dating of orogenic gold mineralization at Paulsens Mine, southern Pilbara

by

IOH Fielding[1], SP Johnson, J-W Zi[1], B Rasmussen[1], JR Muhling[1], DJ Dunkley[1], S Sheppard[1], MTD Wingate, and JR Rogers[2]

Paulsens is a mesothermal orogenic gold deposit situated on the southern margin of the Pilbara Craton in the northern Capricorn Orogen of Western Australia (Fig. 1) and is the only operational gold mine in the region. The mine is hosted within Archean rocks of the 2775–2629 Ma Fortescue Group in the northwestern part of the Wyloo Inlier (Thorne and Trendall, 2001) and is situated adjacent to the Hardey Fault, a splay of the crustal-scale Nanjilgardy Fault (Johnson et al., 2013) (Fig. 1). Regional-scale deformation is believed to be related to the 2215–2145 Ma Ophthalmia (Martin and Morris, 2010; Rasmussen et al., 2005) and 1820–1770 Ma Capricorn Orogenies (Tyler and Thorne, 1990). Despite its economic importance (total endowment of 1 114 000 ounces of gold) little is known about the absolute timing of gold mineralization. However, it has been considered to be associated with either the 1820–1770 Ma Capricorn Orogeny or synchronous with gold mineralization at Mt Olympus to the southeast, which has been dated at c. 1738 Ma (Şener et al., 2005). Understanding the relationships between the timing of gold mineralization, hydrothermal alteration, and the regional structural evolution will provide a more robust exploration model for the northern part of the Capricorn Orogen.

Ore deposit geology

Gold at Paulsens is hosted in a 40 m-wide quartz–sulfide vein that occurs within a folded and faulted gabbro sill, the c. 2701 Ma Paulsens mine gabbro (Fielding et al., in prep.) within the Hardey Formation of the Fortescue Group. The gold predominantly occurs along the margins of the quartz vein in two lodes termed Paulsens upper zone and Paulsens lower zone.

The two mineralized lodes have unique characteristics making them easy to differentiate (Fielding et al., in prep.). Upper zone mineralization has massive to brecciated pyrite. Visible gold is rarely present in hand specimens, although petrographic studies show that microscopic free gold is present in two distinct styles. Early gold forms as rounded inclusions up to 200 µm in size within the cores of massive pyrite crystals (Fig. 2a). This style of gold has silver contents ranging from 8 – 8.5 wt% and has a simple monocrystalline twinned microstructure (Hancock and Thorne, 2016). The second style of gold is located along the grain boundaries of fractured and brecciated pyrite (Fig. 2b) and represents either a local remobilization of pre-existing gold from the massive pyrite cores, or the introduction of new gold from a secondary hydrothermal event. This style of gold has a lower silver content of 6.6 – 7.2 wt% and has a simple monocrystalline microstructure and some twin planes, suggesting that they were not subject to any major deformation (Hancock and Thorne, 2016).

Lower zone mineralization is predominantly sulfide free, but contains abundant graphitic stylolites and wall rock inclusions of carbonaceous shale that form parallel to the vein margin giving it a laminated appearance (Fielding et al., in prep.). Abundant visible gold forms along the wallrock inclusions and graphitic stylolites. This style of gold is similar to the second phase of gold in the upper zone; it contains a silver content of 6.8 – 7.6 wt% and has a simple polycrystalline microstructure with both polysynthetic and incoherent twins (Hancock and Thorne, 2016).

Age of gold mineralization and hydrothermal activity

Euhedral xenotime crystals interlocking with massive pyrite (Fig. 2c) that contains rounded inclusions of gold were dated at 2403 ± 5 Ma (Fielding et al., in prep.). Additionally, in situ analysis of monazite from hydrothermally altered parts of the Paulsens mine gabbro adjacent to mineralization has been dated at 2398 ± 37 Ma, and monazite intergrown with white mica from highly altered sedimentary rocks surrounding other mineralized veins are dated at 2403 ± 38 Ma (Fig. 2d) (Fielding et al., in prep.). The c. 2400 Ma age is interpreted to date the timing of crystallization of the auriferous quartz–sulfide veins and hence the primary gold mineralizing event.

In areas where the pyrite has been brecciated by subsequent deformation, xenotime grains have undergone dissolution and reprecipitation reactions whereby primary

1 Department of Applied Geology, Curtin University, Kent Street, Bentley WA 6102

2 Northern Star Resources Ltd, Level 1, 388 Hay Street, Subiaco WA 6008

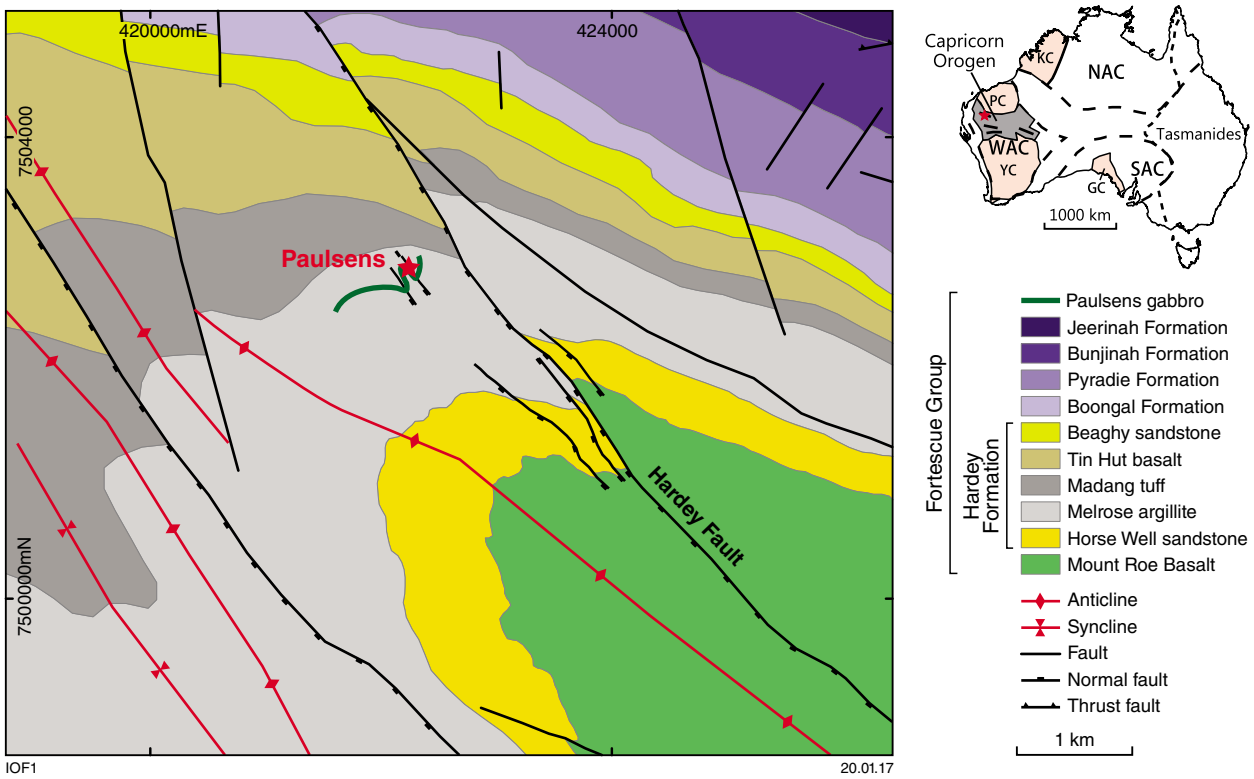

Figure 1. Local geology map showing the Paulsens gold mine in the northwestern part of the Wyloo Inlier and the stratigraphy of the Hardey Formation subdivided into five informal members. Abbreviations: GC, Gawler Craton; KC, Kimberley Craton; NAC, North Australian Craton; PC, Pilbara Craton; SAC, South Australian Craton; WAC, West Australian Craton; YC, Yilgarn Craton (after Fielding et al., in prep).

xenotime cores dated at c. 2403 Ma are surrounded by newly grown xenotime dated at 1680 ± 9 Ma (Fig. 2e) (Fielding et al., in prep.). Additionally, euhedral xenotime from a calcite vein associated with gold values of 48 ppm Au is dated at 1655 ± 37 Ma (Fielding et al., in prep.). The c. 1680 Ma age is interpreted to date the timing of deformation and hydrothermal activity associated with pyrite brecciation and the growth of secondary gold that forms along fractures and grain boundaries, as well as the emplacement of auriferous calcite veins. However, it is not certain if the gold has been remobilized locally from the massive pyrite grains during deformation or if the event represents the introduction of new gold during hydrothermal activity.

Additional hydrothermal activity in the region is recorded within two carbonaceous phyllites containing monazite–florencite porphyroblasts (Fig. 2f). Monazite within the porphyroblasts yielded dates of 1730 ± 28 Ma and 1721 ± 32 Ma (Fielding et al., in prep.) indicating hydrothermal activity at this time.

Regional-scale tectono-thermal activity

The ages obtained for the two main hydrothermal alteration and gold mineralizing events are intriguing as they do not correspond to any of the known tectono-thermal events in the northern Capricorn Orogen including the Ophthalmia and Capricorn Orogenies. However, they can be correlated to events elsewhere in the Pilbara Craton and Capricorn Orogen. At c. 2400 Ma widespread hydrothermal activity is recorded throughout the western Pilbara by the growth of monazite in low-grade phyllitic schists (Rasmussen et al., 2005), as well as by the resetting of high uranium zircons from tuffaceous mudstones of the Hamersley Group (Pickard, 2002). The growth of monazite–florencite porphyroblasts at c. 1730 Ma is coeval with the timing of gold mineralization and dextral strike slip faulting at the Mt Olympus deposit (Şener et al., 2005) to the southeast. The timing of gold mineralization, deformation and hydrothermal activity at c. 1680 Ma is synchronous with 1680–1620 Ma Mangaroon Orogeny that affected rocks of the Gascoyne Province farther to the south (Sheppard et al., 2005), and is synchronous with the growth of hydrothermal monazite and xenotime within crustal scale faults at Tom Price and the Soansville Group in the Pilbara Craton (Rasmussen et al., 2007a,b). These results suggest that lithospheric-scale faults such as the Nanjilgardy Fault, or their splays such as the Hardey Fault, were reactivated multiple times, each time acting as a conduit for potential mineralizing hydrothermal fluids.

At the Paulsens gold mine, two mineralizing events are defined at c. 2400 and 1680 Ma. With this knowledge, the exploration search area can be extended to include older rocks in the Pilbara region while focusing exploration efforts around major lithospheric-scale faults and their splays.

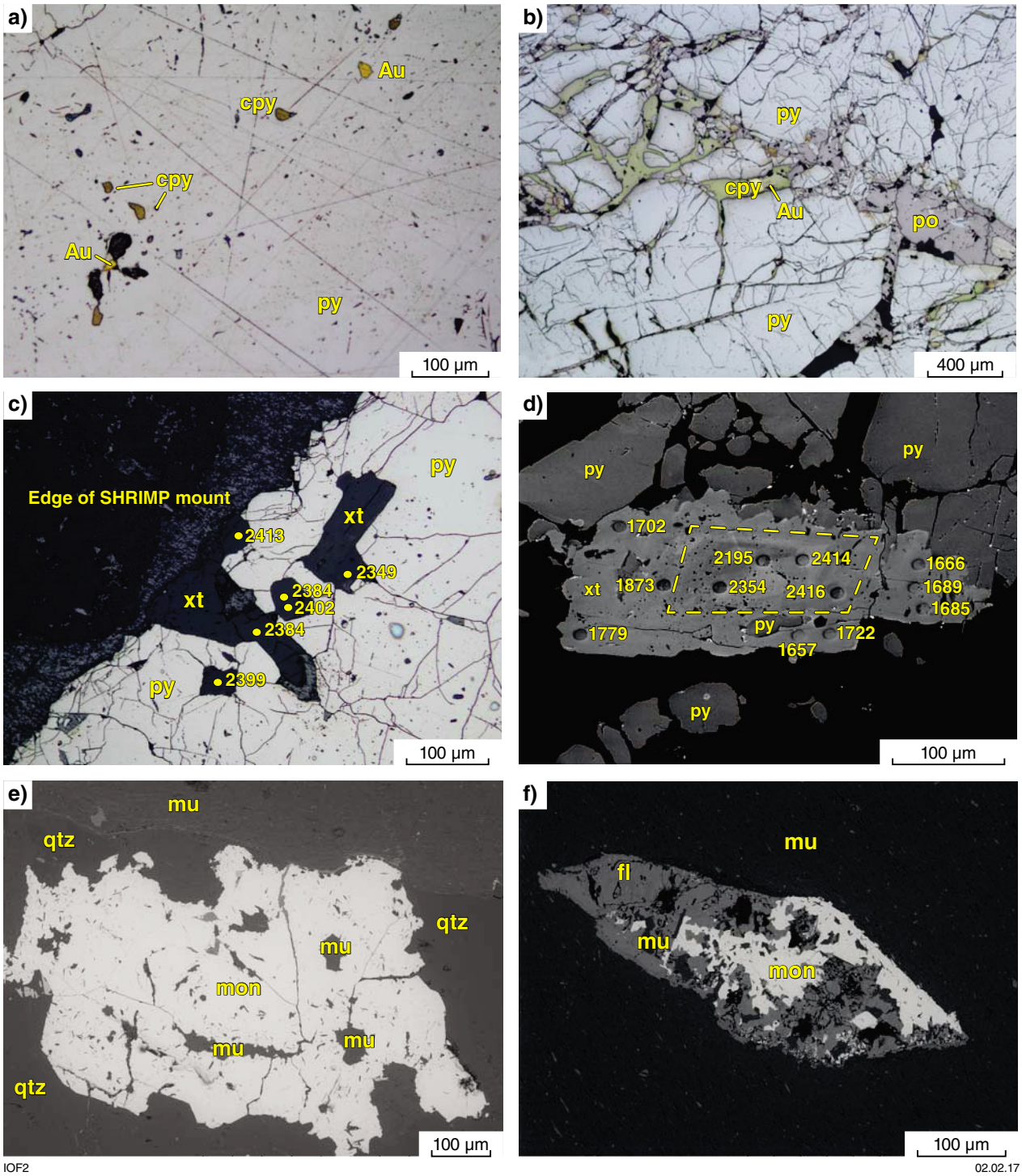

Figure 2. **a) Rounded inclusions of gold and chalcopyrite contained within pyrite; b) brecciated pyrite with free gold, chalcopyrite and pyrrhotite along the fractures; c) reflected light image (RFL) of interlocking crystals of euhedral xenotime and pyrite, SHRIMP analysis spots shown by yellow dots; d) high-contrast back scattered electron scanning microscope (BSE-SEM) images of subhedral xenotime crystals that have undergone dissolution and reprecipitation reactions resulting in c. 2400 Ma cores surrounded by newly grown c. 1680 Ma rims. The oval pits are SHRIMP analysis sites; e) BSE-SEM image of monazite intergrown with muscovite and quartz from the alteration zone surrounding a mineralized quartz vein; f) BSE-SEM image of monazite-florencite porphyroblasts within a carbonaceous phyllite. Abbreviations: Au, gold; cpy, chalcopyrite; fl, florencite; mon, monazite; mu, muscovite; po, pyrrhotite; py, pyrite; qtz, quartz and xt, xenotime**

Acknowledgements

This project is funded by an ARC Linkage grant (LP130100922) and Northern Star Resources Ltd. We acknowledge Northern Star Resources Ltd for supplying samples and for permission to publish.

References

Fielding, IOH, Johnson, SP, Zi, J-W, Rasmussen, B, Muhling, JR, Dunkley, DJ, Sheppard, S, Windgate, MTD and Rogers, JR in prep., Using in situ SHRIMP U–Pb monazite and xenotime geochronology to determine the age of orogenic gold mineralization: an example from the Paulsens mine, southern Pilbara Craton: Economic Geology.

Hancock, EA and Thorne, AM 2016, Mineralogy of gold from the Paulsens and Mount Olympus deposits, northern Capricorn Orogen: Geological Survey of Western Australia, Record 2016/14, 16p.

Johnson, SP, Thorne, AM, Tyler, IM, Korsch, RJ, Kennett, BLN, Cutten, HN, Goodwin, J, Blay, O, Blewett, RS, Joly, A, Dentith, MC, Aitken, ARA, Holzschuh, J, Salmon, M, Reading, A, Heinson, G, Boren, G, Ross, J, Costelloe, RD and Fomin, T 2013, Crustal architecture of the Capricorn Orogen, Western Australia and associated metallogeny: Australian Journal of Earth Sciences, v. 60, no. 6–7, p. 681–705.

Martin, DMcB and Morris, PA 2010, Tectonic setting and regional implications of ca 2.2 Ga mafic magmatism in the southern Hamersley Province, Western Australia. Australian: Journal of Earth Sciences, v. 57, no. 7, p. 911–931.

Pickard, AL 2002, SHRIMP U–Pb zircon ages of tuffaceous mudrocks in the Brockman Iron Formation of the Hamersley Range, Western Australia: Australian Journal of Earth Sciences, v. 49, no. 3, p. 491–507.

Rasmussen, B, Fletcher, IR and Muhling, JR 2007a, In situ U–Pb dating and element mapping of three generations of monazite: Unravelling cryptic tectonothermal events in low-grade terranes: Geochimica et Cosmochimica Acta, v. 71, no. 3, p. 670–690.

Rasmussen, B, Fletcher, IR, Muhling, JR, Thorne, W and Broadbent, GC 2007b, Prolonged history of episodic fluid flow in giant hematite ore bodies: Evidence from in situ U–Pb geochronology of hydrothermal xenotime: Earth and Planetary Science Letters, v. 258, no. 1–2, p. 249–259.

Rasmussen, B, Fletcher, IR and Sheppard, S 2005, Isotopic dating of the migration of a low-grade metamorphic front during orogenesis: Geology, v. 33, no. 10, p. 773–776.

Şener, AK, Young, C, Groves, DI, Krapez, B and Fletcher, IR 2005, Major orogenic gold episode associated with Cordilleran-style tectonics related to the assembly of Paleoproterozoic Australia?: Geology, v. 33, no. 3, p. 225–228.

Sheppard, S, Occhipinti, SA and Nelson, DR 2005, Intracontinental reworking in the Capricorn Orogen, Western Australia: the 1680–1620 Ma Mangaroon Orogeny: Australian Journal of Earth Sciences, v. 52, no. 3, p. 443–460.

Thorne, AM and Trendall, AF 2001, Geology of the Fortescue Group, Pilbara Craton, Western Australia: Geological Survey of Western Australia, Bulletin 144, 249p.

Tyler, IM and Thorne, AM 1990, The northern margin of the Capricorn Orogen, Western Australia—an example of an Early Proterozoic collision zone: Journal of Structural Geology, v. 12, no. 5–6, p. 685–701.

Making sense of the Eastern Goldfields stratigraphic story

by

MC De Paoli, J Sapkota, and S Wyche

Introduction

Since Woodall (1965) defined the first formal stratigraphy for the Kalgoorlie greenstones, various researchers, explorers and miners have used a plethora of names to describe the Archean geological units in the Eastern Goldfields. Local stratigraphic components shown on published 1:250 000- and 1:100 000-scale geological maps in the Eastern Goldfields region of the Archean Yilgarn Craton are based mainly on mapped outcrop distribution. As much of the geology is poorly exposed and deeply weathered, field relationships are difficult to establish in many places.

The Geological Survey of Western Australia (GSWA) is developing a seamless geological interpretation map of the Eastern Goldfields based on published mapping enhanced by new geochronological, geochemical and geophysical data. While there have been previous stratigraphic interpretations of Eastern Goldfields geology (e.g. Gemuts and Theron, 1975; Williams, 1976), this map will be the first synthesis of formal stratigraphy for the entire Eastern Goldfields region. The current project area (Fig. 1) extends between Leinster in the north and Norseman in the south. The first release, in 2014, covered the Lawlers and Coolgardie–Kambalda regions. Recent annual releases have included the Teutonic Bore, Leonora–Kookynie and Ora Banda – Siberia regions. The next release, in 2017, will include the geological interpretation around Menzies and Davyhurst.

Rationale

In current representations of Yilgarn Craton geology, the Eastern Goldfields Superterrane (Cassidy et al., 2006) constitutes the eastern part of the craton that is separated from the Youanmi Terrane to the west by a major crustal feature, which is evident in geophysical (Wyche et al., 2013) and isotopic (Wyche et al., 2012) data. This feature broadly coincides with a mapped structure, the Ida Fault (Fig. 1). The superterrane is bounded to the north by the Capricorn Orogen and to the south by the Albany–Fraser Orogen. Its eastern edge is covered by Phanerozoic rocks of the Canning Basin.

The Eastern Goldfields Superterrane is a structural entity that has been divided into fault-bounded tectono-stratigraphic terranes. The most widely published subdivision comprises four terranes: the Kalgoorlie, Kurnalpi, Burtville, and Yamarna Terranes (Fig. 1; Cassidy et al. 2006; Pawley et al., 2012). Terranes were defined on the basis of distinct lithological associations, geochemistry, and ages of volcanism (Swager, 1997). Other versions of the Eastern Goldfields terrane configuration (e.g. Barley et al., 2008) show different boundaries suggesting different lithological associations.

By analogy with other Archean cratons, the Yilgarn terrane model was interpreted to suggest that the present configuration of the Yilgarn Craton is a result of accretion of a number of pre-existing 'continents' in a series of collisional events between c. 2800 and 2650 Ma (e.g. Myers, 1995). With the completion of more comprehensive mapping over the region (Geological Survey of Western Australia, 2016b), and the acquisition of a substantial body of geochronological (e.g. Kositcin et al., 2008; Geological Survey of Western Australia, 2016a) and geochemical (e.g. Barnes et al., 2012; Geological Survey of Western Australia, 2016c) data, more complex evolutionary models that might involve rifting with or without accretion have been suggested (e.g. Czarnota et al., 2010; Barnes et al., 2012).

New geophysical, geochronological and geochemical data, combined with regional mapping programs, across the Yilgarn Craton, have highlighted problems and limitations with the terrane representation. There is a broad correspondence between the terranes and geochemical and stratigraphic associations, and isotopic data suggest different episodes of crust generation that also broadly correspond to the terranes (Wyche et al., 2012). However, there are many examples where clearly related lithological units transgress terrane boundaries.

The new geological interpretation incorporates formal stratigraphy (Fig. 2), which is described in detailed explanatory notes that are routinely prepared and published in the online GSWA Explanatory Notes System (ENS) database. Entries include type sections or areas, geochronological constraints and detailed lithological descriptions. All formally named units are registered in Geoscience Australia's Australian Stratigraphic Units Database. As the new interpretation proceeds, the new formal stratigraphy will more faithfully reflect the geology as seen on the ground.

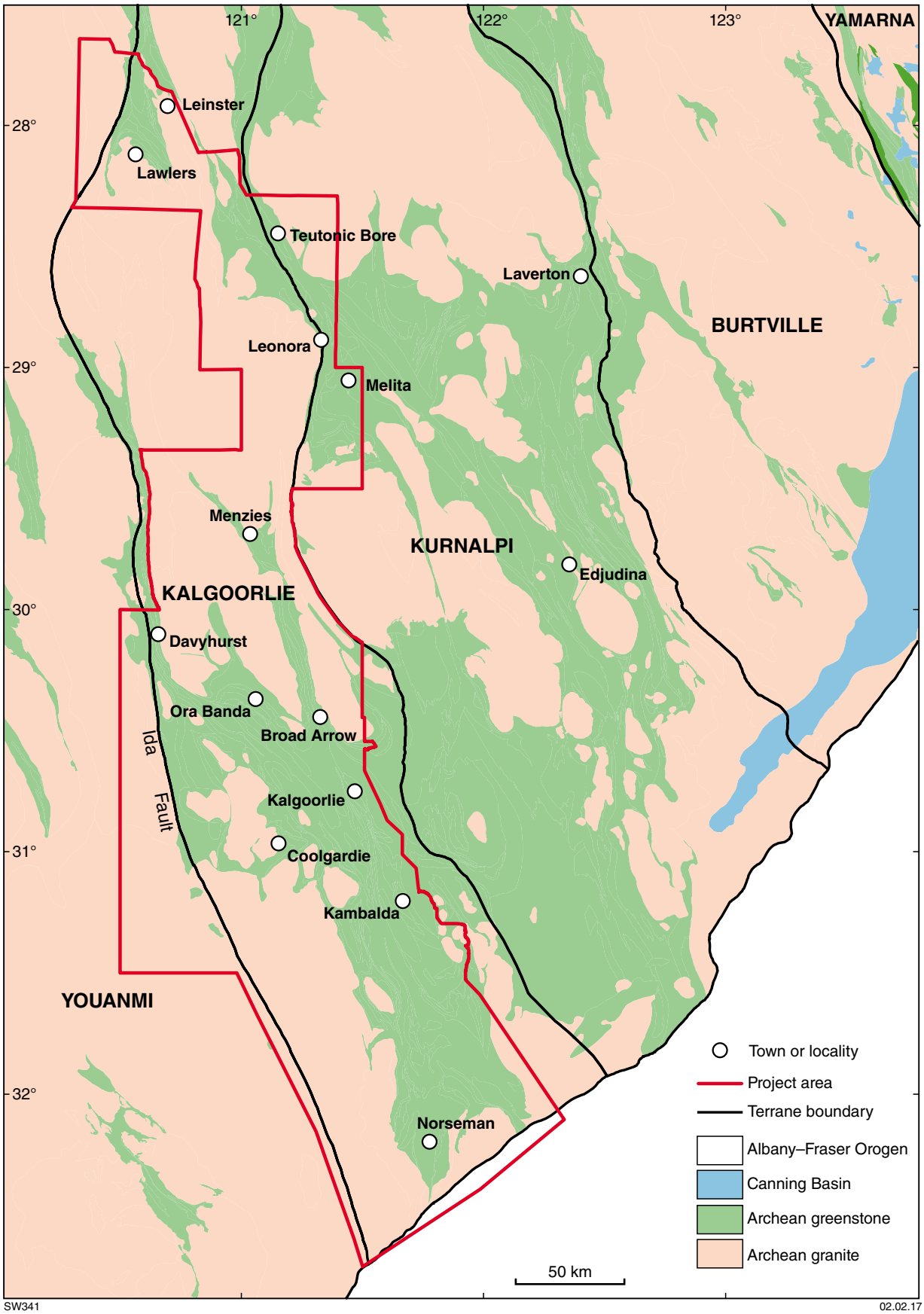

Figure 1. Current extent of the seamless geological bedrock interpretation over the Eastern Goldfields Superterrane

Eastern Goldfields stratigraphy

The current program involves interpretation of the western part of the Eastern Goldfields Superterrane between Norseman and Leinster (Fig. 1). Associations largely assigned to the Kalgoorlie Terrane form the Kalgoorlie, Black Flag and Mount White Groups. The Gindalbie Group, in the western part of the Kurnalpi Terrane of Cassidy et al. (2006) includes volcanic associations that Barley et al. (2008) assigned to their Gindalbie Terrane. Overlying siliciclastic successions, the 'late, syntectonic basins' of Swager (1997), have been distinguished as separate formations. It is likely that the Kalgoorlie, Black Flag, Mount White and Gindalbie Groups, along with other volcanic associations to the east and north within the Cassidy et al. (2006) Kalgoorlie and Kurnalpi Terranes will ultimately be assigned to an 'Eastern Goldfields Supergroup'.

Age constraints

Most mafic–ultramafic successions cannot be dated directly because of the lack of suitable minerals, typically zircon, for analysis. Thus age ranges for formations and their components are inferred from such things as maximum depositional ages of interbedded, overlying or underlying sedimentary rocks; intrusive rocks that can be dated such as granite or differentiated mafic sills; and ages of overlying or underlying felsic volcanic rocks that can also be dated.

Kalgoorlie Group

The Kalgoorlie Group (2726–2680 Ma), comprises most of the lower mafic–ultramafic package in greenstone belts between Norseman and Leinster. It locally overlies, or is structurally juxtaposed against, older (>2800 Ma) mafic–ultramafic successions such as the Trevors Bore Formation around Leonora and the Cock Robin Formation around Menzies. The various rock successions that form the greenstone belts within the Kalgoorlie Group are not physically continuous but they have similar stratigraphy and the same age range. Variations in detailed stratigraphy and the chemical character of stratigraphically equivalent units across major structures and between greenstone belts suggest that, although products of the same geological event, at least some of the successions may have been deposited in distinct basins. Where there are continuous successions, they have been distinguished as subgroups (Fig. 2). To date, the mapped subgroups include the Hannans (Kalgoorlie–Kambalda area), Coolgardie, Vetters (Ora Banda area), Broad Arrow, Marshall Pool (Teutonic Bore area) and Two Sisters Subgroups (Lawlers area). At Lawlers and Coolgardie, the typical Kalgoorlie Group succession appears to be underlain by a mafic–ultramafic succession with similar characteristics but there are presently no geochronological or geochemical constraints that allow this succession to be assigned to the Kalgoorlie Group.

The Kalgoorlie Group has been intruded by mafic–ultramafic sill complexes, such as the Bounty Igneous Complex near Lawlers and the Williamstown Dolerite near Kalgoorlie, at different stratigraphic levels.

Black Flag and Mount White Groups

The Black Flag Group (2692–2665 Ma), which comprises felsic and mafic volcanic and volcaniclastic rocks, overlies the Kalgoorlie Group in the Kalgoorlie–Coolgardie–Kambalda region. To the north, in the Lawlers region, the Mount White Group, which is similar to the Black Flag Group in lithofacies characteristics, age and stratigraphic relationships, is exposed in a syncline west of Leinster. Equivalent successions to the Black Flag Group have not been recognized in the Leonora area.

Both the Black Flag and Mount White Groups have been extensively intruded by mafic sills such as the Powder Gabbro that intrudes the Black Flag Group west of Kalgoorlie.

Gindalbie Group

The Gindalbie Group, which outcrops in volcanic centres at Melita and Teutonic Bore, comprises bimodal (basaltic to rhyolitic) and calc-alkaline volcanic successions with associated intrusive rocks and quartz-rich sedimentary rocks. It hosts volcanogenic massive sulfide mineralization at Teutonic Bore. Felsic volcanic rocks of the Gindalbie Group have been directly dated from a number of volcanic centres and range in age from c. 2694 to 2680 Ma.

Uppermost siliciclastic sequences

Siliciclastic and felsic volcaniclastic rocks that unconformably overlie the Mount White and Black Flag Groups include the Scotty Creek Formation (2662–2640 Ma) in the Lawlers region, the Pig Well Formation (2664–2662 Ma) to the east and southeast of Leonora, the Navajo Sandstone (2657–2640 Ma) southwest of Kalgoorlie, and the Merougil Formation (2664–2640 Ma) west of Kambalda.

The Kurrawang Formation (<2657 Ma) overlies the Black Flag Group and Navajo Sandstone west of Kalgoorlie along a low-angle unconformity. The lower part of the Kurrawang Formation has an exotic clast provenance represented by banded iron-formation, granite, gneiss, metasedimentary rocks and felsic volcanic rocks.

The future

The next stage of the program will see completion of interpretation of the successions between Norseman in the south and Wiluna, to the north of Leinster, that correspond to the area typically shown as the Kalgoorlie Terrane. Future interpretation to the east will embrace the region of relatively juvenile crust indicated in isotopic data (Wyche et al., 2012) that corresponds to the Kurnalpi Terrane.

GSWA is also acquiring a large amount of high-quality geochemical data, mainly derived from diamond drillholes where available. These data will be used to characterize various stratigraphic components and will provide fundamental constraints on tectonic models. The most comprehensive overview of Yilgarn granites is that of Cassidy et al. (2002). New geochemical, geophysical

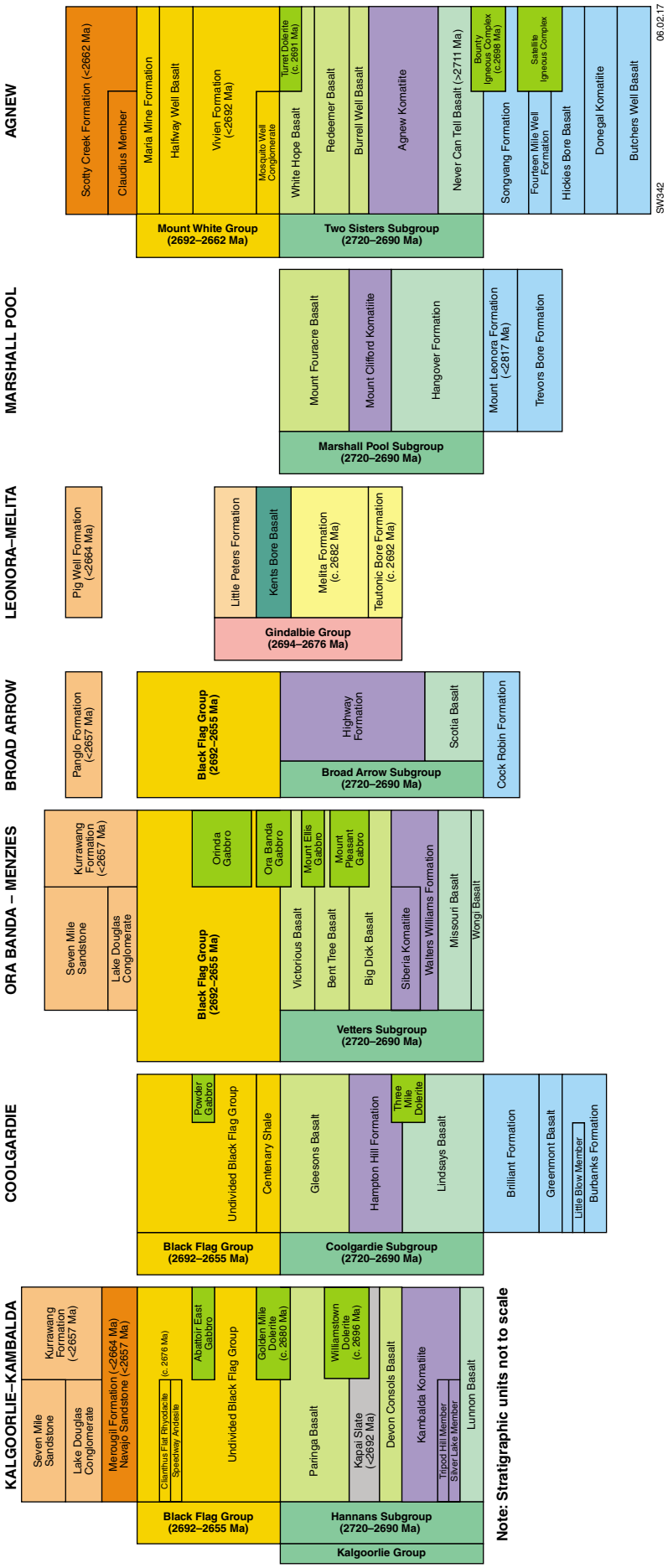

Figure 2. Formal stratigraphic associations between Kambalda and Leinster in the current release of the East Yilgarn seamless geology. The thickness of the stratigraphic units is not to scale.

and geochronological data are being used to implement a granite nomenclature scheme (Cassidy et al., 2002) that is consistent with formal stratigraphy across the craton.

References

Barley, ME, Brown, SJA, Krapež, B and Kositcin, N 2008, Physical volcanology and geochemistry of a Late Archaean volcanic arc: Kurnalpi and Gindalbie Terranes, Eastern Goldfields Superterrane, Western Australia: Precambrian Research, v. 161, p. 53–76.

Barnes, SJ, Van Kranendonk, MJ and Sonntag, I 2012, Geochemistry and tectonic setting of basalts from the Eastern Goldfields Superterrane, Yilgarn Craton: Australian Journal of Earth Sciences, v. 59, no. 5, p. 707–735.

Cassidy, KF, Champion, DC, Krapež, B, Barley, ME, Brown, SJA, Blewett, RS, Groenewald, PB and Tyler, IM 2006, A revised geological framework for the Yilgarn Craton, Western Australia: Geological Survey of Western Australia, Record 2006/8, 8p.

Cassidy, KF, Champion, DC, McNaughton, N, Fletcher, IR, Whitaker, AJ, Bastrakova, IV and Budd, A 2002, The characterisation and metallogenic significance of Archaean granitoids of the Yilgarn Craton, Western Australia: Minerals and Energy Research Institute of Western Australia (MERIWA), Project no. M281/AMIRA Project no. 482, Report no. 222 (unpublished).

Czarnota, K, Champion, DC, Cassidy, KF, Goscombe, B, Blewett, R, Henson, PA and Groenewald, PB 2010, Geodynamics of the eastern Yilgarn Craton: Precambrian Research, v. 183, p. 175–202.

Gemuts, I and Theron, A 1975, The Archaean between Coolgardie and Norseman — stratigraphy and mineralization, *in* Economic geology of Australia and Papua New Guinea, Volume 1. Metals *edited by* CL Knight: Australasian Institute of Mining and Metallurgy, Monograph 5, p. 66–74.

Geological Survey of Western Australia 2016a, Compilation of geochronology information, 2016: Geological Survey of Western Australia, Digital Data Package.

Geological Survey of Western Australia 2016b, East Yilgarn, 2016: Geological Survey of Western Australia, Geological Information Series.

Geological Survey of Western Australia 2016c, GeoChem Extract: Geochemistry database: Department of Mines and Petroleum, East Perth, Western Australia, <http://geochem.dmp.wa.gov.au/geochem/>.

Kositcin, N, Brown, SJA, Barley, ME, Krapež, B, Cassidy, KF and Champion, DC 2008, SHRIMP U–Pb zircon age constraints on the Late Archaean tectonostratigraphic architecture of the Eastern Goldfields Superterrane, Yilgarn Craton, Western Australia: Precambrian Research, v. 161, p. 5–33.

Myers, JS 1995, The generation and assembly of an Archaean supercontinent: evidence from the Yilgarn Craton, Western Australia, in Early Precambrian Processes edited by MP Coward and AC Reis: Geological Society, London, Special Publication 95, p. 143–154.

Pawley, MJ, Wingate, MTD, Kirkland, CL, Wyche, S, Hall, CE, Romano, SS and Doublier, MP 2012, Adding pieces to the puzzle: episodic crustal growth and a new terrane in the northeast Yilgarn Craton, Western Australia: Australian Journal of Earth Sciences, v. 59, no. 5, p. 603–623, doi:10.1080.08120099.2012.696555.

Swager, CP 1997, Tectono-stratigraphy of late Archaean greenstone terranes in the southern Eastern Goldfields, Western Australia: Precambrian Research, v. 83, p. 11–42.

Williams, IR 1976, Regional interpretation map of the Archaean geology of the southeast part of the Yilgarn Block (parts of SH51 and SI51): Geological Survey of Western Australia, 1:1 000 000 scale map.

Woodall, R 1965, Structure of the Kalgoorlie goldfield, *in* Geology of Australian Ore Deposits (2nd edition) *edited by* J McAndrew: 8th Commonwealth Mining and Metallurgical Congress, Australia and New Zealand, 1965; Publications 1, p. 71–79.

Wyche, S, Ivanic, TJ and Zibra, I (compilers) 2013, Youanmi and southern Carnarvon seismic and magnetotelluric (MT) workshop 2013: Geological Survey of Western Australia, Record 2013/6, 180p.

Wyche, S, Kirkland, CL, Riganti, A, Pawley, MJ, Belousova, E and Wingate, MTD 2012, Isotopic constraints on stratigraphy in the central and eastern Yilgarn Craton, Western Australia: Australian Journal of Earth Sciences, v. 59, no. 5 (Archean evolution — Yilgarn Craton), p. 657–670.

A hydrogeochemistry atlas for Western Australia

by

DJ Gray*

In collaboration with the Geological Survey of Western Australia (GSWA), CSIRO is undertaking the processing, modelling and interpretation of hydrogeochemical data from various sources (Fig. 1) for Western Australia. This will include results from soon-to-be-completed programs (Capricorn and Eucla; Fig. 1), and will be released as the Hydrogeochemical Atlas of Western Australia in 2018.

The Atlas will include:

- a summary of main data sources, QA/QC metadata (when known) and their availability
- description of data modelling techniques
- brief geological description of Western Australia (GSWA)
- discussion of Western Australian-relevant groundwater processes
- plots of various solutes and other variables, including
  - i. salinity and other environmental/health parameters
  - ii. individual elements, with their application to lithology (e.g. F) or exploration (e.g. U)
  - iii. major elements (Na, K, Mg, Ca, Sr, Rb, B, Cl, Br, SO_4), also plotted as various indices (e.g. Fig. 2) to emphasize geochemical trends (Gray et al., 2016)
  - iv. mineral saturation (e.g. gypsum, carnotite) as a guide to geochemical processes (Gray et al., 2016)
  - v. isotopes, particularly ^{2}H and ^{18}O, as a guide to aquifer processes.

  Each of these will be a double-page spread (e.g. Fig. 3), including an Australia-wide, and a Western Australia-wide distribution map, a discussion of the chemical parameter being mapped, and summary of implications.
- a geological modelling section, detailing the uses of the chemical data and some implications for Western Australia with regard to mineral exploration, health and environment.

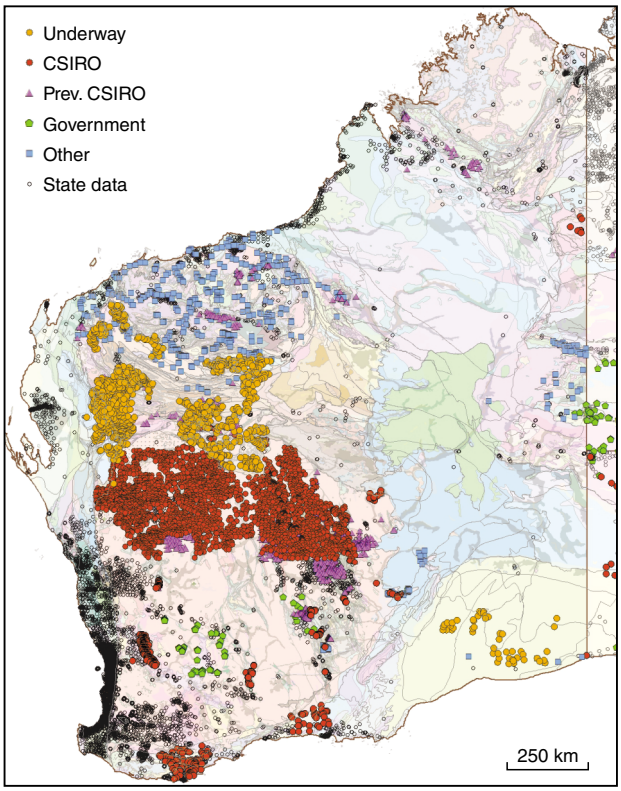

Figure 1. Hydrogeochemical datasets for Western Australia already identified, with the yellow dots showing the Capricorn and Eucla hydrogeochemical surveys still underway. Many of the data sources are listed in Bardwell and Gray (2016).

* Mineral Resources, CSIRO, 26 Dick Perry Ave, Kensington WA 6151

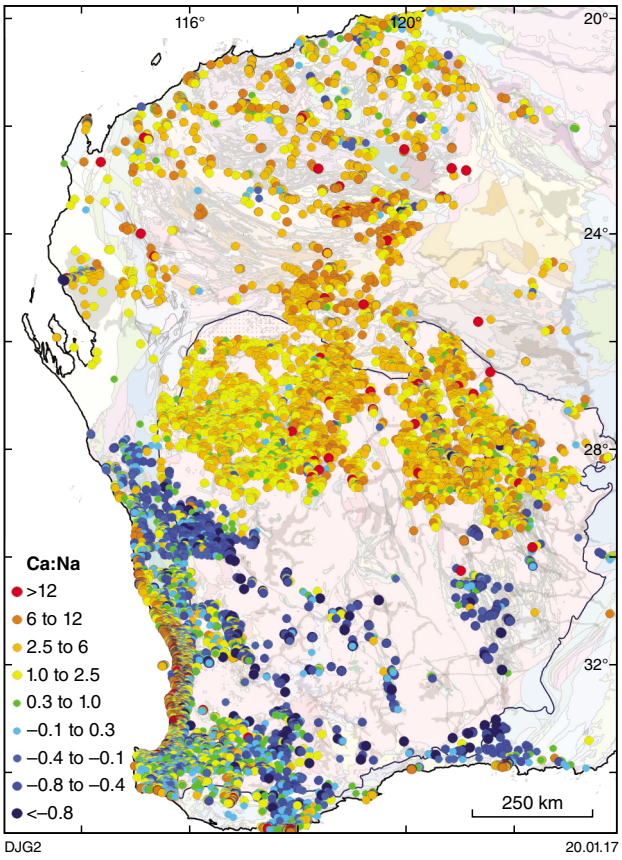

Figure 2. Example of the use of ion indices (in this case Ca:Na, for the Yilgarn and Pilbara) in lithological and regolith discrimination

There has been extensive groundwater sampling (>3000 samples) in the northern Yilgarn by CSIRO (Fig. 1; Gray et al., 2016), which is now being extended into the Capricorn Orogen. The northern Yilgarn data are available online (http://doi.org/10.4225/08/5756B35D5B217), along with other datasets. This initial research has demonstrated the utility of groundwater chemistry for lithological discrimination and prospectivity analysis for the northern Yilgarn Craton (Gray et al., 2016). It is presently being developed for other areas of Western Australia, including the Capricorn, Pilbara, Albany–Fraser and the Eucla (Fig. 1). As part of the Atlas, hydrogeochemistry will be used to demonstrate critical geochemical trends and boundaries across the State, correlated with established (and potentially new) geological transitions. Once resolved and understood, this should be a source of important geological information. Additionally, at the exploration scale, a regional understanding of groundwater 'baseline' chemistry would enable better resolution of hydrogeochemical anomalism.

Two major controlling factors in groundwater are salinity and pH. There is a broad saline zone across the south of Australia, from the southern part of Western Australia, through the southern half of South Australia, and into the SW Murray Basin. In Western Australia, this saline region is strongly correlated with low pH groundwaters, sitting south of the EW Menzies Line, a botanical, soil, and groundwater (Gray, 2001) division of the Yilgarn Craton. In these acid/salty groundwaters, base levels for various ion ratios differ from the north (e.g. Fig. 2), base metals, rare earth elements (REE) and U (which are highly soluble in these waters; Gray, 2001) have much higher background concentrations (Fig. 3), and oxyanions such as As and Mo (which have low solubility in acid groundwaters; Gray, 2001) will work poorly for prospecting using groundwater. Further delineating these processes will be critical to mapping anomalies and prospectivity mapping in these regions.

Ion ratios identify deviations from the seawater evaporation trend for ion pairs. For example, the Ca:Na index (Fig. 2) identifies the Eromanga Basin as a zone of low Ca:Na, although with internal differentiation. Critically, the saline groundwaters of the southern Yilgarn also have low Ca:Na, which is indicated to be an absolute Ca depletion (based on ion difference calculations; Bardwell and Gray, 2016). Many other ion indices show spatial patterns related to geology or landform effects (Gray et al., 2016), as will be demonstrated in the Atlas.

Mineral saturation analysis can complement these studies. There is high SO_4:Cl across much of central Australia. Where this correlates with waters at or near gypsum ($CaSO_4.H_2O$) saturation (Bardwell and Gray, 2016), this suggests S dissolving into the groundwaters, probably from gypsum beds. In contrast, the southern Yilgarn groundwaters are saline, with low SO_4:Cl, low Ca:Na (Fig. 2), and close to gypsum saturation. This suggests that salinization via evaporation is precipitating gypsum, with reduced dissolved Ca and SO_4.

Where present, minor and trace element data can be particularly useful in lithological discrimination and prospectivity analysis. Albany–Fraser rocks around Esperance show high dissolved F, and in the northern Yilgarn Craton, there is a correlation of relatively higher dissolved F with granitic rocks. Dissolved U is higher in granitic rocks, whereas mafic–ultramafic elements such as Cr and Ni can effectively discriminate more basic rocks.

Dissolved U can reach particularly high concentrations (>100 µg/L) in specific areas of the Yilgarn Craton and elsewhere in Australia such as the Curnamona Basin (Fig. 3; de Caritat et al., 2005), reflecting active and potential secondary U deposits in these regions. Other elements such as Mo are high sporadically across the Yilgarn Craton and in specific regions, such as the western Olary and the Stuart Shelf in South Australia. Such data for varying elements such as As and W may become useful for lithological discrimination and detection of hydrothermal dispersion (e.g. Gray et al., 2016).

Additionally, delineation of salinity can be important for agricultural use of groundwater, and better discriminating areas with high levels of solutes of health concern, such as NO_3, may be important for remote communities.

This brief introduction to the Atlas is to indicate the potential of this publication. This will also be followed up through meetings and workshops, presentations in industry and scientific conferences, and through related publications.

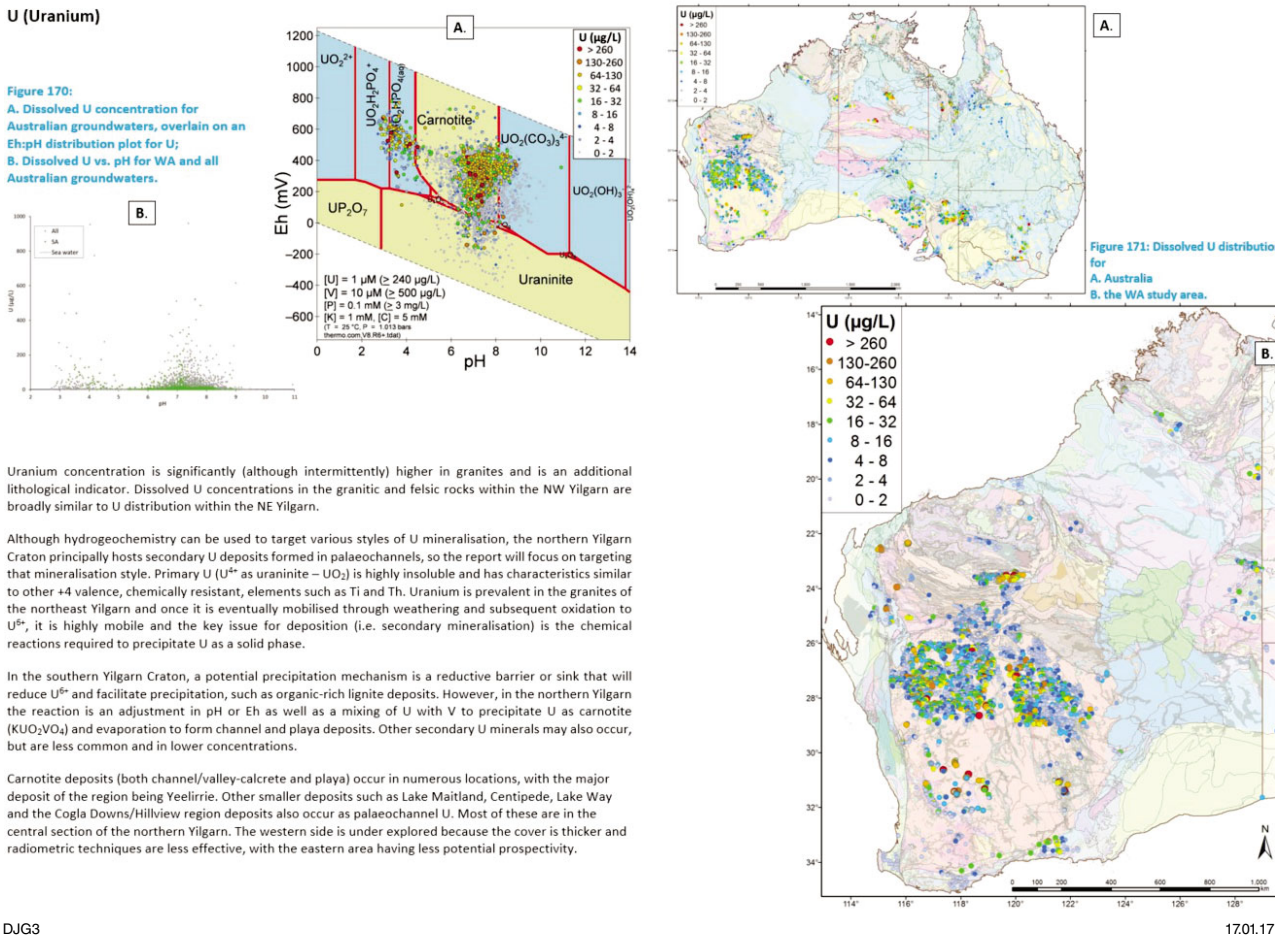

Figure 3. Example of a double-page spread from the Hydrogeochemical Atlas (describing U chemistry and distribution). Note that this will include additional data from Capricorn, Eucla and elsewhere in the final version.

References

Bardwell, N and Gray, DJ 2016, Hydrogeochemistry of Western Australia, data release: Accompanying Notes: EP156404 CSIRO, Australia, 33p.

de Caritat, P, Kirste, D, Carr, G and McCulloch, M 2005, Ground water in the Broken Hill region, Australia; recognising interaction with bedrock and mineralization using S, Sr and Pb isotopes: Applied Geochemistry: 20, p. 767–787.

Gray, DJ 2001, Hydrogeochemistry in the Yilgarn Craton, Geochemistry: Exploration, Environment, Analysis, vol. 1, p. 253–264.

Gray, DJ, Noble RRP, Reid, N, Sutton, GJ and Pirlo, MC 2016, Regional scale hydrogeochemical mapping of the northern Yilgarn Craton, Western Australia: A new technology for exploration in arid Australia, Geochemistry: Exploration, Environment, Analysis, 16, p. 100–115.

Regolith and spinifex chemistry from the Ngururrpa area, northeastern Western Australia

by

PA Morris

Introduction

In areas of extensive regolith cover with few bedrock outcrops, detecting the surface location and subsurface orientation of faults usually relies on geophysical and drillhole data. Faults are a key component in mineral exploration in terms of providing both a migratory pathway and focusing mechanism for mineralizing fluids (e.g. McCuaig and Hronsky, 2014). However, even when fault location and morphology are known, whether the fault is a conduit for mineralizing fluids relies on a number of factors, including its age and movement history (e.g. Johnson et al., 2013). The chemistry of the fine fraction of regolith, and spinifex from two transects across a regional fault in a regolith-dominated area of northeastern Western Australia has been used to better constrain the fault position and provide evidence of a fault-controlled fluid. The fine fraction of regolith (in particular the clay fraction) has a propensity to either weakly bond or adsorb ions held in solution, whereas plant roots can take up elements by either cation exchange or diffusion from soil water (Hawkes and Webb, 1962; Dunn, 2007).

Regional geology and sampling transects

The Ngururrpa area of northeastern Western Australia, which is underlain by quartz-rich siliciclastic sedimentary rocks of the Murraba and Canning Basins (Fig. 1), has about 90% regolith cover. The Stansmore Fault bisects the Ngururrpa area, and has a long history of activity, displacing the Proterozoic basement and being periodically active during deposition of Canning Basin sediments. Recent regolith mapping shows possible Cenozoic fault activity. Regolith samples have been collected along two transects across the Stansmore Fault (Fig. 1), and spinifex samples have been collected along one of these transects.

Transect chemistry

The <50 µm fraction of regolith and the ashed component of spinifex were analysed by inductively coupled plasma (ICP) spectrometry following acid digestion.

SRT transect

On this transect (Fig. 1), the Stansmore Fault separates quartz-rich rocks of the Liveringa Group and undivided Mesozoic sedimentary rocks of the Canning Basin. Ten regolith samples were collected along a 3.5 km transect. Sample SRT10, coincident with the Stansmore Fault trace (Fig. 2a), has notably high concentrations of rare earth elements (REE; La and Y) and fluid-mobile elements such as Li, Tl and Cs (not shown), and Zn. Fluid-immobile elements, such as the high field strength elements Nb and Zr, are not unusually enriched in regolith close to the Stansmore Fault, and transect chemistry shows no compositional differences attributable to bedrock.

SR transect

Regolith and spinifex were collected from 12 sites along a 16 km transect across the Stansmore Fault. The transect takes in the Liveringa Group and an upfaulted block of Noonkanbah Formation, bounded to the east by the Stansmore Fault, and to the west by an unnamed fault. Heritage issues prevented collecting regularly spaced samples, including on the inferred trace of the Stansmore Fault. The highest concentrations of La and Y in regolith are in sample SR9, about 900 m east of the inferred Stansmore Fault trace (Fig. 2b). Unlike regolith samples from the SRT transect, fluid-mobile elements in regolith, such as Li, show no positive expression in this sample. However, spinifex from SR9 shows a strong positive response for fluid-mobile elements such as Li and B, as well as Zn and REE. Boron, Li, and Zn also show elevated concentrations in spinifex from SR14, which is coincident with the unnamed fault in the western part of the transect.

Discussion

The behavior of low ionic potential elements such as Li in the fine fraction of regolith (SRT transect) and Li and B in spinifex (SR transect) has the potential to locate fault traces accurately. Both Zn and the REE are less fluid mobile, yet they are in relatively high concentrations in samples of regolith and/or spinifex close to faults. The high concentrations of Zn in spinifex could be explained by preferential uptake, as Zn is an essential element for plant metabolism (Dunn, 2007).

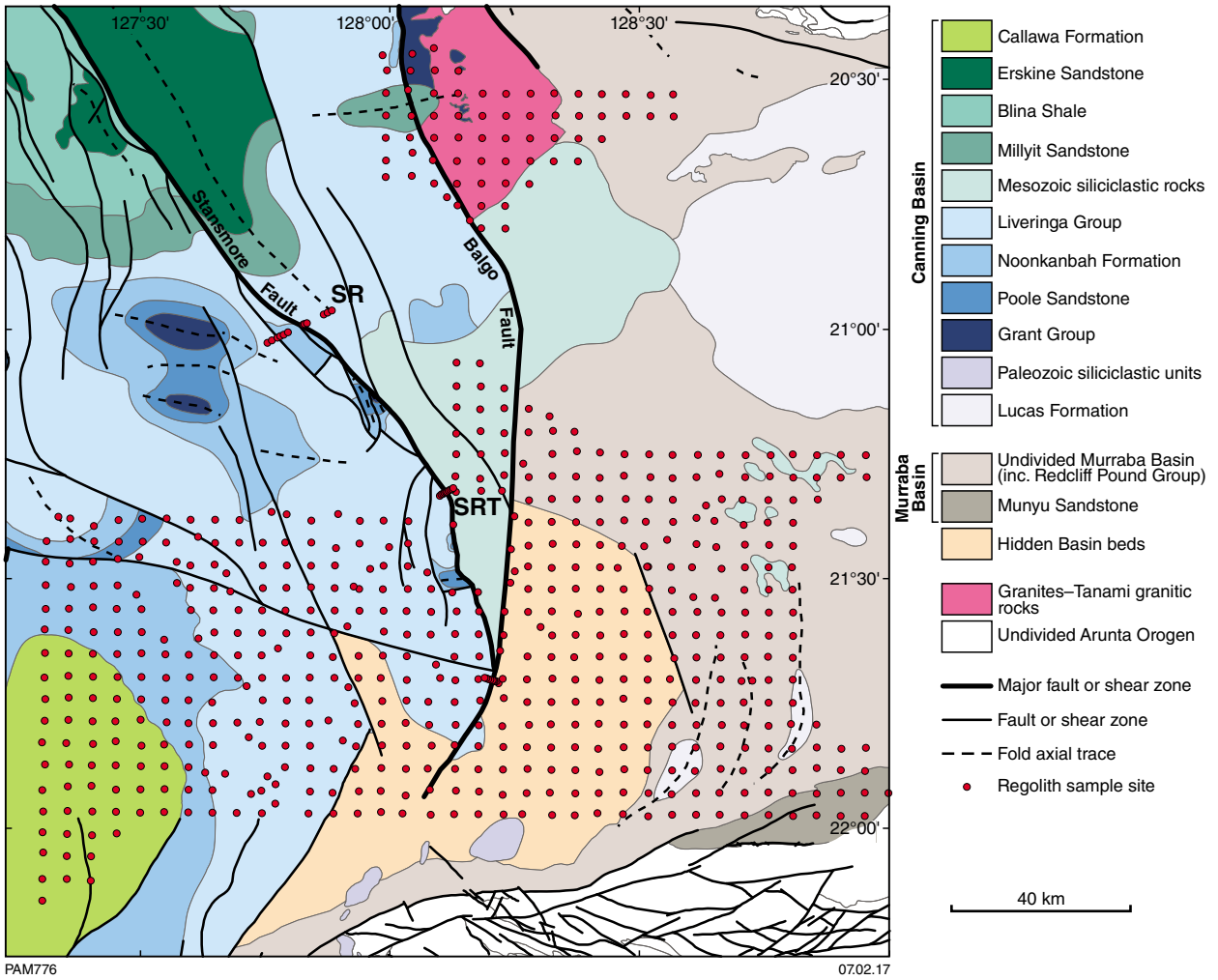

Figure 1. 1:500 000 interpreted bedrock geology (GSWA, 2016) of the Ngururrpa program area, showing the location of the two transects over the Stansmore Fault

However, regolith coincident with the Stansmore Fault on the SRT transect has the highest Zn content from the Ngururrpa program (70 ppm), and it is likely that this is a reflection of the fault-controlled fluid. The REE are not essential for plant health, but are similar to Zn, and sample SRT10 has elevated REE (Fig. 2a), which is also likely to be a characteristic of the fault-controlled fluid.

References

Dunn, CE 2007, Biogeochemistry in Mineral Exploration: Handbook of Exploration and Environmental Geochemistry, Volume 9, 480p.

Geological Survey of Western Australia 2016, 1:500 000 State interpreted bedrock geology of Western Australia, 2016: Geological Survey of Western Australia, <www.dmp.wa.gov.au/geoview>.

Hawkes, HE and Webb, JS 1962, Geochemistry in Mineral Exploration: Harper and Row, New York, 415p.

Johnson, SP, Thorne, AM, Tyler, IM, Korsch, RJ, Kennett, BLN, Cutten, HN, Goodwin, J, Blay, OA, Blewett, RS, Joly, A, Dentith, MC, Aitken, ARA, Holzschuh, J, Salmon, M, Reading, A, Heinson, G, Boren, G, Ross, J, Costelloe, RD and Fomin, T 2013, Crustal architecture of the Capricorn Orogen, Western Australia and associated metallogeny: Australian Journal of Earth Sciences, v. 60, no. 6–7, p. 681–705, doi:10.1080/08120099.2013.826735.

McCuaig, TC and Hronsky, JMA 2014, The mineral system concept: the key to exploration targeting, *in* Building Exploration Capability for the 21st Century *edited by* KD Kelley and HC Golden: Society of Economic Geologists, Inc., Special Publication Number 18, p. 153–175.

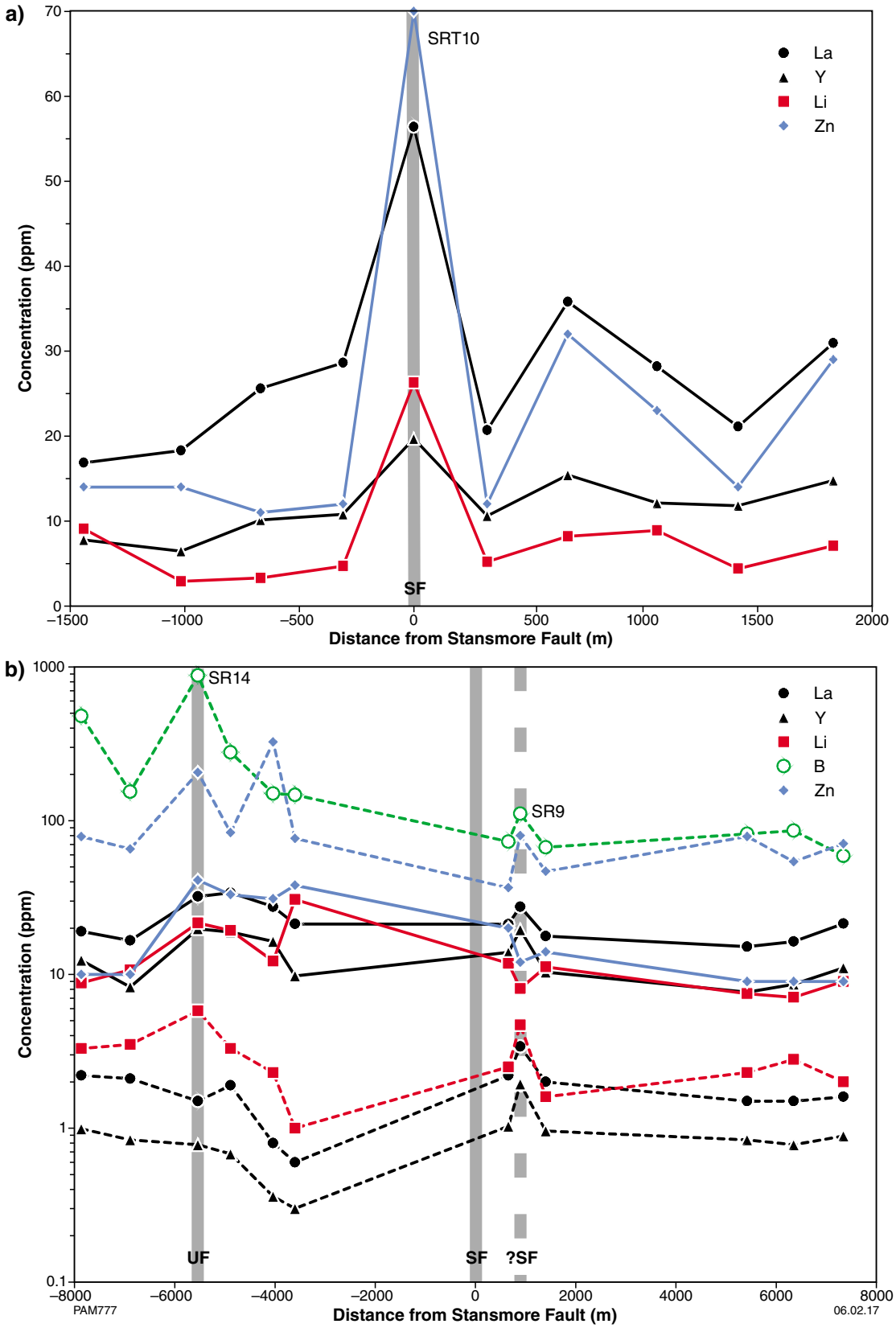

Figure 2. Chemistry of regolith and/or spinifex samples along two transects over the mapped trace of the Stansmore Fault. All values in ppm. X axis is distance (metres) from the Stansmore Fault (SF). Solid lines – regolith; dotted lines – spinifex. a) SRT transect; b) SR transect. UF is an unnamed fault separating the Liveringa Group and Noonkanbah Formation and ?SF is the possible location of the Stansmore Fault based on regolith and spinifex chemistry. Samples from particular locations on each transect (SRT10, SR9, SR14) are shown.

Digging up the dirt on Western Australian coal exploration, northern Perth Basin

by

AS Millar

The first reported coal discovered by Europeans in Western Australia was in the Irwin River by explorers A and FT Gregory in September 1846 (Le Blanc Smith and Mory, 1995) within what is now known as the Permian Irwin River Coal Measures. Thin seams of Permian coal were also intersected in the Irwin River Coal Measures in drillholes located on the Beagle Ridge (MacTavish, 1965; Romanoff and Shepherd, 1974). Discussion of the exploration of these Permian coals will be covered in a separate Record which is anticipated to be published in 2017. This extended abstract covers the discovery, exploration, evaluation and basic geology of the coal within the Mesozoic of the northern Perth Basin and is part of an ongoing project to document the coal resources of Western Australia.

Early exploration

Mesozoic coal was first intersected in petroleum exploration well Eneabba 1, drilled by West Australian Petroleum Pty Ltd (WAPET) in 1961 (Pudovskis, 1962) (Fig. 1). The section was not cored and was interpreted from basic wireline logs as containing 11.5 m of coal in five seams ranging from 1 to 3.3 m in thickness within the interval 1942.5 – 1963.2 m. The coal was considered high quality with weak coking properties which encouraged WAPET to explore known outcrops of the 'Cockleshell Gully Formation' in the Hill River area. WAPET completed two programs of stratigraphic and shallow test drilling; however, final results indicated the shallow coal was of poor quality and structurally complex, prompting WAPET to withdraw from the program in late 1963. No further exploration occurred in the area until the early 1970s, following the discovery of shallow coal in a water bore near Eneabba and a reinvestigation in the late 1970s and early 1980s of the areas previously explored by WAPET to the south in the Gairdner Range and Hill River areas. Exploration targeting coal on the Greenough Shelf farther north commenced in 1980 following the reporting of Jurassic coal in petroleum well Bookara 3 drilled by WAPET in 1967 (Bowering, 1967).

Eneabba

Gold Fields Exploration Pty Ltd (GFEL) completed an extensive evaluation program at Eneabba during the early 1980s. By the end of November 1981, GFEL had drilled at total of 14 550 m in 139 holes in and immediately around the defined coal area. The drilling density was considered sufficient for seam correlation, structure definition for 'reserve calculation' purposes, and for analytical testing. The deposit was estimated to contain about 153 Mt of coal to a maximum depth of 195 m or 123 Mt to a depth of 130 m (Morgan, 1981).

In 2004 Aviva Corporation purchased the now-named Central West Coal project and recommenced an evaluation program. In 2007, Aviva announced total Coal Reserves (JORC, 2004) of 72 Mt within a 130 m deep pit at strip ratio of 7.2 m^3/run-of-mine (ROM) tonne. The resource was updated in 2008 with Aviva reporting a resource (JORC, 2004) calculated to a depth of 130 m to the floor of the Eneabba Main Seam (EMS) split G of 89.3 Mt total Coal Resources (McElroy Bryan Geological Services Pty Ltd, 2008). In April 2009 Aviva released the project Public Environmental Review (PER) documents for public review. In October 2009 Synergy informed Aviva that it was not the preferred tenderer for the 2009 electricity supply procurement program, hence removing the potential market for electricity produced from the Coolimba Power Project associated with any mine development. In February 2011 the Environmental Protection Authority (EPA) recommended that the Minister for Environment not approve the Central West Coal Pty Ltd proposal to mine and supply coal to the proposed Coolimba Power Project.

Gairdner Range – Cowla Peak – Brazier

Numerous exploration companies explored the broader area during the late 1970s and 1980s resulting in only one other major discovery in the Gairdner Range – Cowla Peak – Brazier area south of the defined Eneabba Deposit. This project was formed from a number of joint ventures and led by the then CRA Exploration which estimated a non-JORC resource in excess of 500 Mt of coal over five adjacent deposits, of which about 90 Mt was considered to be extractable by opencut mining. The project was taken through a full evaluation process from 1988 to 1991. Approximately half of the identified resource (Compston, 2002) now lies within the boundaries of the Mt Lesueur National Park which was gazetted in 1992. The main coal deposits remain under title; however, little additional technical work has been completed.

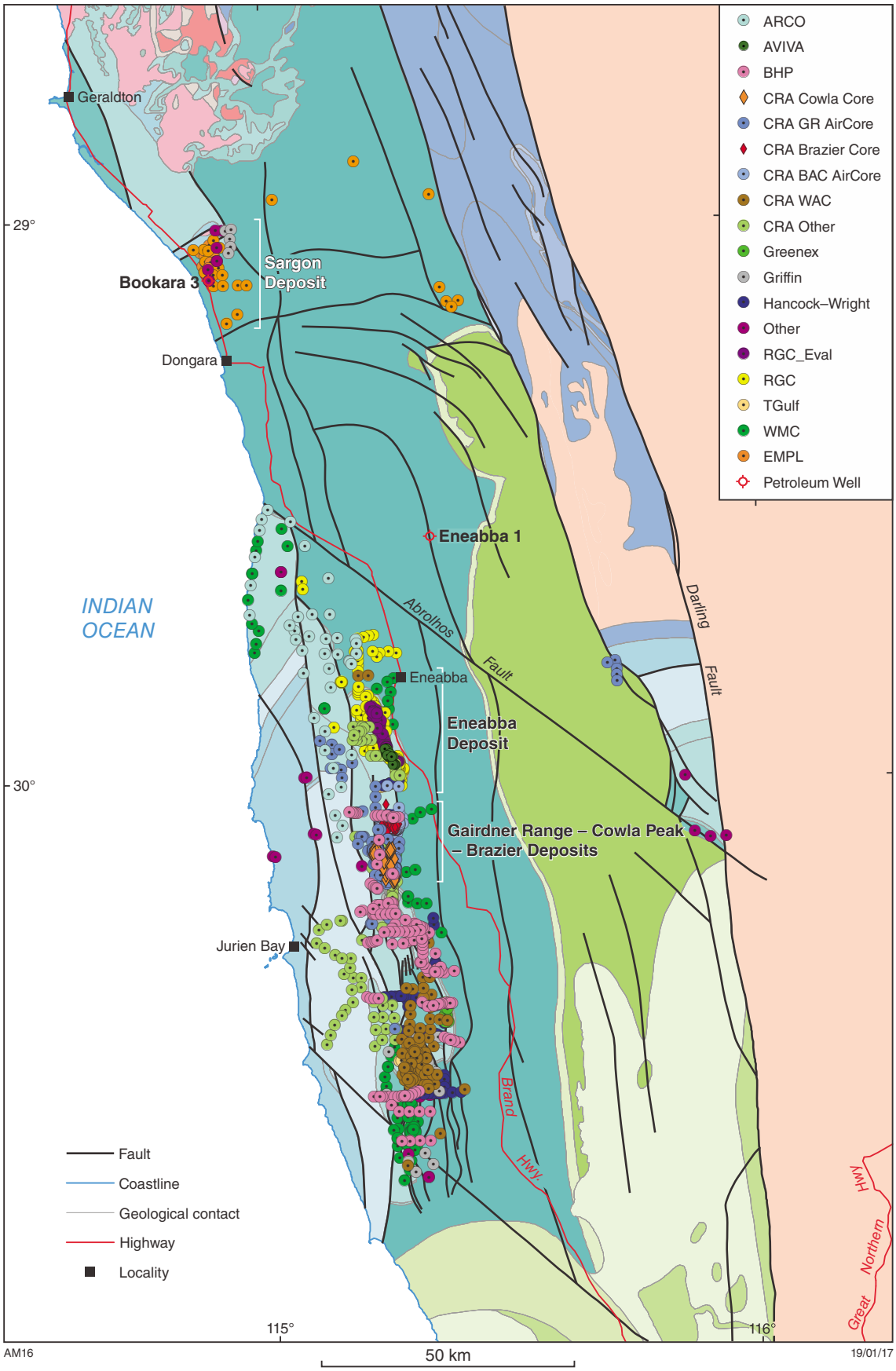

Figure 1. Location of drillholes targeting Mesozoic coal in the northern Perth Basin, coloured by company and main drilling method. Background image 1:500 000 geology (GSWA, 2016)

Bookara

Exploration for coal on the Greenough Shelf in the Bookara area was initiated in the early 1980s with limited economic success. In 2004 Eneabba Gas Limited commenced exploration for coal seam methane (CSM) on their Sargon Project. Initial results from this program indicated that coal rank was low and that the gas content was very low to non-existent. The project then changed to targeting coal suitable for Underground Coal Gasification (UCG). By 2008 the company had completed an evaluation program allowing them to define a coal resource suitable for UCG, resulting in the reporting of a total Coal Resource of 194 Mt, which was revised up to 205 Mt in 2012 (Eneabba Gas Ltd, 2012; Westblade, 2013) under the now superseded 2004 JORC Code (JORC, 2004, 2012).

Geology

All of the defined Mesozoic coal resources are located on the Greenough Shelf and Cadda Terrace and almost all of the coal exploration has been within these structural units and the adjacent Beagle Ridge, with only minor targeted coal exploration elsewhere.

The Cattamarra Coal Measures is the principal coal-bearing unit within the Mesozoic of the northern Perth Basin. Originally named the 'Cattamarra Coal Member' for the coal-bearing unit within the Lower Jurassic 'Cockleshell Gully Formation', the name 'Cockleshell Gully Formation' was abandoned and formally replaced with the Cattamarra Coal Measures and the Eneabba Formation by Mory (1994a,b). However, the use of the abandoned terminology persists in some reporting and the historical 'Cockleshell Gully Formation' is not subdivided in most old reports.

The Cattamarra Coal Measures consists of fine- to coarse-grained sandstone interbedded with carbonaceous mudstone and seams of coal (Kristensen, 1983). Based on detailed lithotype, microlithotype and maceral analyses at the Gairdner Range – Cowla Peak – Brazier Deposit, the depositional environment is interpreted as a telmatic wet forest swamp of a brackish to upper–lower delta plain (Suwarna, 1993, 1999). Trace element analysis, palynology, the common association of bioturbation of sediments, and elevated organic sulfur levels in the coal indicate a marine influence during peat deposition.

Coal rank varies throughout the deposits, generally in the range of sub-bituminous B to sub-bituminous A (ASTM classification) with some areas of the Gairdner block of Gairdner Range – Cowla Peak – Brazier Deposit reaching high-volatile bituminous C (Kristensen, 1991). The coals are high in vitrinite and inertinite and typically low in liptinite. Vitrinite reflectance values range from 0.3% at Bookara and Eneabba up to 0.5% for the Gairdner Range – Cowla Peak – Brazier Deposit. Figure 2 is a combined plot of short spaced density (uncalibrated) and caliper logs alongside a simplified coal lithology log with summary coal quality data for the main seam (Seam G) for drillhole CPCH 23, Gairdner Range – Cowla Peak – Brazier Deposit (Park, 1987; Kristensen, 1991).

References

Bowering, OJW 1967, Bookara No.3 Stratigraphic Well, Northern Perth Basin. Well Completion Report; West Australian Petroleum Pty Ltd: Geological Survey of Western Australia, Statutory petroleum exploration report, W 385 A1.

Compston, DM 2002, Combined Annual Report, M70/381, M70/382, M70/383, M70/490, M70/491, M70/492, M70/543, M70/639, c71/1999 for the period 8 May 2001 – 7 May 2002; Australian Gold Resources Ltd: Geological Survey of Western Australia, Statutory mineral exploration report, A65371.

Eneabba Gas Ltd 2012, Coal Resource on Sargon Tenements increased to 205 million tonnes: Report to ASX, 27 November 2012.

Geological Survey of Western Australia 2016, 1:500 000 State interpreted bedrock geology of Western Australia, digital data layer, <www.dmp.wa.gov.au/geoview>.

JORC 2004, Australasian Code for Reporting of Exploration Results, Mineral Resources and Ore Reserves (The JORC Code): The Joint Ore Reserves Committee of The Australasian Institute of Mining and Metallurgy, Australian Institute of Geoscientists and Minerals Council of Australia.

JORC 2012, Australasian Code for Reporting of Exploration Results, Mineral Resources and Ore Reserves (The JORC Code): The Joint Ore Reserves Committee of The Australasian Institute of Mining and Metallurgy, Australian Institute of Geoscientists and Minerals Council of Australia.

Kristensen, S 1983, Annual Report for 1982 on Coal Mining Leases 70/2284-91, 70/3980-89, 70/4047-78, Cowla Peak Coal Prospect, Hill River, Western Australia. Report 11924; CRA Exploration Pty Ltd: Geological Survey of Western Australia, Statutory mineral exploration report, A36063.

Kristensen, SE 1991, Annual Report for 1990 on the Hill River Project - Group 1 Tenements. Report 17170; CRA Exploration Pty Ltd: Geological Survey of Western Australia, Statutory mineral exploration report, A36318.

Le Blanc Smith, G and Mory, AJ 1995, Geology and Permian coal resources of the Irwin Terrace, Perth Basin, Western Australia: Geological Survey of Western Australia, Report 44, 60p.

MacTavish, RA 1965, Completion Report BMR 10 and 10A, Beagle Ridge, Western Australia: Bureau of Mineral Resources, Geology and Geophysics 80.

McElroy Bryan Geological Services Pty Ltd 2008, Statement of Coal Resources, Central West Coal Project, Western Australia. Prepared for Aviva Corporation Ltd. Appendix 1; Aviva Corporation Ltd: Geological Survey of Western Australia, Statutory mineral exploration report, A82840.

Morgan, AM 1981, Eneabba Coal Project, Geology and Reserves, November 1981; Gold Fields Exploration Pty Ltd: Geological Survey of Western Australia, Statutory mineral exploration report, A36032.

Mory, AJ 1994a, Geology of the Arrowsmith – Beagle Islands 1:100 000 sheet: Geological Survey of Western Australia, 1:100 000 Geological Series Explanatory Notes, 26p.

Mory, AJ 1994b, Geology of the Hill River –– Green Head 1:100 000 sheet: Geological Survey of Western Australia, 1:100 000 Geological Series Explanatory Notes, 29p.

Park, WJ 1987, Annual Report for 1986 on 70/2284-2291, 3980-3989, 4047-4050, 4052-4054, 4060, 4061, 4064-4068, ELA 70/236, Cowla Peak, Hill River, SH-50-09, Western Australia. Repot No. 14402; CRA Exploration: Geological Survey of Western Australia, Statutory mineral exploration report, A36067.

Pudovskis, V 1962, Eneabba No.1 Well Completion Report; West Australian Petroleum Pty Ltd: Geological Survey of Western Australia, Statutory petroleum exploration report, W 34 A2.

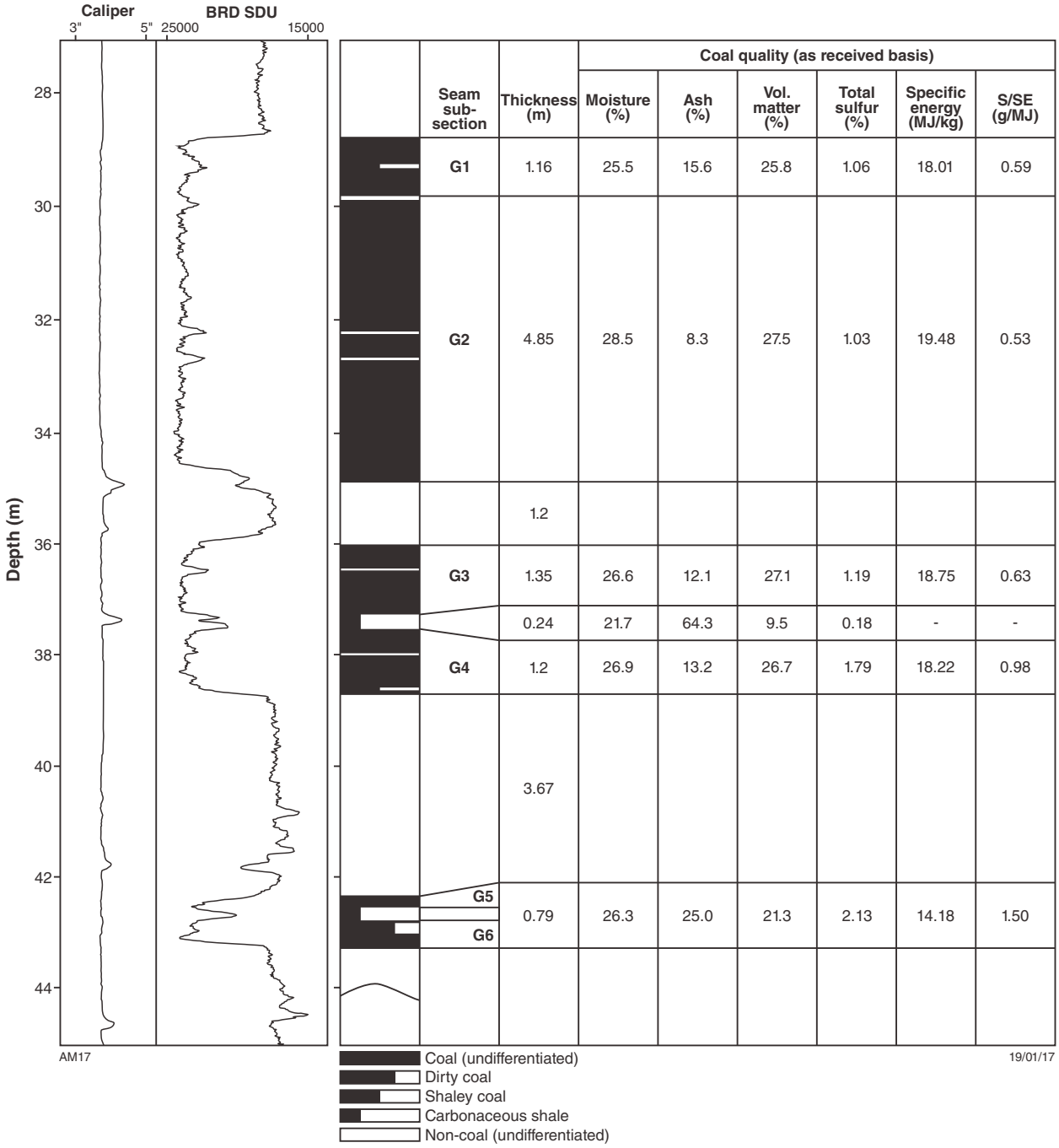

Seam sub-section	Thickness (m)	Coal quality (as received basis) Moisture (%)	Ash (%)	Vol. matter (%)	Total sulfur (%)	Specific energy (MJ/kg)	S/SE (g/MJ)
G1	1.16	25.5	15.6	25.8	1.06	18.01	0.59
G2	4.85	28.5	8.3	27.5	1.03	19.48	0.53
	1.2						
G3	1.35	26.6	12.1	27.1	1.19	18.75	0.63
	0.24	21.7	64.3	9.5	0.18	-	-
G4	1.2	26.9	13.2	26.7	1.79	18.22	0.98
	3.67						
G5	0.79	26.3	25.0	21.3	2.13	14.18	1.50
G6							

Figure 2. Combined plot of short spaced density (uncalibrated) and caliper logs alongside a simplified coal lithology log and summary coal quality data for the main seam (Seam G) for drillhole CPCH 23, Gairdner Range – Cowla Peak Deposit (modified after Park, 1987 and Kristensen, 1991)

Romanoff, A and Shepherd, N 1974, Green Head Coal Prospect, Green Head, Western Australia, Final Report; AMAX Exploration (Australia) Inc.: Geological Survey of Western Australia, Statutory mineral exploration report, A35874.

Suwarna, N 1993, Petrology of Jurassic Coal, Hill River Area, Perth Basin, Western Australia: Curtin University of Technology, Perth, PhD thesis (unpublished).

Suwarna, N 1999, Jurassic coal in Western Australia and its depositional environment, in GEOSEA '98: Geological Society of Malaysia; Bulletin 45, p. 275–289.

Westblade, D 2013, Sargon Project, Annual report for the period 15 November 2011 to 14 November 2012, E70/2758; Eneabba Mining Pty Ltd: Geological Survey of Western Australia, Statutory mineral exploration report, A96234.

Revised tectono-stratigraphy of the Kimberley Basin, northern Western Australia

by

C Phillips, DW Maidment, and Y Lu

The Kimberley region of northern Western Australia is dominated by sedimentary rocks of the Paleoproterozoic Speewah and Kimberley Groups that currently comprise the Speewah and Kimberley Basins, respectively. The Speewah Group unconformably overlies older Paleoproterozoic meta-igneous and metasedimentary rocks of the Lamboo Province and is in turn overlain by the Kimberley Group (Figs 1, 2; Griffin et al., 1993; Tyler et al., 1995; Sheppard et al., 2012). The Speewah and lower Kimberley Groups are intruded by sills of the Hart Dolerite which has an average SHRIMP U–Pb zircon and baddeleyite age of 1795 ± 15 Ma (Sheppard et al., 2012; Wingate et al., in prep.). The Hart Dolerite is correlated with mafic volcanism in the Carson Volcanics (Fig. 2; Kimberley Group) and together constitutes the Hart–Carson Large Igneous Province. The age of igneous activity is considered a good approximation for the timing of deposition of the Speewah and lower Kimberley Groups.

Kimberley Basin — revised nomenclature

Field relationships, comparative lithofacies and detrital zircon U–Pb geochronology suggest that the Kimberley Basin should be redefined to incorporate both the Speewah and Kimberley Groups.

There is low-angle unconformity or disconformity locally between the Bedford Sandstone at the top of the Speewah Group and the overlying King Leopold Sandstone (Fig. 2; Williams, 1969). However, recent mapping by the Geological Survey of Western Australia (GSWA) found that at most localities the transition between the two groups is conformable and locally gradational with no distinct change in paleocurrent direction (i.e. from the northeast; Gellatly et al., 1970). These low-angle unconformities are not considered here to be a basinwide feature, but rather a series of local erosive surfaces between coarse-grained quartz sandstone at the top of the Bedford Sandstone and cobble to boulder conglomerates at the base of the King Leopold Sandstone. Conglomeratic lithofacies in the lower King Leopold Sandstone have previously been interpreted as glacial outwash following a low-latitude glaciation — the King Leopold glaciation (Williams, 2005; Schmidt and Williams, 2008). Features described as glacial striations, frost fissures and tillite produced by the westward flow of ice (Williams, 2005) are reinterpreted here to be a part of a broad, prograding fluvial, partly deltaic plain, derived from the northeast. This system fines to the west, as is evident by the presence of granule and pebble sandstones that were deposited with a shallow-marine influence, and no evidence of glaciation has been observed.

North and east of the Mueller Range, the Kimberley Group rests unconformably on the Lamboo Province (Fig. 1). Since the Speewah Group does not crop out east of the Greenvale–Dunham–Ivanhoe Fault system (Fig. 1) it has previously been interpreted to have been deposited in a fault-bound trough. There is no obvious change in thickness of Speewah Group sedimentary rocks toward the faults suggesting that they might not have controlled deposition. It is possible that uplift of the Lamboo Province exerted a strong topographic control on deposition of the fluvial rocks at the base of the Speewah Group. Areas north and east of the Mueller Range might represent former topographic highs that were onlapped by Speewah Group sedimentary rocks that were subsequently drowned during deposition of the laterally extensive Kimberley Group.

Detrital zircon geochronology

Detrital zircon geochronology of the Speewah and Kimberley Groups (Hollis et al., 2014), including recent SHRIMP U–Pb and laser ablation (LA-ICP-MS) data, is broadly dominated by Paleoproterozoic (1880–1850 Ma) and Neoarchean (2525–2480 Ma) detrital components (Fig. 3). There is an increase in Neoarchean-dominated age components from Speewah to Kimberley Group samples possibly indicating a change in provenance, possibly linked to basin-forming processes (Hollis et al., 2014). However, this pattern is reinterpreted here as a gradual increase in sedimentary detritus supplied from a Neoarchean magmatic source or reworking of older sedimentary units. A Neoarchean source is evident throughout the Speewah Group but it is generally in low abundance (Fig. 3). Additional information from the Bedford Sandstone at the top of the Speewah Group, for which no data currently exist, would help resolve these conflicting hypotheses.

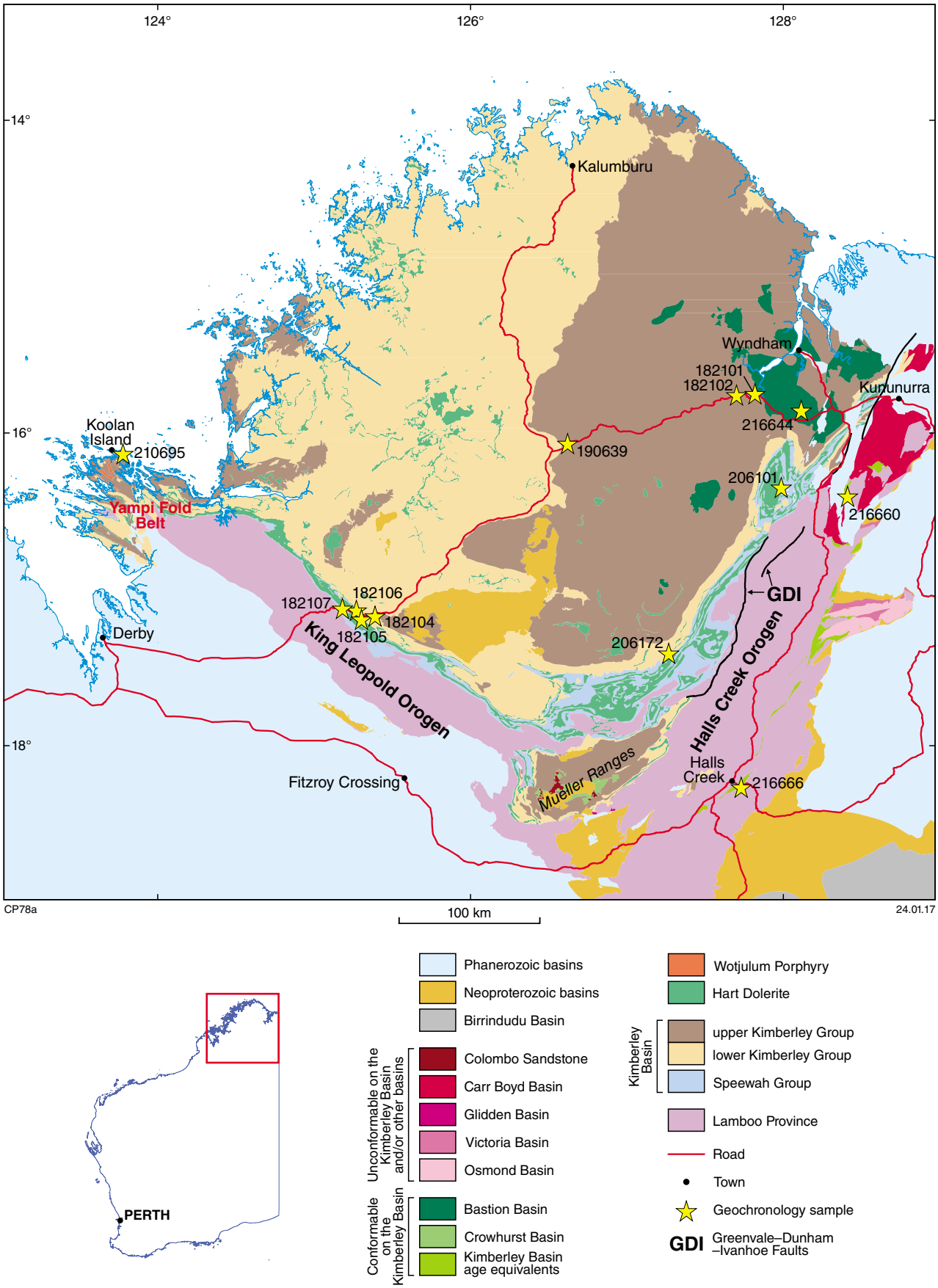

Figure 1. Simplified geology of the Kimberley region showing the sites of samples taken for detrital zircon geochronology (results presented in Figure 3)

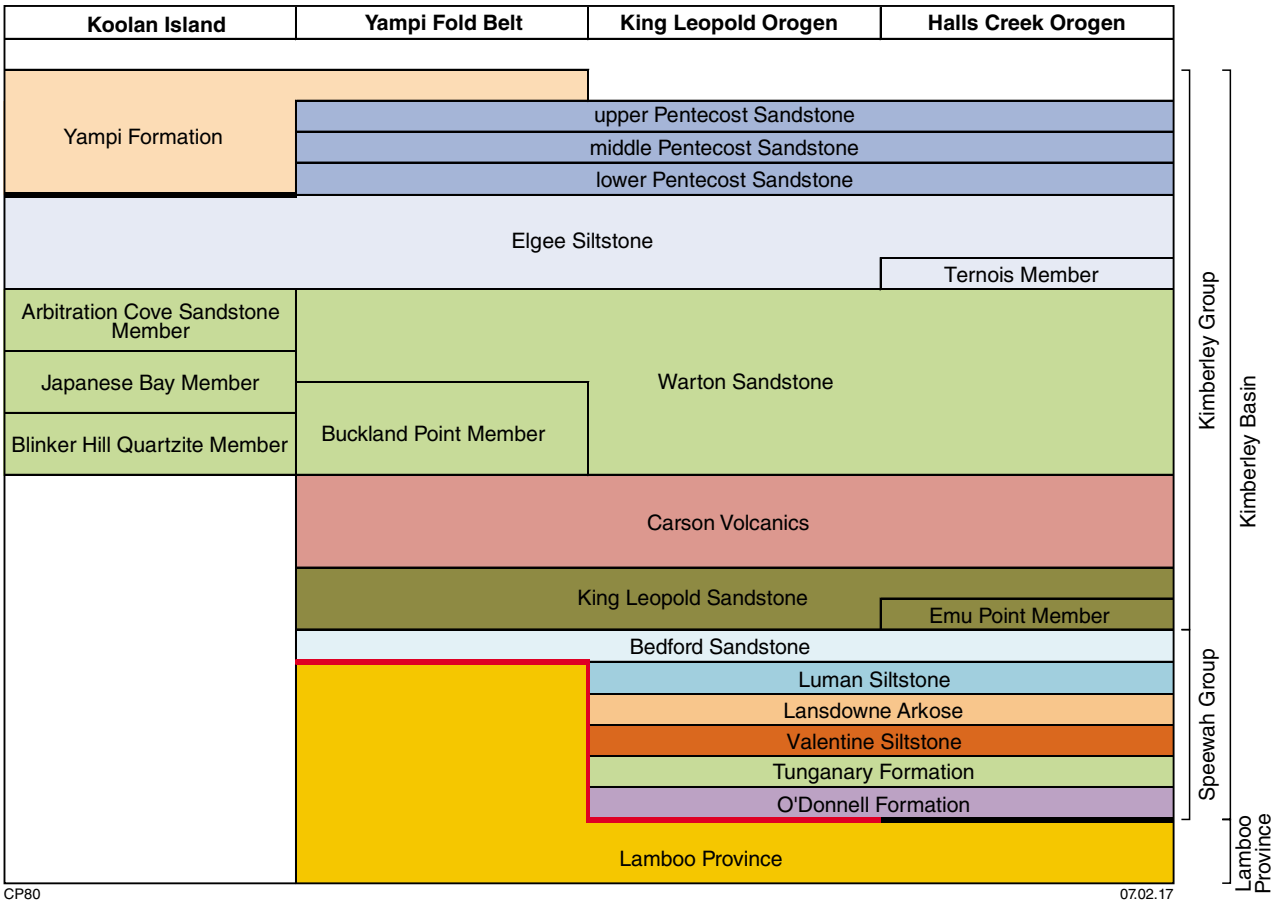

Figure 2. A time–space plot showing the revised stratigraphy and distribution of Kimberley Basin units. Thick black lines represent dominantly unconformable contacts, and thick red lines indicate a fault contact between units.

The broad similarity in the ages of source regions for the Speewah and lower Kimberley Groups, coupled with similar paleocurrent directions, is further evidence that there was no major change in basin dynamics during their deposition, which can be viewed in terms of a progressive evolution within a single basin on top of complex basement topography. It is therefore suggested the use of the term 'Speewah Basin' should be discontinued.

Paleoproterozoic–Mesoproterozoic basins

Recent work by GSWA in the east Kimberley region has focused on a number of smaller Paleoproterozoic–Mesoproterozoic sedimentary basin remnants (Fig. 1) for which there are little or no previous geochronological data. New LA-ICP-MS detrital zircon geochronology provides initial constraints on the tectono-stratigraphy of some of these basins.

Revolver Creek Formation

The Revolver Creek Formation is a >1000 m-thick succession of quartz sandstone, feldspathic sandstone, siltstone and shale intercalated with basaltic rocks that rest unconformably on the Lamboo Province (Fig. 1; Dow et al., 1964; Thorne et al., 1999). The formation is currently assigned to the Revolver Creek Basin but is considered to be equivalent of the Kimberley Basin based on similar lithological associations (Plumb et al., 1985; Thorne et al., 1999). This interpretation is supported by paleocurrent measurements from the Revolver Creek Formation, which are consistent with those from the Speewah and lower Kimberley Groups (i.e. from the northeast). New LA-ICP-MS detrital zircon U–Pb geochronology from the Revolver Creek Formation (GSWA 216660) indicates a significant, almost unimodal, Paleoproterozoic age component consistent with data (albeit with lower analytical precision) from the Speewah and lower Kimberley Groups, particularly the O'Donnell Formation (Fig. 3). Although these data do not allow detailed comparison with the lower Kimberley Group, they are consistent with deposition of the Revolver Creek Formation as the first stage of deposition in the Kimberley Basin in the local area, and as a lateral equivalent of the King Leopold Sandstone and Carson Volcanics.

Moola Bulla Formation

Currently assigned to the Moola Bulla Basin, the Moola Bulla Formation is a succession of conglomerate, sandstone and siltstone unconformable on the Lamboo Province and conformably overlain by the Kimberley

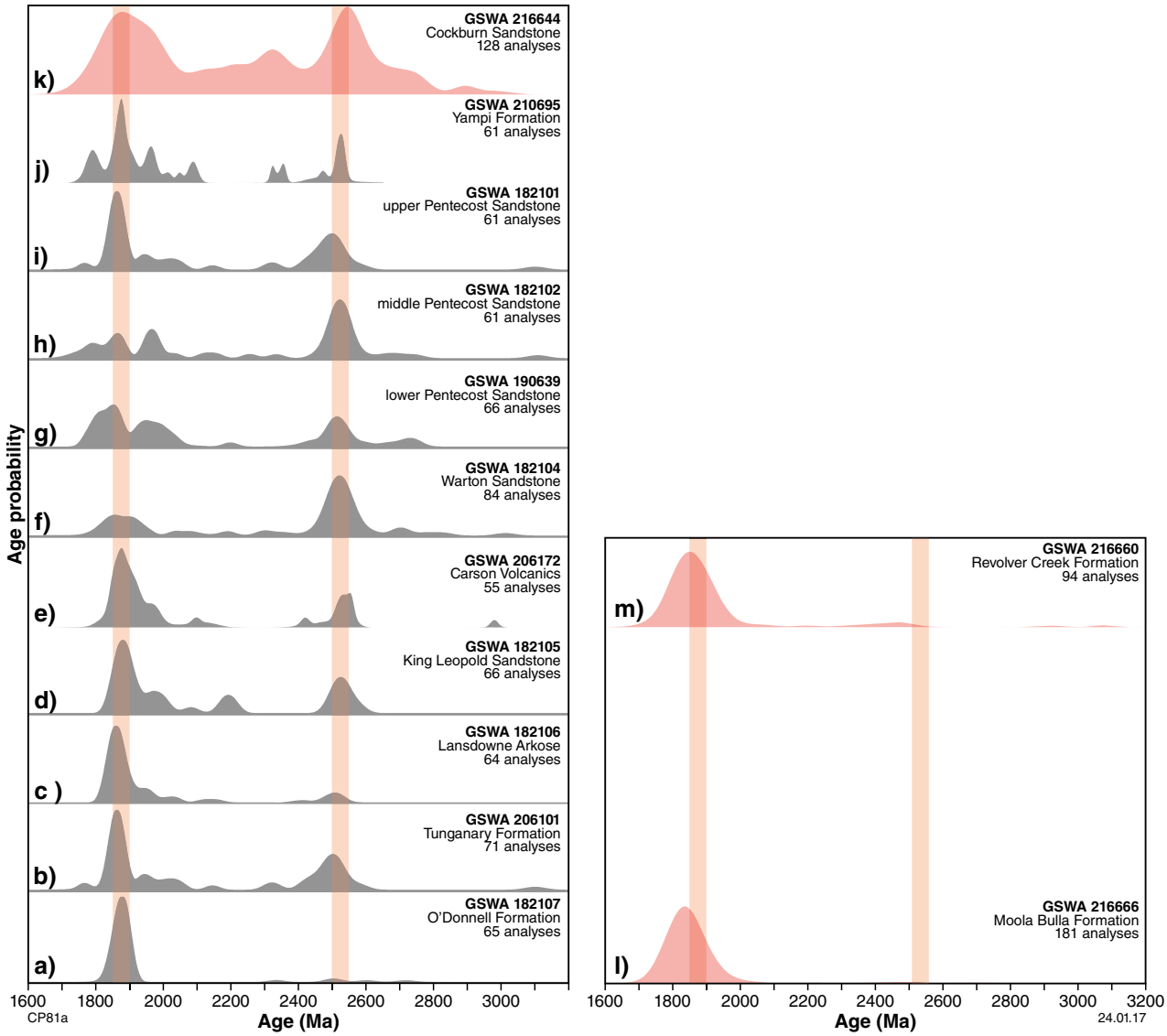

Figure 3. Normalized probability density diagrams of detrital zircon ages (<5% discordant) for sandstone samples from the Speewah and Kimberley Groups. SHRIMP U–Pb data from Hollis et al. (2014) and new SHRIMP U–Pb dating of the Carson Volcanics and Yampi Formation, shown in grey. New LA-ICP-MS detrital zircon geochronology is shown in pink.

Group (Fig. 1). Tentative correlations have been made with the Speewah Group despite contrasting paleocurrent data whereby northeasterly currents dominate the Speewah Group (Gellatly et al., 1970) and southwesterly currents dominate in the Moola Bulla Formation (Blake et al., 1999). New LA-ICP-MS detrital zircon geochronology from the Moola Bulla Formation (GSWA 216666) indicates an almost unimodal Paleoproterozoic detrital zircon population, consistent with detrital age data from the lower Speewah Group (Fig. 3). The Moola Bulla Formation is thus interpreted as an age equivalent to the Speewah Group within the lower Kimberley Basin. Differences in paleocurrent directions can be ascribed to localized irregularities in basement topography, which is likely to have had a significant influence on these fluvial to shallow-marine units.

Bastion and Crowhurst Groups

The Bastion Group consists of fine-grained siliciclastic rocks and quartz sandstone that conformably rest on the Kimberley Group, except west of the Durack Range where unconformable relationships have been described (Thorne et al., 1999). This is the only instance of this relationship which may be locally erosive. Despite the relatively large analytical uncertainties associated with the laser-derived data, new LA-ICP-MS detrital zircon geochronology from the Cockburn Sandstone (GSWA 216644) shows age components at 1880–1850 Ma and 2525–2480 Ma, consistent with detrital age data from the upper Kimberley Group. Likewise, dominantly north and northwest paleocurrent measurements from the Bastion Group are consistent with those from the upper Kimberley Group.

The Crowhurst Group, exposed to the south of the Bastion Group, is conformably overlain by the Kimberley Group; locally, the contact is gradational. The two groups have comparable lithofacies and paleocurrent data (i.e. sediment sourced from the north and northwest; Gellatly et al., 1970). Samples for detrital zircon geochronology collected by GSWA in 2016 are currently being processed.

Based on the conformable relationships, similarity and continuity of sedimentary lithofacies, consistency of paleocurrent data (and with the Bastion Group, consistent detrital zircon age components), it is suggested that the Bastion and Crowhurst Groups represent continued sedimentation in the Kimberley Basin and may, in parts, be correlative.

Future detrital zircon geochronology

Sampling for detrital zircon geochronology in younger Proterozoic sedimentary basins in the east Kimberley region was completed by GSWA during 2015 and 2016. The results of these studies will focus on defining a more robust tectono-stratigraphy for sedimentary succession in the region, including the Glidden, Osmond, Carr Boyd and Victoria Basins, and will be used to construct broader correlations across the Proterozoic of northern Australia.

References

Blake, DH, Tyler, IM, Griffin, TJ, Sheppard, S, Thorne, AM and Warren, RG 1999, Geology of the Halls Creek 1:100 000 Sheet area (4461), Western Australia: Australian Geological Survey Organisation, Explanatory Notes, 36p.

Dow, DB, Gemuts, I, Plumb, KA and Dunnet, D 1964, The Geology of the Ord River region, Western Australia: Australian Bureau of Mineral Resources, Geology and Geophysics, Record 1964/104, 164p.

Gellatly, DC, Derrick, GM and Plumb, KA 1970, Proterozoic palaeocurrent directions in the Kimberley region, northwestern Australia: Geological Magazine, v. 107, p. 249–257.

Griffin, TJ, Tyler, IM and Playford, PE 1993, Explanatory notes on the Lennard River 1:250 000 geological sheet SE/51-8, Western Australia (3rd edition): Geological Survey of Western Australia, Record 1992/5, 85p.

Hollis, JA, Kemp, AIS, Tyler, IM, Kirkland, CL, Wingate, MTD, Phillips, C, Sheppard, S, Belousova, E and Greau, Y 2014, Basin formation by orogenic collapse: zircon U–Pb and Lu–Hf isotope evidence from the Kimberley and Speewah Groups, northern Australia: Geological Survey of Western Australia, Report 137, 46p.

Plumb, KA, Allen, R and Hancock, SL 1985, Proterozoic evolution of the Halls Creek Province, Western Australia: Bureau of Mineral Resouces, Geology and Geophysics, Record 1985/25, 87p.

Schmidt, PW and Williams, GE 2008, Palaeomagnetism of red beds from the Kimberley Group, Western Australia: implications for the palaeogeography of the 1.8 Ga King Leopold Glaciation: Precambrian Research, v. 167, p. 267–280.

Sheppard, S, Page, RW, Griffin, TJ, Rasmussen, B, Fletcher, IR, Tyler, IM, Kirkland, CL, Wingate, MTD, Hollis, J and Thorne, AM 2012, Geochronological and isotopic constraints on the tectonic setting of the c. 1800 Ma Hart Dolerite and the Kimberley and Speewah Basins, northern Western Australia: Geological Survey of Western Australia, Record 2012/7, 28p.

Thorne, AM, Sheppard, S and Tyler, IM 1999, Lissadell, Western Australia (2nd edition): Geological Survey of Western Australia, 1:250 000 Geological Series Explanatory Notes, 68p.

Tyler, IM, Griffin, TJ, Page, RW and Shaw, RD 1995, Are there terranes within the Lamboo Complex of the Halls Creek Orogen?, *in* Geological Survey of Western Australia Annual Review 1993–94: Geological Survey of Western Australia, p. 37–46.

Williams, GE 1969, Stratigraphy and sedimentation in the Mount Bedford area, WA: Melbourne, Report to The Broken Hill Proprietary Company Limited (unpublished).

Williams, GE 2005, Subglacial meltwater channels and fluvioglacial deposits in the Kimberley Basin, WA: 1.8 Ga low-latitude glaciation coeval with continental assembly: Journal of the Geological Society of London, v. 162, p. 111–124.

Structural evolution of the S-bend region, east Albany–Fraser Orogen

by

MA Munro, R Quentin de Gromard, and CV Spaggiari

The margins of Archean cratons have long been recognized as important zones of intense deformation, enhanced magmatism and economically important mineralization. Understanding the tectono-metamorphic and magmatic evolutions of these margins is therefore paramount in establishing temporal and structural frameworks for the formation of these mineral systems. The Albany–Fraser Orogen is an important and prospective example of Archean craton margin modification and deformation. This is because it hosts the Tropicana gold mine within the reworked Archean rocks of the Tropicana Zone, and the Nova–Bollinger Ni–Cu deposit within the mafic to ultramafic, Mesoproterozoic granulite facies rocks of the Fraser Zone. The linear orogen is approximately 1200 km long and is situated along the southern and southeastern margins of the Yilgarn Craton, with the transition zone between the two marked by the Jerdacuttup Fault and the Cundeelee Shear Zone. The eastern extent of the east Albany–Fraser Orogen is marked by the Rodona Shear Zone, an east- to southeast-dipping thrust system that separates the orogen from the Proterozoic Madura Province (Spaggiari et al., 2014a).

The S-bend region (Fig. 1) is informally named as such due to its apparent S-fold geometry and is one of the most structurally complex regions within the orogen. It is an asymmetric interface between the reworked Archean rocks of the Northern Foreland, the Paleoproterozoic orthogneiss-dominated rocks of the Biranup and Nornalup Zones, and the Mesoproterozic interlayered mafic and felsic gneisses of the Fraser Zone (Spaggiari et al., 2014b). This region consists of multiple fold generations affecting a series of faults and shear zones, marking an important regional-scale crustal architecture that provides insight into the structural relationships between these tectonic units, and their evolution. The tectonic units within and adjacent to the S-bend region preserve differences in their structural grain and evolution, and are described below.

Structural evolutions preserved internally within tectonic units

The Biranup Zone

The structural grain of the Biranup Zone to the southwest of the S-bend (Figure 1, area a) is defined by northwest-trending gneissic layering subparallel to the axial traces of folds and shear zones. The folds are upright, isoclinal, gently northwest or southeast plunging, and affect the gneissic layering and layer-parallel leucosomes. Stretching lineations on the axial planar foliation are subparallel to the fold axes, and also parallel to the long axes of boudins of the foliation. This suggests that folding and stretching may have been synchronous, and both symmetric and asymmetric boudins are present. Open, moderately to steeply northeast-plunging folds deform the earlier folds resulting in the formation of Type 3 fold interference patterns (Fig. 2a; Ramsay, 1962). Leucosomes are commonly in situ and show different structural relationships. Some are deformed by, or axial planar to, northwest-trending F_1 folds. Others are axial planar to northeast-trending F_2 refolds. This indicates that partial melting occurred before or during local F_1 folding, and also during local F_2 folding.

To the south and southeast of the Fraser Zone, the structural grain of the Biranup Zone is defined by regional-scale, northeast-trending fold axial traces (Fig. 1, area b). Several northeast-trending folds in this eastern section of the Biranup Zone refold pre-existing folds resulting in both Type 2 and Type 3 interference patterns (Ramsay, 1962). This indicates the refolding of two prior fold generations. The presence of northeast-trending boudins suggests the development of the northeast-trending folds in the centre of the S-bend might also have been associated with a significant component of subhorizontal, strike-parallel stretching. A steeply east-plunging, regional-scale fold (Fig. 1, area c) is manifest in interlayered felsic and mafic gneisses of this section of the Biranup Zone and might represent either a second generation fold, or, alternatively, passive folding within a regional-scale boudin neck adjacent to the shear zone boundary.

Northern Foreland

Early deformation in metasedimentary and metamafic rocks of the Northern Foreland to the northwest of the S-bend produced gently south-plunging, overturned, west-verging isoclinal folds and approximately north–south striking, west-directed thrusts (Fig. 1, area d). These are refolded about near-orthogonal, moderately east-plunging, open folds. This fold overprinting history is bounded to either side by two east-dipping thrusts that have been

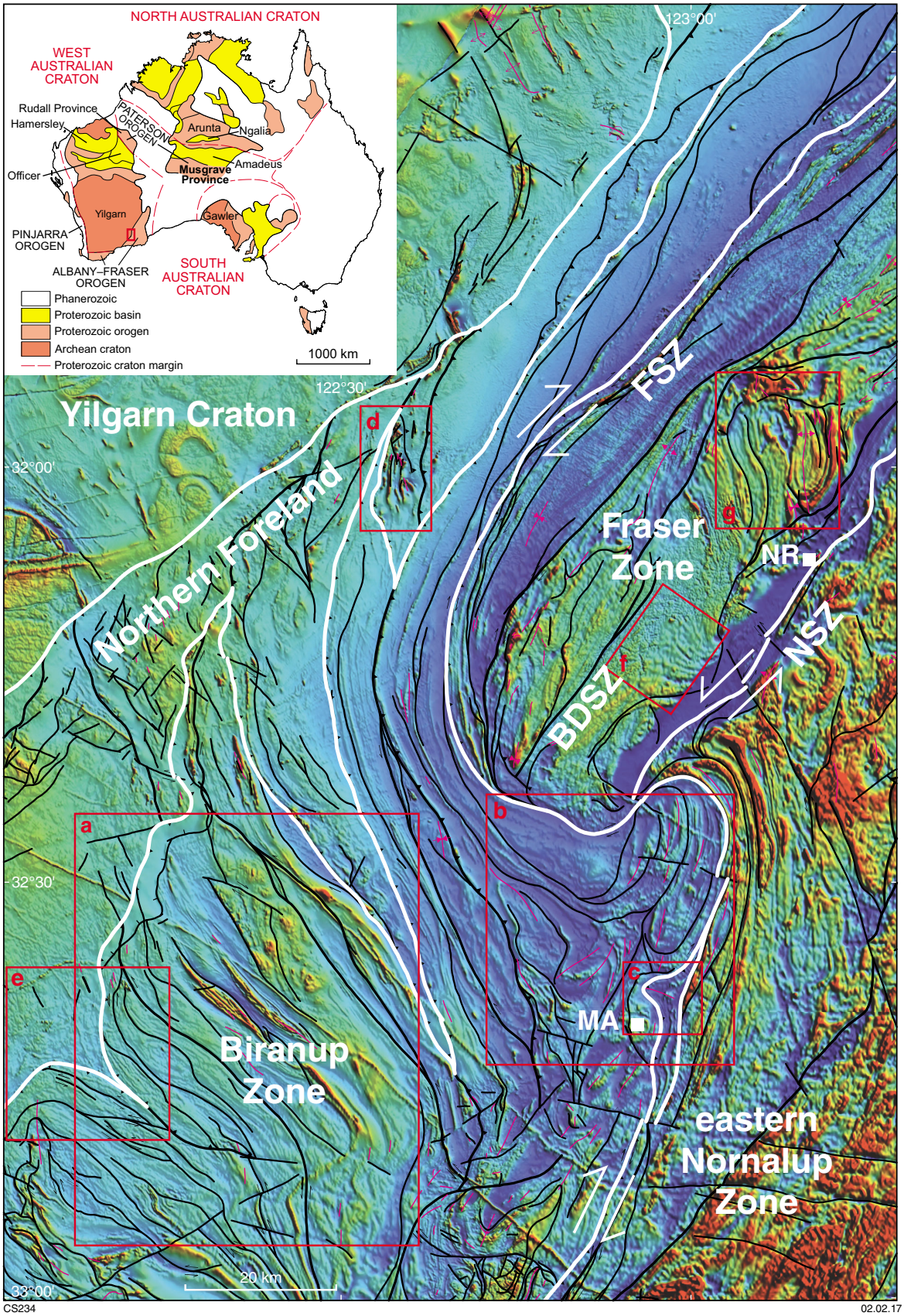

Figure 1. **Reduced-to-pole aeromagnetic image showing the structural relationship between the four tectonic units in the S-bend region. FSZ = Fraser Shear Zone; NSZ = Newman Shear Zone; BDSZ = Browns Dam Shear Zone; NR = Newman Rock; MA = Mount Andrew. Areas a–g mark the positions of key structural domains described in the text.**

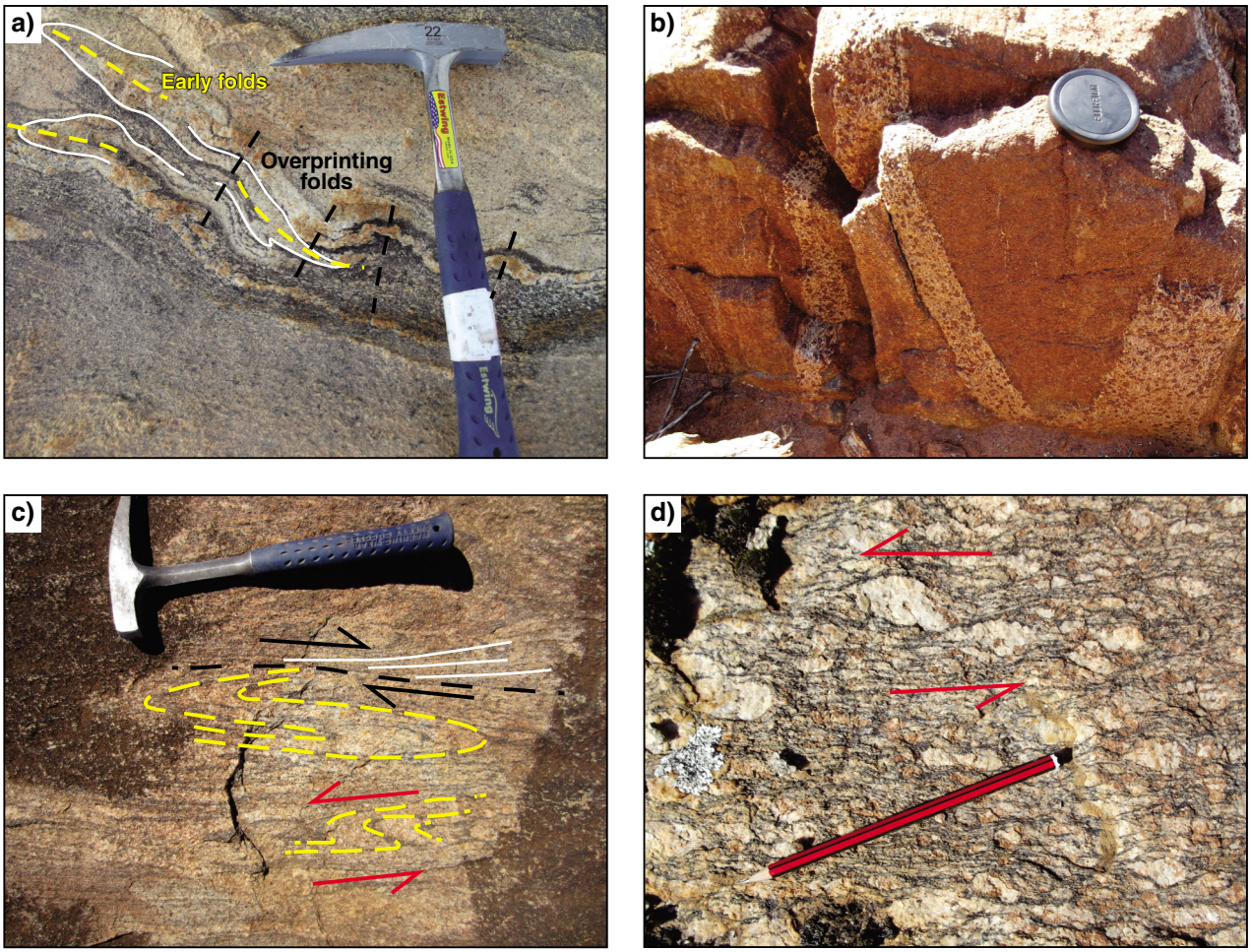

Figure 2. **a) Plan view of early northwest-trending isoclinal folds of gneissic layering and leucosomes (solid white lines show layering; dashed yellow lines show axial traces) in the Biranup Zone, refolded about steeply northeast-plunging, open folds (dashed black lines show axial traces). Hammer head points north; b) a gently northeast-plunging antiform and synform pair in interlayered garnet-bearing sedimentary gneiss, metagabbro and metagranite on the northwestern margin of the Fraser Zone. Photo faces due northeast; c) plan view of asymmetric folds (yellow dashed lines) showing an early sinistral shear history preserved along the Fraser Shear Zone near the centre of the S-bend, overprinted by subsequent discrete dextral shear zones (black dashed line). White markers show the progressive rotation of previous structures into the discrete dextral shear. Hammer head points north; d) plan view of the dominant northeast–southwest striking mylonitic foliation of the Newman Shear Zone. Large sigma-type feldspar porphyroclasts indicate sinistral strike-slip shear sense. Pencil tip points north.**

folded about the S-bend. Along strike to the northeast, an eastward-dipping thrust has been folded about a series of east-trending folds with tighter interlimb angles. The bounding thrust between the Northern Foreland and the Biranup Zone has a curved trace, as interpreted from aeromagnetic data (Fig. 1, area e). This suggests that the margin between the two units has been deformed about northwest-trending folds that parallel the structural grain of this section of the Biranup Zone.

Fraser Zone

The northeast-trending Fraser Zone may be subdivided along the Browns Dam Shear Zone into a northwestern and a southeastern domain (Fig. 1). The northwestern domain is dominated by interlayered paragneiss, metagabbro and metagranite. The northeast-trending structural grain of this domain is defined by the layering and a layering-parallel foliation. Folds are tight to isoclinal, and gently to steeply doubly plunging (Figs 1, 2b). The more competent mafic layers form centimetre- to metre-scale boudins that indicate stretching subparallel to the northeast-trending axial traces of the folds. The southeastern domain is dominated by metagabbroic rocks. Aeromagnetic data show folded magnetic horizons interpreted to represent a 10 km-wide, northeast-trending open fold affecting the magmatic layering within the metagabbroic rocks (Fig. 1, area f). To the northeast of this fold, a series of approximately north-trending magnetic horizons are interpreted to reflect folded and sheared magmatic layering (Fig. 1, area g). The northeast-trending structural grain that dominates the Fraser Zone wraps around this structure.

This structure may be interpreted as a regional-scale boudin whose orientation might have been rotated from its original northeast trend into its current north trend during shearing. Alternatively, this north trend may represent the preservation of an older generation of structures that pre-date the northeast structural grain of the Fraser Zone.

Kinematic history of shear zones bounding the Fraser Zone

The Fraser Shear Zone (FSZ) is a wide zone of mylonitic to ultramylonitic foliations that mark the boundary between the Biranup and Fraser Zones (Fig. 1). Kinematic indicators associated with subhorizontal to gently plunging stretching lineations suggest a protracted history of dextral strike-slip kinematics. The dominant mylonitic foliation contains asymmetric dextral boudins that are overprinted by narrow dextral shear zones that lie at a low angle to the foliation. However, relatively lower strain areas preserve evidence of an earlier sinistral shearing history (Fig. 2c). Large delta-type garnet porphyroclasts and the asymmetries of isoclinal, often rootless, folds indicate sinistral shear sense along the gneissic layering. These earlier structures are truncated by narrow discrete dextral shear zones at low angles to the gneissic layering.

The northeast-trending Newman Shear Zone (NSZ) separates the Fraser Zone from the eastern Nornalup Zone and toward the southern end of the Fraser Zone, coincides with a remarkably low-intensity aeromagnetic signature (Fig. 1). Stretching lineations on the dominant mylonitic foliation vary significantly from steeply plunging to subvertical at localities such as Newman Rock (Fig. 1), to gently plunging and subhorizontal elsewhere along strike. Sinistral and southeast-side-up relative motion can be interpreted from kinematic indicators (e.g. Fig. 2d). Displacement along the shear zone appears to have produced a regional-scale drag fold that affects a series of northeast-trending folds and faults in the Biranup and eastern Nornalup Zones (northeast corner of area b in Figure 1), accentuating the S-bend's geometry. Within the NSZ, narrow, discrete, approximately north-trending sinistral shear zones locally branch out of the mylonitic foliation. Their shear sense and angular relationship with the mylonitic foliation are compatible with representing subsidiary synthetic R shears. However, a series of discrete, approximately east-trending dextral shear zones locally deform the mylonitic foliation and may correlate with other similarly oriented dextral shears that overprint northeast-trending folds in the Biranup Zone.

Conclusions and future directions

The S-bend of the East Albany–Fraser Orogen is an important regional-scale crustal interface between four lithologically and structurally distinct tectonic units. The structural evolution of the S-bend region preserves at least three regionally significant orientations of folds and associated structures: north–south trending, northwest–southeast trending and northeast–southwest trending. A history of gently south-plunging folds near-orthogonally overprinted by moderately east-plunging folds in the Northern Foreland may correlate with an analogous relationship observed in metagabbros and orthogneisses of the Biranup Zone in the S-bend (Fig. 1, area c). The northeast-trending folds that dominate the structural grain of the Fraser Zone appear to correlate with similarly oriented northeast-trending folds in the Biranup Zone that refold earlier northwest-trending folds.

Rheological contrasts and deformation partitioning may have contributed toward the differential preservation of structural orientations throughout the S-bend region. While at least three generations of folding are preserved in the centre of the S-bend just north of Mount Andrew (Fig. 1), elsewhere, evidence of earlier structures and their relative timing has been largely erased during their transposition into parallelism with the dominant northeasterly structural grain during ongoing or subsequent deformation. We interpret that the northwesterly trending structures of the Biranup Zone were preserved due to their proximity to the relatively competent metagabbro-dominated Fraser Zone. The regional-scale S-fold geometry may therefore have developed by the overprinting of multiple structures oriented at high angle to one another, as opposed to a straightforward sinistral shear development as might be expected to produce such geometry. The FSZ preserves a dextral shear-dominated kinematic evolution. However, an earlier history of sinistral kinematics is locally preserved. The FSZ is interpreted as a relatively old structure that was later folded about the S-bend with associated northeast-trending folds. Younger sinistral and east-side-up components of relative motion along the NSZ subsequently produced an apparent regional-scale drag fold that overprinted northeast-trending folds, accentuating the S-bend geometry.

The determination of the structural evolution for the S-bend region represents an important step toward a holistic tectono-metamorphic and magmatic framework for the east Albany–Fraser Orogen and the economically important mineralization that it hosts. Future work will combine oriented microstructural analysis with the field- and aeromagnetic-based structural observations, thermodynamic modelling, and in situ dating of microstructurally constrained accessory phases to establish the pressure–temperature–time–deformation (P–T–t–d) histories of the different tectonic units.

References

Ramsay, JG 1962, Interference patterns produced by the superposition of folds of 'similar' type: Journal of Geology v. 70, p. 466–481.

Spaggiari, CV, Kirkland, CL, Smithies, RH, Occhipinti, SA and Wingate, MTD 2014b, Geological framework of the Albany–Fraser Orogen, *in* Albany–Fraser Orogen seismic and magnetotelluric (MT) workshop 2014: extended abstracts *compiled by* CV Spaggiari and IM Tyler: Geological Survey of Western Australia, Record 2014/6, p. 12–27.

Spaggiari, CV, Occhipinti, SA, Korsch, RJ, Doublier, MP, Clark, DJ, Dentith, MC, Gessner, K, Doyle, MG, Tyler, IM, Kennett, BLN, Costelloe, RD, Fomin, T and Holzschuh, J 2014a, Interpretation of Albany–Fraser seismic lines 12GA-AF1, 12GA-AF2 and 12GA-AF3: implications for crustal architecture, *in* Albany–Fraser Orogen seismic and magnetotelluric (MT) workshop 2014: extended abstracts *compiled by* CV Spaggiari and IM Tyler, Geological Survey of Western Australia, Record 2014/6, p. 28–51.

Post-Giles Event evolution of the Musgrave Province constrained by (multi-method) thermochronology

by

R Quentin de Gromard, HM Howard, CL Kirkland*, RH Smithies, MTD Wingate, and F Jourdan*

The Musgrave Province is a Mesoproterozoic orogen exposed at the junction between the North, West, and South Australian Cratons. Over the last decade, the Geological Survey of Western Australia (GSWA) has focused its efforts in identifying and characterizing the crust-forming events of the west Musgrave Province (see Howard et al., 2015 for review). However, the post-Mesoproterozoic exhumation history of the province remains poorly known. We show that the interpretation of previous and new field mapping, deep seismic reflection, and U–Pb and Ar–Ar geochronological data impose significant constraints on the evolution of the province after the 1085–1040 Ma Giles Event, requiring revision of the evolution of parts of central Australia.

Geology of the west Musgrave Province

The oldest known rocks of the west Musgrave Province are poorly exposed gneisses of the c. 1600 Ma Warlawurru Supersuite and granitic rocks of the c. 1400 Ma Papulankutja Supersuite (Howard et al., 2011; Quentin de Gromard et al., 2016). The first main tectono-magmatic event identified is the Mount West Orogeny during which granitic rocks of the 1345–1293 Ma Wankanki Supersuite were emplaced and volcano-sedimentary rocks of the 1340–1270 Ma Wirku Metamorphics were deposited (Smithies et al., 2010; Howard et al., 2011; Evins et al., 2012). All of these rocks were metamorphosed at ultra-high temperature during the Musgrave Orogeny which was also accompanied by the emplacement of the 1220–1150 Ma Pitjantjatjara Supersuite (Edgoose et al., 2004; Smithies et al., 2010). The Musgrave Province refers to all rocks formed during, or affected by, the Musgrave Orogeny and constitutes the basement to rocks of the 1085–1040 Ma Giles Event. Volcano-sedimentary rocks of the c. 1085 Kunmarnara Group are interpreted as the lowermost unit deposited during the Giles Event (Evins et al., 2010). Igneous rocks formed during the Giles Event belong to the Warakurna Supersuite and include the layered mafic–ultramafic Giles intrusions, mixed and mingled gabbros and leucogranites, Alcurra Dolerite intrusions and bimodal volcanic rocks of the Talbot Supervolcano (Howard et al., 2009; Evins et al., 2010; Smithies et al., 2015). Apart from minor mafic dyke intrusion at c. 1000, 825 and 750 Ma (Wingate et al., 1998), the Musgrave Province is commonly regarded as tectonically quiescent until intracontinental reactivation during the 580–520 Ma Petermann Orogeny. Deformation during the Petermann Orogeny produced east-trending crustal-scale faults and shear zones that dissect the entire Musgrave Province (Lambeck and Burgess, 1992; Camacho and McDougall, 2000; Aitken et al., 2009). Metamorphic conditions during the Petermann Orogeny approached eclogite facies south of the Woodroffe Thrust, and amphibolite facies or lower in the north-verging Petermann Nappe Complex (Scrimgeour and Close, 1999; Edgoose et al., 2004; Raimondo et al., 2010).

Structure and thermochronology of the west Musgrave Province

The study area is subdivided, from south to north, into the Talbot Sub-basin, the Mitika area, and the Wanarn area (Fig. 1). The Wanarn area, between the Mitika Fault and the Woodroffe Thrust, represents a gneissic core that formed after the Giles Event.

The structure of the Talbot Sub-basin is characterized by a west- to northwest-trending open anticline and south-directed reverse faults (Fig. 1). Ar–Ar analyses of muscovite from kyanite-bearing schists yielded a date of c. 715 Ma. Igneous zircons from a nearby metagranitic rock yielded a U–Pb date of 1079 ± 8 Ma, interpreted as the time of crystallization of the granite protolith. U–Pb titanite dates from this rock show a bimodal population. One population yielded results ranging from c. 1100 to 942 Ma. The latter date is interpreted as the time the granite cooled below 600 °C (the retention temperature of the U–Pb system in titanite). The second population of titanite dates yielded a peak at 715 ± 7 Ma, similar to the Ar–Ar date. The c. 715 Ma date is interpreted as the age of metamorphic growth of muscovite and titanite resulting from thickening of the Talbot Sub-basin during north–south compression.

* Department of Applied Geology, Western Australian School of Mines, Curtin University, Bentley WA 6102

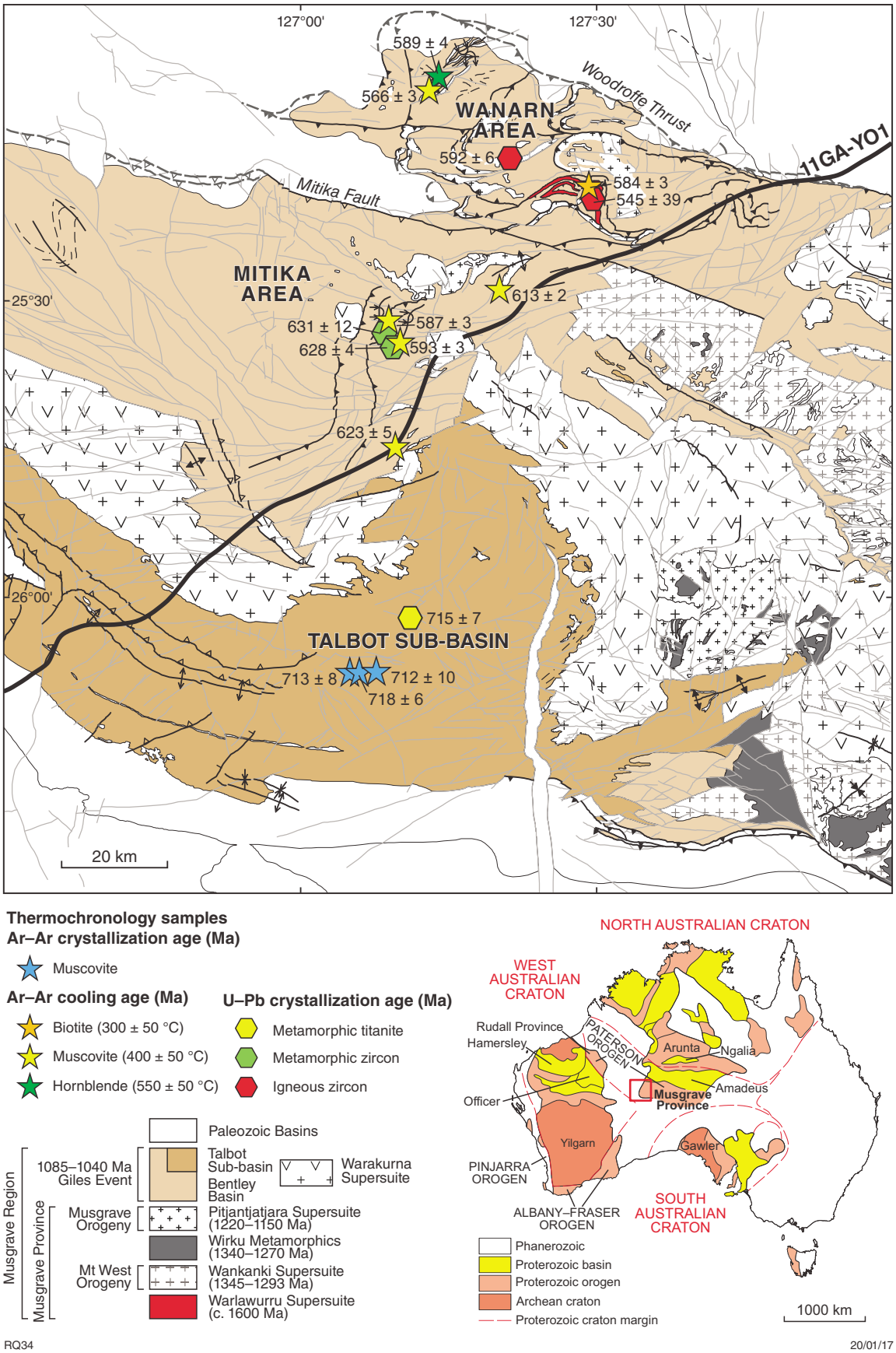

Figure 1. Interpreted bedrock geology map of the study area (tectonic map of Australia is inset for location) showing the thermochronology sample locations and the trace of the deep seismic reflection profile 11GA-YO1

The structure of the Mitika area consists of a west-verging fold and thrust system. Zircon overgrowths from garnet–kyanite schists yielded U–Pb dates of c. 630 Ma, interpreted as the time of peak metamorphism during east–west shortening. This was followed by exhumation and cooling below 400 °C (the retention temperature of argon in muscovite) at c. 590 Ma, dated by Ar–Ar on muscovite. The lower-grade periphery of the Mitika area cooled below 400 °C at 623 ± 5 Ma to the south and 613 ± 2 Ma to the north.

The Wanarn area is a zone of complex ductile deformation where basement rocks of the Musgrave Province are tectonically interleaved with rocks of the Kunmarnara Group. Pegmatite veins intruding the Kunmarnara Group yield U–Pb zircon dates of 592 ± 6 Ma and 545 ± 39 Ma, interpreted as the age of pegmatite crystallization. The southern Wanarn area cooled below 300 °C at 584 ± 3 Ma, while the northern area cooled below 550 °C at 589 ± 4 Ma, as indicated by Ar–Ar analyses of biotite and hornblende, respectively. This suggests differential cooling of the Wanarn area and that minor pegmatitic melt was generated and crystallized during exhumation. The northern Wanarn area was then cooled below 400 °C at 567 ± 3 Ma, as indicated by Ar–Ar analyses of muscovite.

A lengthy period of post-Giles Event tectono-metamorphic evolution

The deep seismic reflection line 11GA-YO1 runs northeast through the west Musgrave Province (Fig. 1). A reinterpretation of the seismic section is proposed (Fig. 2). Thermochronology data projected onto this section clearly show the overall younging of ages toward the north, expressing an overall northward exhumation over a period of nearly 200 Ma. This period partly overlaps, but largely pre-dates, the 580–520 Ma Petermann Orogeny. Thus, the Musgrave Province preserves a much lengthier post-Giles tectono-metamorphic history than previously recognized.

These results indicate that the exhumation of the exposed part of the Musgrave Province is not the sole result of the 580–520 Ma Petermann Orogeny. Rather, it spanned a much longer time period that started as early as c. 715 Ma. This period is marked by discrete events in central Australia: north–south shortening at c. 715 Ma, followed by 630–615 Ma east–west shortening, and finally 590–565 Ma northeast–southwest shortening related to the Petermann Orogeny. All these events involved fluid mobility as indicated by muscovite, titanite and zircon growth as well as pegmatite generation.

The reinterpretation of the seismic section forms the backbone of a time–temperature-constrained evolution model (Fig. 3). The geothermal gradient used in the model is non-linear and derived from published P–T estimates (e.g. 600 °C at 6 kbar and 750 °C at 12 kbar, Scrimgeour and Close, 1999; Raimondo et al., 2010; Walsh et al., 2013). Line-length balancing of the section south of the Woodroffe Thrust, using the base of the Kunmarnara Group as a marker line, indicates a total shortening of 67 km (i.e. –27%), where 90% (i.e. 59 km) of the total shortening is concentrated in the Wanarn Area alone.

References

Aitken, ARA, Betts, PG and Ailleres, L 2009, The architecture, kinematics, and lithospheric processes of a compressional intraplate orogen occurring under Gondwana assembly: the Petermann Orogeny, central Australia: Lithosphere, v. 1, no. 6, p. 343–357.

Camacho, A and McDougall, I 2000, Intracratonic, strike-slip partitioned transpression and the formation of eclogite facies rocks: an example from the Musgrave Block, central Australia: Tectonics, v. 19, p. 978–996.

Edgoose, CJ, Scrimgeour, IR and Close, DF 2004, Geology of the Musgrave Block, Northern Territory: Northern Territory Geological Survey, Report 15, 46p.

Evins, PM, Kirkland, CL, Wingate, MTD, Smithies, RH, Howard, HM and Bodorkos, S 2012, Provenance of the 1340–1270 Ma Ramarama Basin in the west Musgrave Province, central Australia: Geological Survey of Western Australia, Report 116, 39p.

Evins, PM, Smithies, RH, Howard, HM, Kirkland, CL, Wingate, MTD and Bodorkos, S 2010, Redefining the Giles Event within the setting of the 1120–1020 Ma Ngaanyatjarra Rift, west Musgrave Province, central Australia: Geological Survey of Western Australia, Record 2010/6, 36p.

Howard, HM, Smithies, RH, Kirkland, CL, Evins, PM and Wingate, MTD 2009, Age and geochemistry of the Alcurra Suite in the western Musgrave Province and implications for orthomagmatic Ni–Cu–PGE mineralization during the Giles Event: Geological Survey of Western Australia, Record 2009/16, 16p.

Howard, HM, Smithies, RH, Kirkland, CL, Kelsey, DE, Aitken, A, Wingate, MTD, Quentin de Gromard, R, Spaggiari, CV and Maier, WD 2015, The burning heart — the Proterozoic geology and geological evolution of the west Musgrave Region, central Australia: Gondwana Research, v. 27, no. 1, p. 64–94.

Howard, HM, Werner, M, Smithies, RH, Evins, PM, Kirkland, CL, Kelsey, DE, Hand, M, Collins, AS, Pirajno, F, Wingate, MTD, Maier, WD and Raimondo, T 2011, The geology of the west Musgrave Province and the Bentley Supergroup — a field guide: Geological Survey of Western Australia, Record 2011/4, 116p.

Lambeck, K and Burgess, G 1992, Deep crustal structure of the Musgrave Block, central Australia: results from teleseismic travel-time anomalies: Australian Journal of Earth Sciences, v. 39, p. 1–20.

Quentin de Gromard, R, Wingate, MTD, Kirkland, CL, Howard, HM and Smithies, RH 2016, Geology and U–Pb geochronology of the Warlawurru Supersuite and MacDougall Formation in the Mitika and Wanarn areas, west Musgrave Province: Geological Survey of Western Australia, Record 2016/4, 29p.

Raimondo, T, Collins, AS, Hand, M, Walker-Hallam, A, Smithies, RH, Evins, PM and Howard, HM 2010, The anatomy of a deep intracontinental orogen: Tectonics, v. 29 (TC4024), doi:10.1029/2009TC002504.

Scrimgeour, IR and Close, DF 1999, Regional high pressure metamorphism during intracratonic deformation: the Petermann Orogeny, central Australia: Journal of Metamorphic Geology, v. 17, p. 557–572.

Smithies, RH, Howard, HM, Evins, PM, Kirkland, CL, Kelsey, DE, Hand, M, Wingate, MTD, Collins, AS, Belousova, E and Allchurch, S 2010, Geochemistry, geochronology, and petrogenesis of Mesoproterozoic felsic rocks in the west Musgrave Province, Central Australia, and implications for the Mesoproterozoic tectonic evolution of the region: Geological Survey of Western Australia, Report 106, 73p.

Smithies, RH, Howard, HM, Kirkland, CL, Korhonen, FJ, Medlin, CC, Maier, WD, Quentin de Gromard, R and Wingate, MTD 2015, Piggy-back supervolcanoes — long-lived, voluminous, juvenile rhyolite volcanism in Mesoproterozoic central Australia: Journal of Petrology, v. 56, no. 4, p. 735–763.

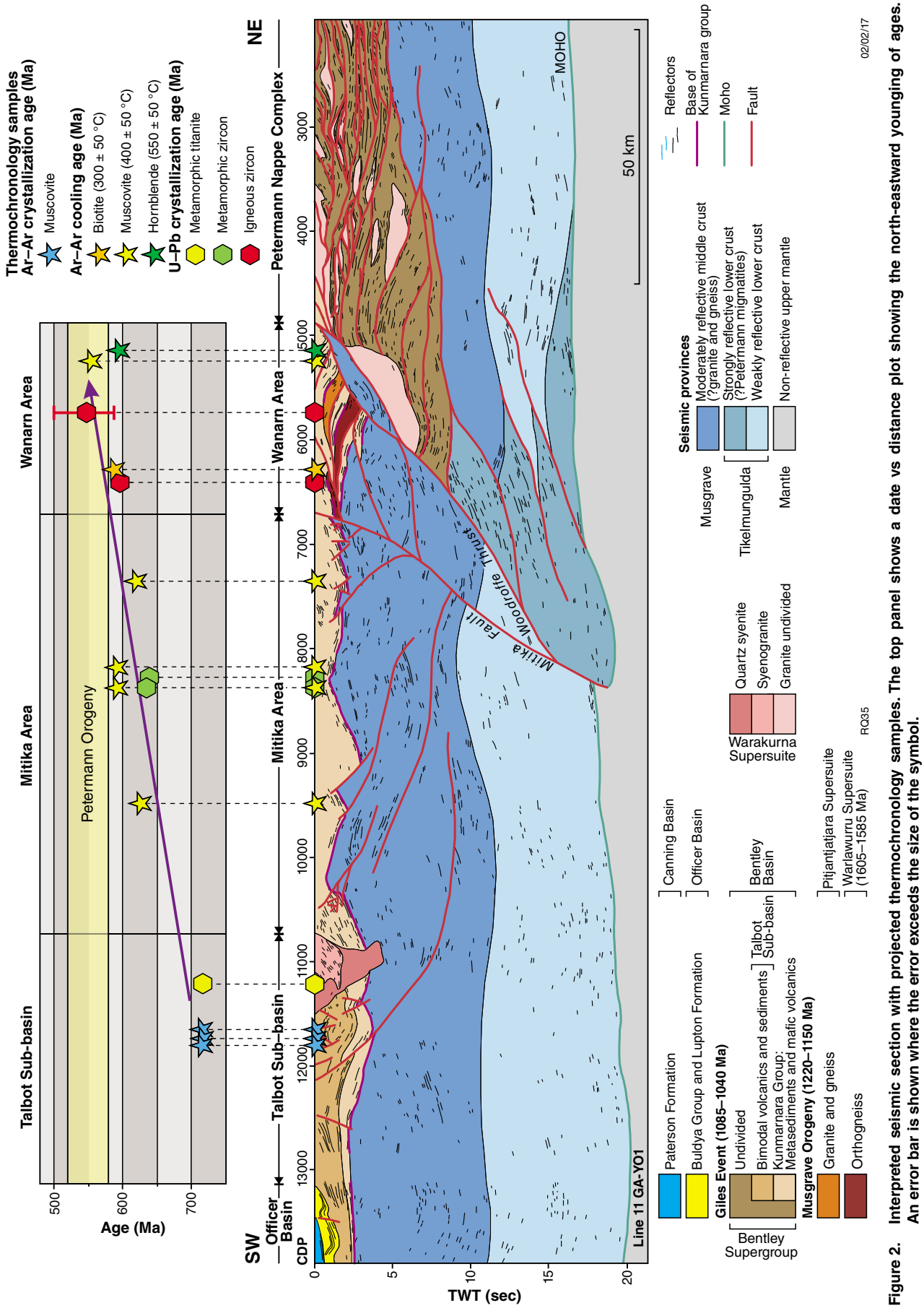

Figure 2. Interpreted seismic section with projected thermochronology samples. The top panel shows a date vs distance plot showing the north-eastward younging of ages. An error bar is shown where the error exceeds the size of the symbol.

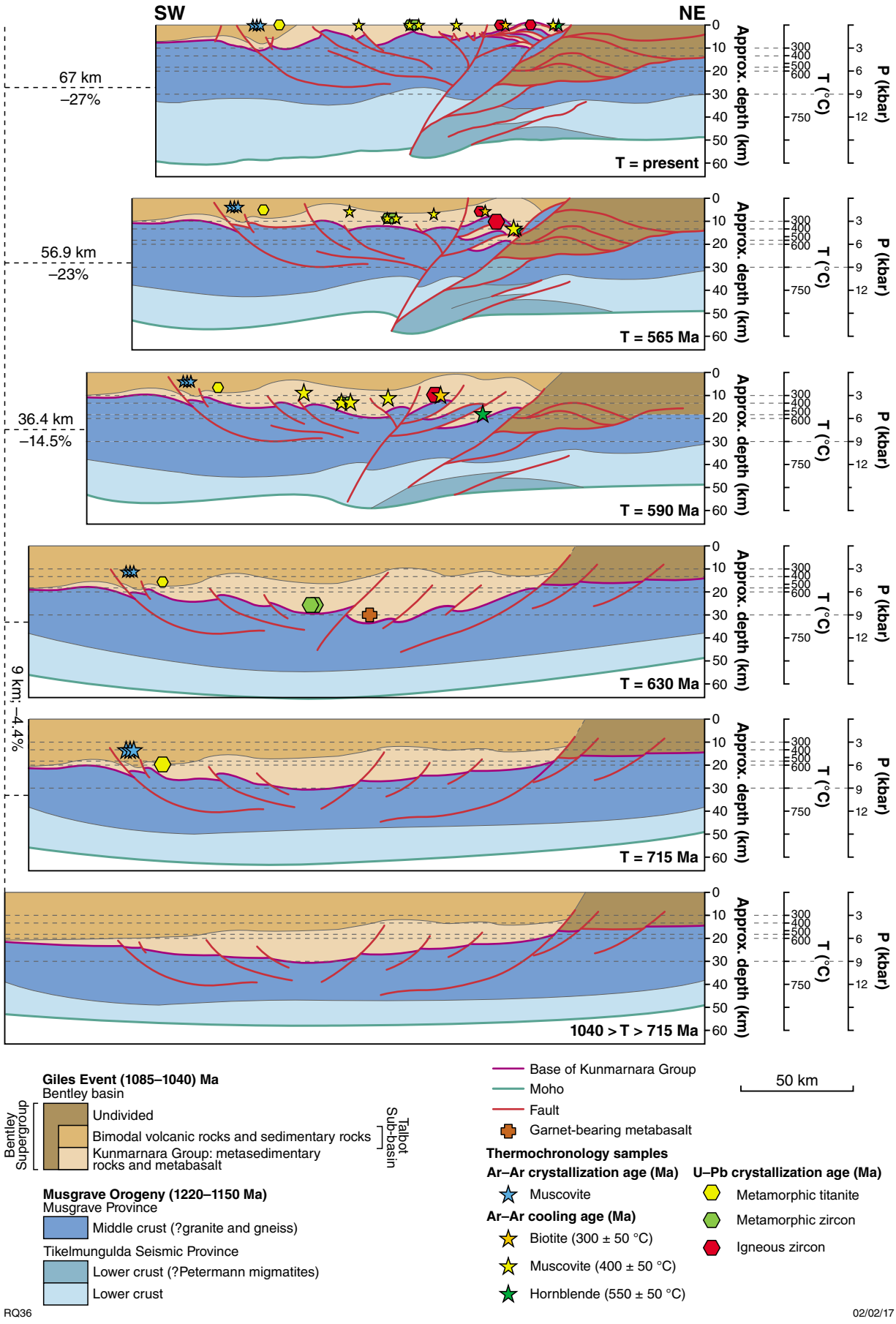
SW
NE
67 km
–27%
56.9 km
–23%
36.4 km
–14.5%
9 km; –4.4%
T = present
T = 565 Ma
T = 590 Ma
T = 630 Ma
T = 715 Ma
1040 > T > 715 Ma
Approx. depth (km)
T (°C)
P (kbar)
Giles Event (1085–1040) Ma
Bentley basin
Bentley Supergroup
Undivided
Bimodal volcanic rocks and sedimentary rocks
Kunmarnara Group: metasedimentary rocks and metabasalt
Talbot Sub-basin
Musgrave Orogeny (1220–1150 Ma)
Musgrave Province
Middle crust (?granite and gneiss)
Tikelmungulda Seismic Province
Lower crust (?Petermann migmatites)
Lower crust
Base of Kunmarnara Group
Moho
Fault
Garnet-bearing metabasalt
50 km
Thermochronology samples
Ar–Ar crystallization age (Ma)
Muscovite
Ar–Ar cooling age (Ma)
Biotite (300 ± 50 °C)
Muscovite (400 ± 50 °C)
Hornblende (550 ± 50 °C)
U–Pb crystallization age (Ma)
Metamorphic titanite
Metamorphic zircon
Igneous zircon
RQ36
02/02/17

Figure 3. (left) Time–temperature constrained evolution model showing amount of calculated shortening over time. The geothermal gradient used is 30 °C/km for the first 20 km and 7.5 °C/km for the next 20 km (see text for references). Line-length balanced and reconstructed only south of the Woodroffe Thrust. Granites of the Warakurna Supersuite and rocks of the Canning and Officer Basins were omitted deliberately.

Walsh, AK, Raimondo, T, Kelsey, DE, Hand, M, Pfitzner, HL and Clark, C 2013, Duration of high-pressure metamorphism and cooling during the intraplate Petermann Orogeny: Gondwana Research, v. 24, no. 3–4, p. 969–983.

Wingate, MTD, Campbell, IH, Compston, W and Gibson, GM 1998, Ion microprobe U–Pb ages for Neoproterozoic basaltic magmatism in south-central Australia and implications for the breakup of Rodinia: Precambrian Research, v. 87, no. 3–4, p. 135–159, doi: 10.1016/S0301-9268(97)00072-7.

This Record is published in digital format (PDF) and is available as a free download from the DMP website at <www.dmp.wa.gov.au/GSWApublications>.

Further details of geological products produced by the Geological Survey of Western Australia can be obtained by contacting:

Information Centre
Department of Mines and Petroleum
100 Plain Street
EAST PERTH WESTERN AUSTRALIA 6004
Phone: (08) 9222 3459 Fax: (08) 9222 3444
www.dmp.wa.gov.au/GSWApublications